Source apportionment of PM_{10} and $PM_{2.5}$ in Nelson Airshed A

T. Ancelet
P.K. Davy
W.J. Trompetter

GNS Science Consultancy Report 2013/146
December 2013

GNS SCIENCE
TE PŪ AO

DISCLAIMER

This report has been prepared by the Institute of Geological and Nuclear Sciences Limited (GNS Science) exclusively for and under contract to Nelson City Council. Unless otherwise agreed in writing by GNS Science, GNS Science accepts no responsibility for any use of, or reliance on any contents of this Report by any person other than Nelson City Council and shall not be liable to any person other than Nelson City Council, on any ground, for any loss, damage or expense arising from such use or reliance.

The data presented in this Report are available to GNS Science for other use from June 2013.

BIBLIOGRAPHIC REFERENCE

Ancelet, T.; Davy, P. K.; Trompetter, W. J. 2013. Source apportionment of PM_{10} and $PM_{2.5}$ in Nelson Airshed A, *GNS Science Consultancy Report* 2013/146. 95 p.

CONTENTS

FIGURES

TABLES

APPENDICES

APPENDIX FIGURES

APPENDIX TABLES

EXECUTIVE SUMMARY

This report presents the results of an analysis of particulate matter (PM_{10} and $PM_{2.5}$) concentrations and composition in Nelson City Council's 'Airshed A' in Nelson South. The compositional data has been used in a receptor modelling study to apportion particulate matter concentrations to those emission sources contributing to ambient concentrations in the airshed.

Key results from the study are:

1. Emissions from solid fuel fires for home heating are the primary source of $PM_{2.5}$ and PM_{10} in the Nelson South airshed and responsible for exceedances of the PM_{10} National Environmental Standard for Air Quality (NES) of 50 $\mu g\ m^{-3}$.
2. On high pollution nights during winter most of the particulate matter is in the fine fraction ($PM_{2.5}$) and It was found that there were many more days where $PM_{2.5}$ exceeds the New Zealand Ambient Air Quality Guidelines (NZAAQG) compared to PM_{10} NES exceedances. The data suggests that it will take significantly longer to comply with the $PM_{2.5}$ monitoring guideline than the PM_{10} NES. The implications of this are that the health related effects due to high $PM_{2.5}$ concentrations from combustion sources will continue despite compliance with the PM_{10} NES.
3. The data shows that both PM_{10} and Black Carbon (BC) concentrations have been decreasing over the years 2006–2012, indicating that it was most likely to be a reduction in combustion source emissions affecting PM_{10} concentrations with the most significant reductions occurring during winter months. When the sources of BC were accounted for, the winter decrease was found to be entirely from reductions in biomass combustion-associated black carbon. This demonstrates that measures introduced by Nelson City Council to mitigate the winter domestic fire air pollution problem have been effective.
4. The multi-site particulate matter monitoring campaign undertaken during the 2011 winter showed that the St. Vincent Street site regularly records the highest PM_{10} concentrations in the Nelson South airshed, with down-valley katabatic drainage on cold and calm nights the main particulate matter transport mechanism observed during peak PM_{10} events. The study also found that the observed morning (7am – 9am) peak in PM_{10} concentrations was likely to be due to relighting of domestic solid fuel heating appliances.
5. Arsenic contamination in particulate matter has been found in urban air across New Zealand and the Nelson South airshed is no exception as shown in Figure 1.1. Average annual concentrations calculated from the Ion Beam Analysis elemental data indicates that the New Zealand Ambient Air Quality Guideline for arsenic (5.5 ng m^{-3} annual average) is substantially exceeded every year in Nelson South (Figure 1.2), with the highest concentrations during winter (maxima around 90 ng m^{-3}). The arsenic was strongly associated with the biomass combustion source and therefore, the arsenic contamination is considered to be from the use of copper chrome arsenate (CCA)-treated timber as fuel for domestic fires.
6. During peak PM_{10} pollution events, up to 20 % of PM_{10} is from natural and secondary sources which should be factored into any PM_{10} pollution reduction strategy since nothing can be done with regard to PM_{10} from these sources.

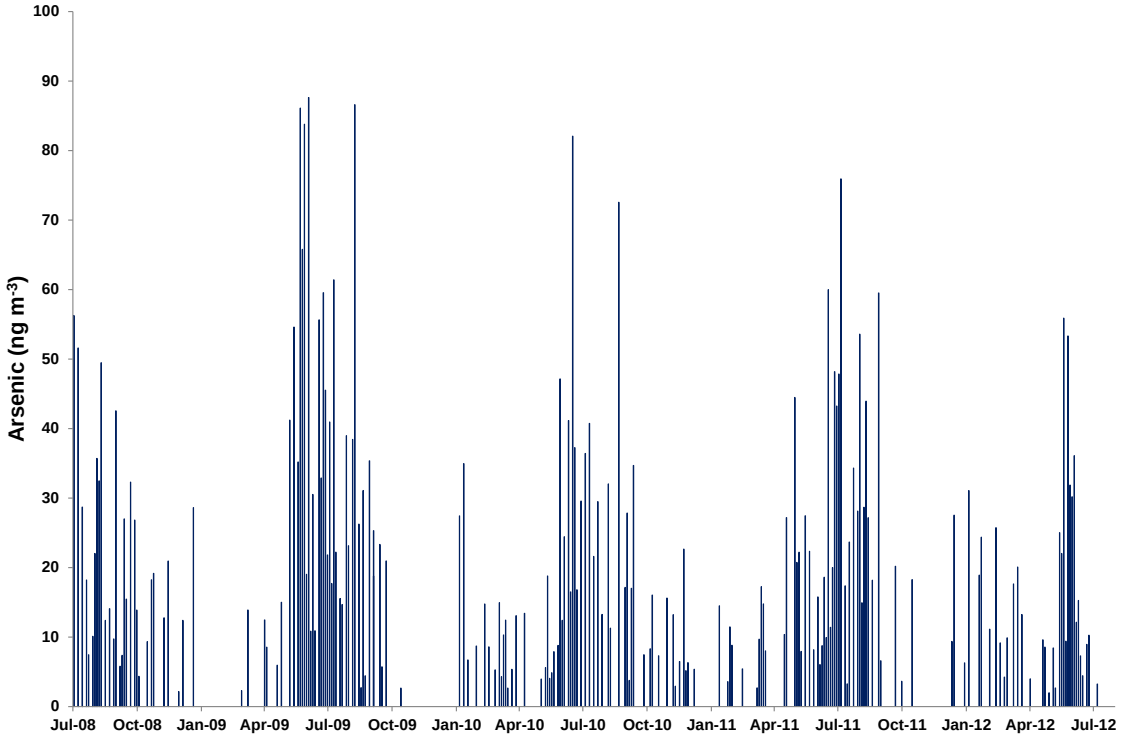

Figure 1.1 Arsenic concentrations at the St. Vincent Street site.

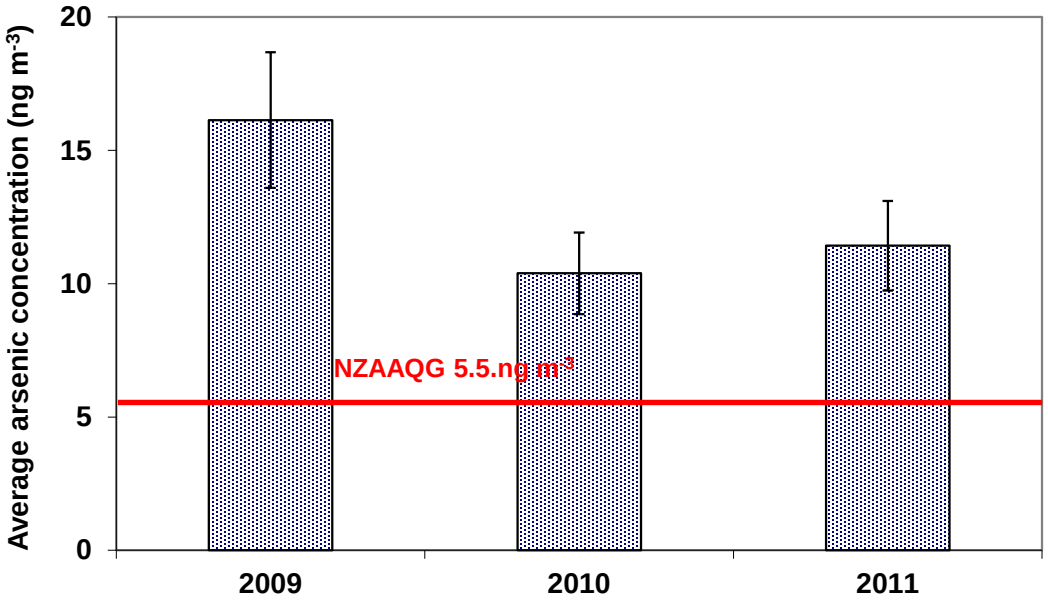

Figure 1.2 Annual average arsenic concentrations at the St. Vincent Street site.

1.0 INTRODUCTION

This report presents results from a receptor modeling study of two size fractions of airborne particles collected at an ambient air quality monitoring site on St. Vincent Street, in Nelson Airshed A (Nelson South). This work was commissioned by the Nelson City Council (NCC) as part of their ambient air quality monitoring strategy and was partially funded by Envirolink grants (1273-NLCC 71 & 1291-NLCC72) from the Ministry of Business, Innovation and Employment.

1.1 REQUIREMENT TO MANAGE AIRBORNE PARTICLE POLLUTION

In response to growing evidence of significant health effects associated with airborne particle pollution, the New Zealand Government introduced a National Environmental Standard (NES) in 2005 of 50 µg m^{-3} for particles less than 10 µm in aerodynamic diameter (denoted as PM_{10}). The NES places an onus on regional councils to monitor PM_{10} and publicly report if the air quality in their region exceeds the standard. Initially, regional councils were required to comply with the standard by 2013 or face restrictions on the granting of resource consents for discharges that contain PM_{10}, but the NES has since been revised, extending the target date for regional councils to comply with the standard. The new target dates are September 1, 2016 for airsheds with between 1 and 10 exceedances and September 1, 2020 for airsheds with 10 or more exceedances. In areas where the PM_{10} standard is exceeded, information on the sources contributing to those air pollution episodes is required to effectively manage air quality and formulate appropriate mitigation strategies.

In addition to the PM_{10} NES, the Ministry for the Environment issued ambient air quality guidelines for air pollutants in 2002 that included a guideline value of 25 µg m^{-3} for particles less than 2.5 µm in aerodynamic diameter ($PM_{2.5}$) (24-hour average). More recently, the World Health Organisation (WHO) has confirmed a $PM_{2.5}$ ambient air quality guideline value of 25 µg m^{-3} (24-hour average) based on the relationship between 24-hour and annual PM concentrations (WHO, 2006). The WHO annual average guideline for $PM_{2.5}$ is 10 µg m^{-3}. These are the lowest levels at which total, cardiopulmonary and lung cancer mortality have been shown to increase with more than 95% confidence in response to exposure to $PM_{2.5}$. The WHO recommends the use of $PM_{2.5}$ guidelines over PM_{10} because epidemiological studies have shown that most of the adverse health effects associated with PM_{10} are because of $PM_{2.5}$.

1.2 IDENTIFYING THE SOURCES OF AIRBORNE PARTICLE POLLUTION

Measuring the mass concentration of particulate matter (PM) provides little or no information on the identities of the contributing sources. Airborne particles are composed of many elements and compounds emitted from various sources and receptor modeling allows the determination of relative mass contributions from sources impacting the total PM mass of samples collected at a monitoring site. First, gravimetric mass is measured and then a variety of methods can be used to determine the elements and compounds present in a sample. In this study, elemental concentrations in the samples were determined using ion beam analysis (IBA) techniques at the New Zealand Ion Beam Analysis facility operated by GNS Science in Lower Hutt.

Ion beam analysis describes a range of mature analytical techniques that provide the non-destructive determination of multi-elemental concentrations in samples. Using elemental

concentrations, coupled with appropriate statistical techniques and purpose-designed mathematical models, the sources contributing to each ambient sample can be identified. In general, the more ambient samples that are included in the analysis, the more robust the receptor modeling results.

In Nelson Airshed A, an emissions inventory was developed in 2006 by NCC, but the accuracy of this inventory with respect to source emissions and types is unclear. It is critical for NCC to effectively manage air quality that all of the PM sources and their contributions in Nelson Airshed A are identified. Therefore, this study aimed to identify, using the receptor modeling technique positive matrix factorisation (PMF), the sources contributing to PM concentrations in Nelson Airshed A and their mass contributions. Importantly, source contributions from natural sources, like marine aerosol, which are difficult or impossible to quantify using emissions inventories, were examined. Temporal variations in source contributions were also analysed to identify how source contributions varied seasonally and annually, and to assess the effectiveness of NCC-implemented air quality management measures.

1.3 REPORT STRUCTURE

This report is comprised of 11 main chapters. Briefly, the remaining chapters have been broken down as follows:

1. Chapter 2 describes the methodology and analytical techniques used for the receptor modeling analysis.
2. Chapter 3 describes the Nelson Airshed A ambient air quality monitoring site, temporal trends in PM_{10} concentrations and local meteorology.
3. Chapter 4 presents the receptor modeling results for PM_{10} and $PM_{2.5}$, including temporal variations and seasonality.
4. Chapter 5 presents a discussion of the receptor modeling results.
5. Chapter 6 presents results from an hourly PM sampling campaign undertaken at the St. Vincent Street site.
6. Chapter 7 presents analyses of trends in black carbon concentrations.
7. Chapter 8 presents analyses of arsenic concentrations.
8. Chapter 9 provides comparisons of the receptor modeling results with the 2006 NCC Emissions Inventory.
9. Chapter 10 compares the results obtained in this study with those from a study at Tahunanui (Nelson Airshed B).
10. Chapter 11 provides a summary of the research findings.

2.0 METHODOLOGY

PM_{10} and $PM_{2.5}$ samples on filters were collected at the NCC monitoring site on St. Vincent Street, Nelson. Figure 2.1 presents the location of the monitoring site. All PM sampling and systems maintenance at the sampling site was carried out by NCC, and as such, NCC maintains all records of equipment, flow rates and sampling methodologies used for the PM sampling regimes. Filter conditioning, weighing and re-weighing for PM_{10} and $PM_{2.5}$ gravimetric mass determinations were performed by the Cawthron Institute, Nelson.

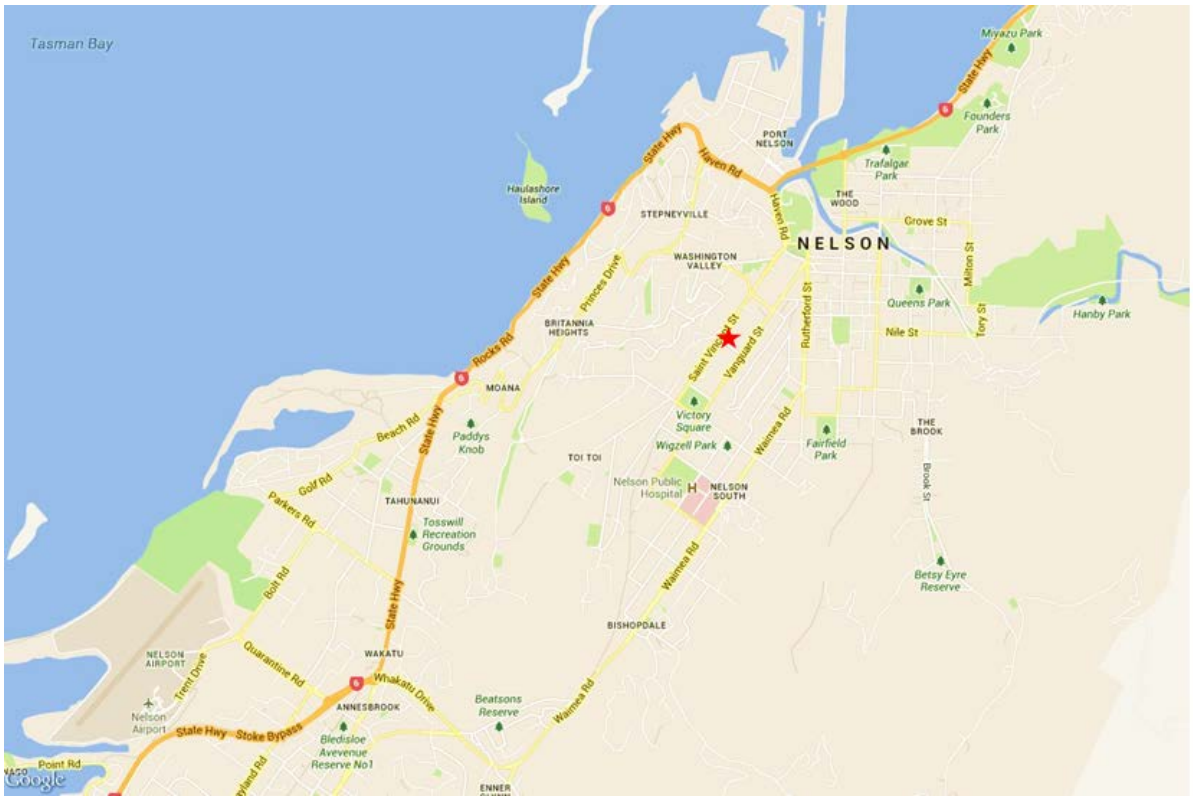

Figure 2.1 Location of the Tahunanui monitoring site in the Nelson area (★) (source: Wises Maps www.wises.co.nz)

Elemental concentrations in the PM_{10} and $PM_{2.5}$ samples were determined using IBA techniques at the New Zealand Ion Beam Analysis Facility in Gracefield, Lower Hutt. The full suite of analyses included particle-induced X-ray emission (PIXE), particle-induced gamma-ray emission (PIGE), Rutherford backscattering (RBS) analysis and particle elastic scattering analysis (PESA). Black carbon (BC) concentrations were determined using light reflection techniques. Full descriptions of the analytical and data analysis techniques used in this study are provided in Appendix 1.

The authors visited the monitoring site and noted typical activities occurring in the surrounding area that may contribute to PM concentrations. These observations are reflected in the conceptual receptor model described in Chapter 3.

2.1 DATA ANALYSIS AND REPORTING

The receptor modeling results within this report have been produced in a manner that provides as much information as possible on the relative contributions of sources to PM concentrations so that it may be used for monitoring strategies, air quality management and policy development. The data have been analysed to provide the following outputs:

1. masses of elemental species apportioned to each source;
2. source elemental profiles;
3. average PM_{10} and $PM_{2.5}$ mass apportioned to each source;
4. temporal variations in source mass contributions (timeseries plots);
5. seasonal variations in source mass contributions. For the purposes of this study, summer has been defined as December–February, autumn as March–May, winter as June–August and spring as September–November;
6. analysis of source contributions on peak PM days. Table 2.1 presents the relevant standards, guidelines and targets for PM concentrations.

Table 2.1 Standards, guidelines and targets for PM concentrations

Particle Size	Averaging Time	Ambient Air Quality Guideline	MfE* 'Acceptable' air quality category	National Environmental Standard	Allowable Exceedances per Annum
PM_{10}	24 hours	50 µg m^{-3}	33 µg m^{-3}	50 µg m^{-3}	3 (by 2020)
	Annual	20 µg m^{-3}	13 µg m^{-3}		
$PM_{2.5}$	24 hours	25 µg m^{-3}	17 µg m^{-3}		

*Ministry for the Environment air quality categories taken from the Ministry for the Environment, October 1997 – ***Environmental Performance Indicators: Proposals for Air, Fresh Water and Land***.

3.0 ST. VINCENT STREET MONITORING SITE AND SAMPLING METHODOLOGY

3.1 SITE DESCRIPTION

Size-resolved PM samples (PM_{10} and $PM_{2.5}$) were collected at an ambient air quality monitoring station located on a property off of St. Vincent Street, Nelson (Lat: –41.164150°, Long: 173.162447°, elevation: 5 m). Figure 3.1 presents the site location on a map of the local area.

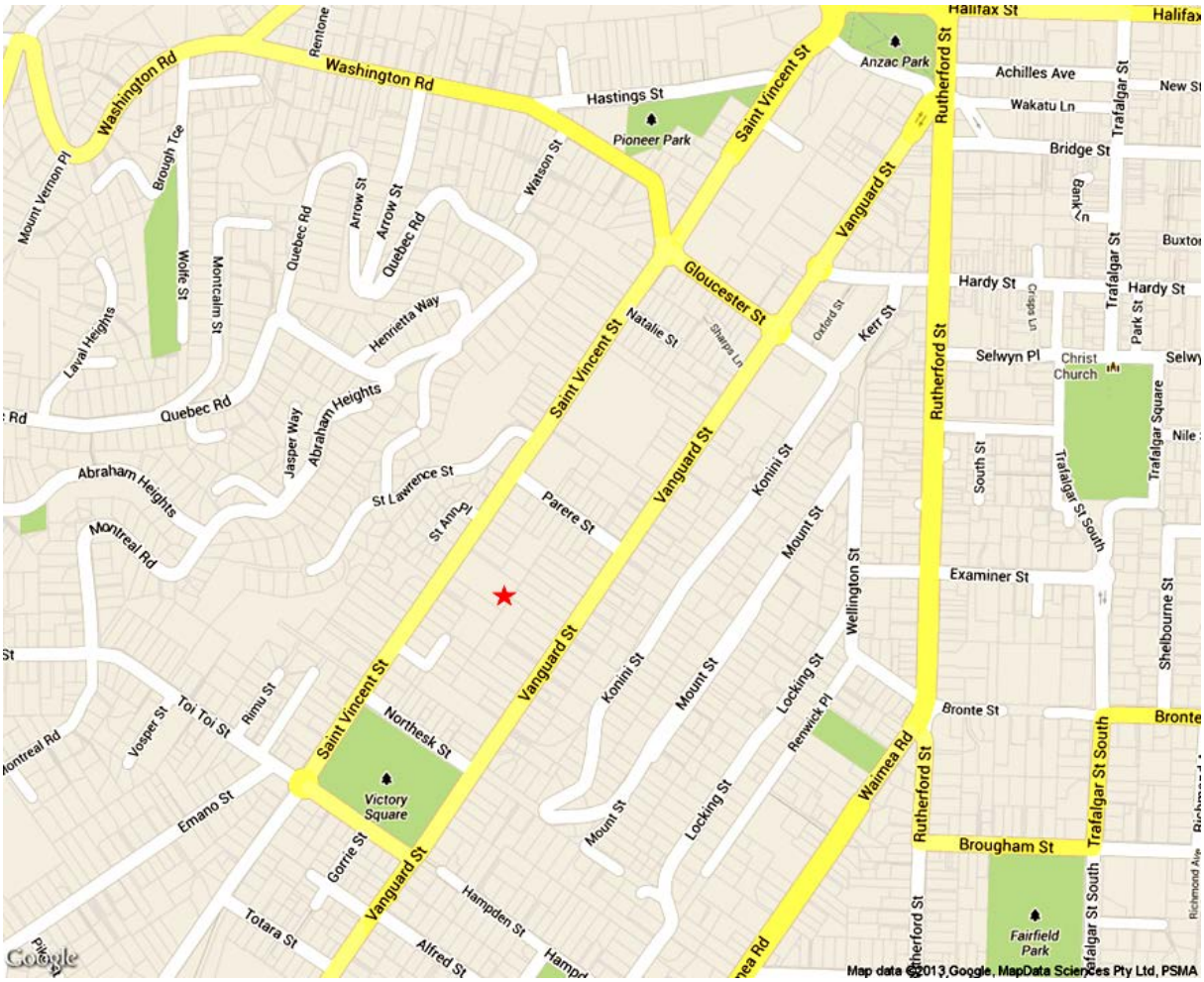

Figure 3.1 Map showing the location of the St. Vincent Street monitoring site (★) (source: Wises Maps www.wises.co.nz).

St. Vincent Street is located near (within 600 m) the Nelson CBD. The site was approximately 90 m from the nearest road and surrounded by open space or buildings no more than two stories high. Figure 3.2 provides an aerial photo of the St. Vincent Street monitoring site and its immediate environs.

Figure 3.2 Aerial view of the St. Vincent Street monitoring site and its immediate environs (from Google Earth).

3.2 PARTICULATE MATTER SAMPLING AND MONITORING PERIOD

Samples of PM_{10} and $PM_{2.5}$ were collected for analysis in this study. Overall 190 PM_{10} and 200 $PM_{2.5}$ samples were collected using a Partisol (satellite and hub) sampler system from July 2008–July 2012. Samples were collected on an alternating one-day-in-six (midnight to midnight) sampling regime for each of the size fractions so that a sample was collected every third day alternating between PM_{10} and $PM_{2.5}$. Mass concentrations of PM_{10} and $PM_{2.5}$ were determined gravimetrically, where a filter of known weight was used to collect the PM samples from a known volume of sampled air. The loaded filters were the re-weighed to obtain the mass of collected PM. The average PM concentration in the sampled air was then calculated.

3.3 CONCEPTUAL RECEPTOR MODEL FOR PM AT ST. VINCENT STREET

An important part of the receptor modeling process is to formulate a conceptual model of the receptor site. This means understanding and identifying the major sources that may influence ambient PM concentrations at the site. For the St. Vincent Street site, the initial conceptual model includes local emission sources:

- Motor vehicles – all roads in the area act as line sources, and roads with higher traffic densities and congestion will dominate;
- Domestic activities – likely to be dominated by biomass burning activities like emissions from solid fuel fires used for domestic heating during the winter;
- Local wind-blown soil or road dust sources may contribute because there are empty lots and vehicle access ways in close proximity.

Sources that originate further from the monitoring site would also be expected to contribute to ambient particle loadings, and these include:

- Marine aerosol;
- Secondary PM resulting from atmospheric gas-to-particle conversion processes – includes sulphates, nitrates and organic species;
- Potential industrial emissions from combustion processes (boilers) and dust generating activities.
- Emissions from ships in the Port area.

Another category of emission sources that may contribute are those considered to be 'one-off' emission sources:

- Fireworks displays and other special events (e.g. Guy Fawkes day);
- Short-term road works and demolition/construction activities.

The variety of sources described above can be recognised and accounted for using appropriate data analysis methods such as examination of seasonal differences, temporal variations and receptor modeling itself.

3.4 LOCAL METEOROLOGY AT THE ST. VINCENT STREET SITE

A meteorological station was located at the monitoring site and is owned and operated by NCC. The predominant wind directions at St. Vincent Street were from the southwest and northeast, as shown in Figure 3.3. The meteorology at the St. Vincent Street site is defined and constrained by the local topography because the site is located inside a narrow valley running in the southwest to northeast direction. Few contributions from other wind directions were apparent. Little seasonality was apparent in wind directions, as shown in Figure 3.4. However, wind speeds during autumn and winter were lower than during other seasons.

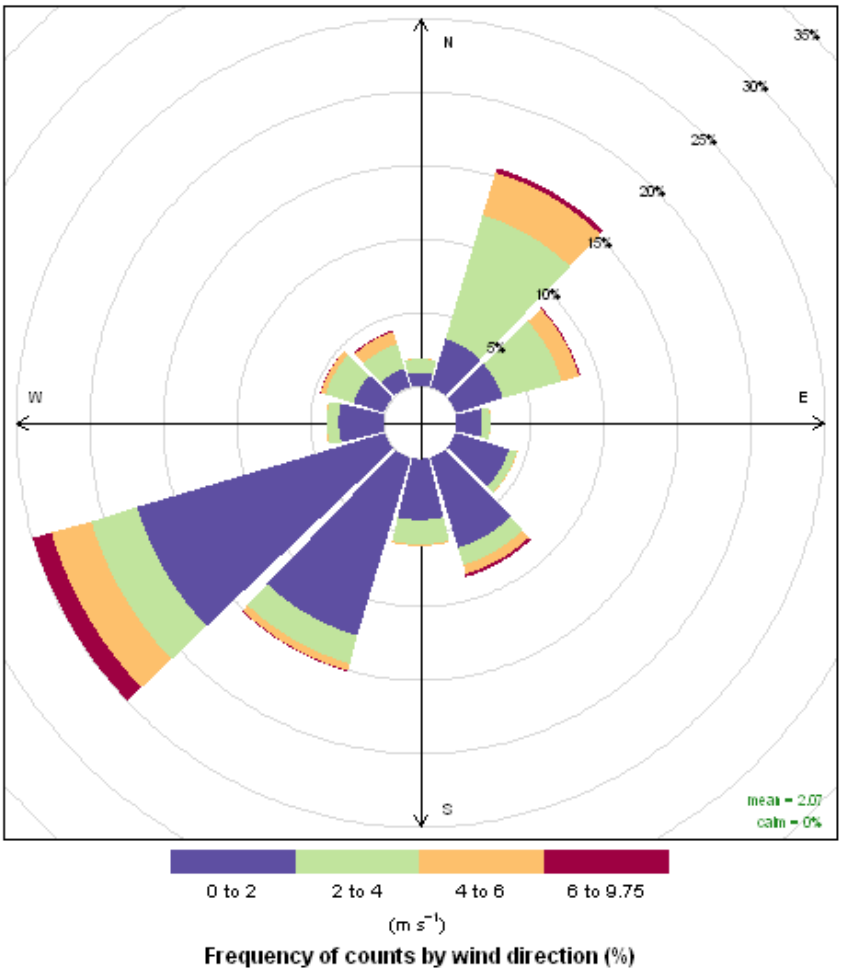

Figure 3.3 Wind rose for entire monitoring period (July 2008–July 2012).

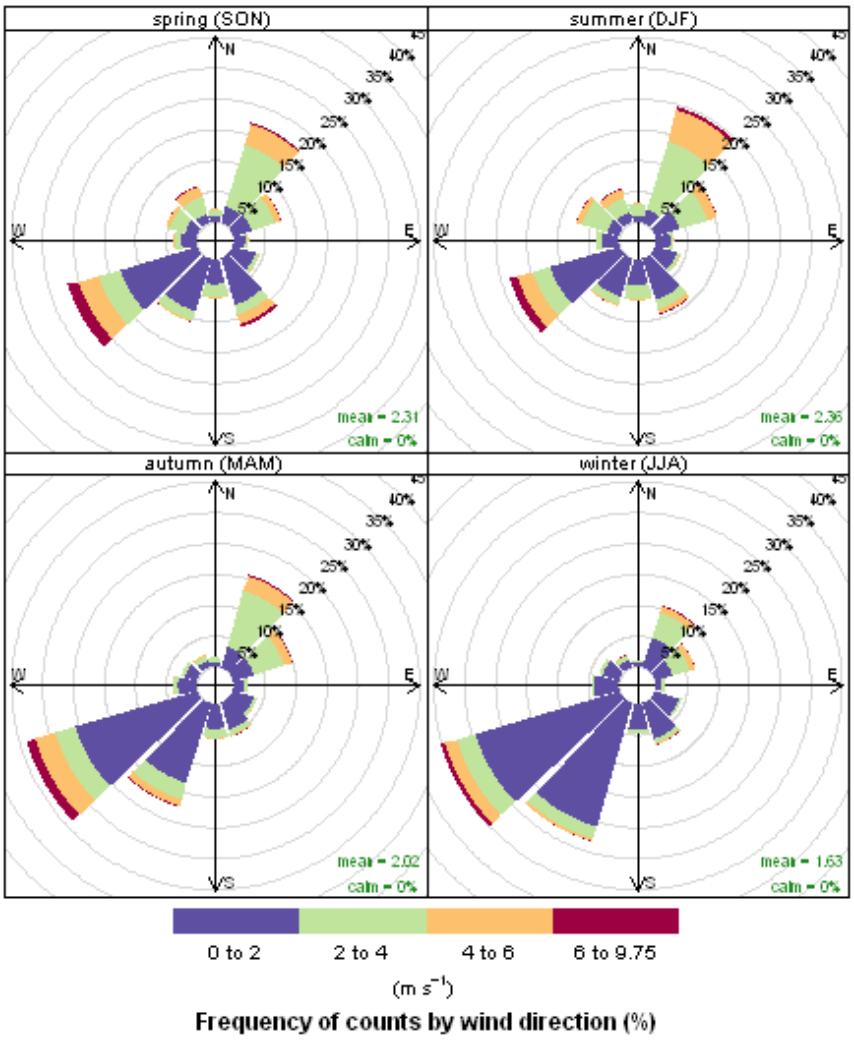

Figure 3.4 Wind roses by season over the entire monitoring period (July 2008–July 2012).

3.5 PM_{10} CONCENTRATIONS AT THE ST. VINCENT STREET SITE

PM_{10} concentrations were continuously monitored at the St. Vincent Street site using a Thermo-Anderson FH62 Beta-particle Attenuation Monitor (BAM) operated according to AS/NZS 3580.9.11.2008. Figure 3.5 presents the BAM PM_{10} monitoring results (midnight to midnight) over the monitoring period (July 2008–July 2012).

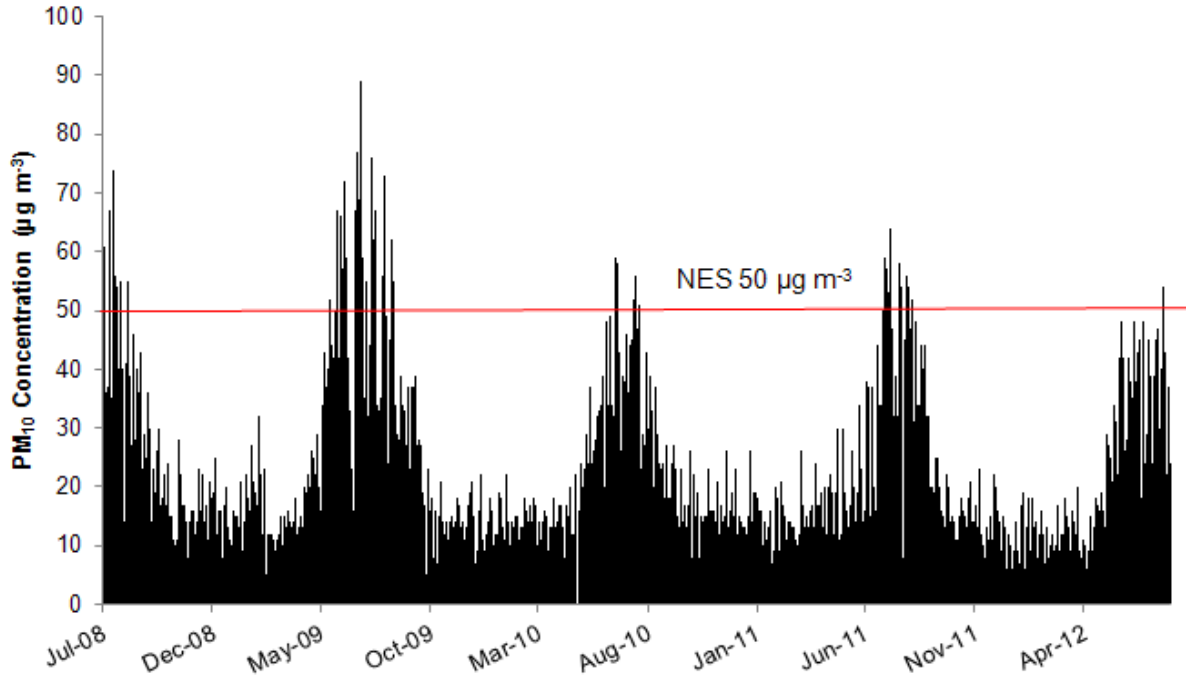

Figure 3.5 PM_{10} (BAM) concentrations at the St. Vincent Street site (supplied by NCC).

Figure 3.5 shows that PM_{10} concentrations at St. Vincent Street have seasonal patterns, with peak concentrations occurring in winter. During the monitoring period, 64 exceedances of the NES were recorded (www.nelsoncitycouncil.co.nz/air-monitoring). NCC does not continuously monitor $PM_{2.5}$ at the St. Vincent Street monitoring site.

4.0 RECEPTOR MODELING ANALYSES FOR PM_{10} AT ST. VINCENT STREET

4.1 ANALYSIS OF PM_{10} AND $PM_{2.5}$ AT ST. VINCENT STREET

The PM_{10} and $PM_{2.5}$ samples from the St. Vincent Street site were collected using a Partisol (hub and satellite) sampler system on an alternating one-day-in-three sampling regime, as discussed in Section 3.2, from July 2008–July 2012. PM_{10} and $PM_{2.5}$ concentrations were determined gravimetrically and elemental and BC concentrations were determined using IBA techniques and light reflection, respectively, as described in Appendix 1. Gravimetric results for the PM_{10} and $PM_{2.5}$ samples are presented in Figure 4.1and 4.2, respectively. Clear seasonal patterns are apparent from Figures 4.1 and 4.2, with PM_{10} and $PM_{2.5}$ concentrations peaking from May–August. Outside of the winter season, PM_{10} and $PM_{2.5}$ concentrations at St. Vincent Street were low. Gaps present in Figures 4.1 and 4.2 resulted from missed sample days or samples removed as part of the quality assurance process, which could include, but would not be limited to, samples being collected on the wrong side of the filter, double exposure of filters, no volumetric data available, or equipment failure.

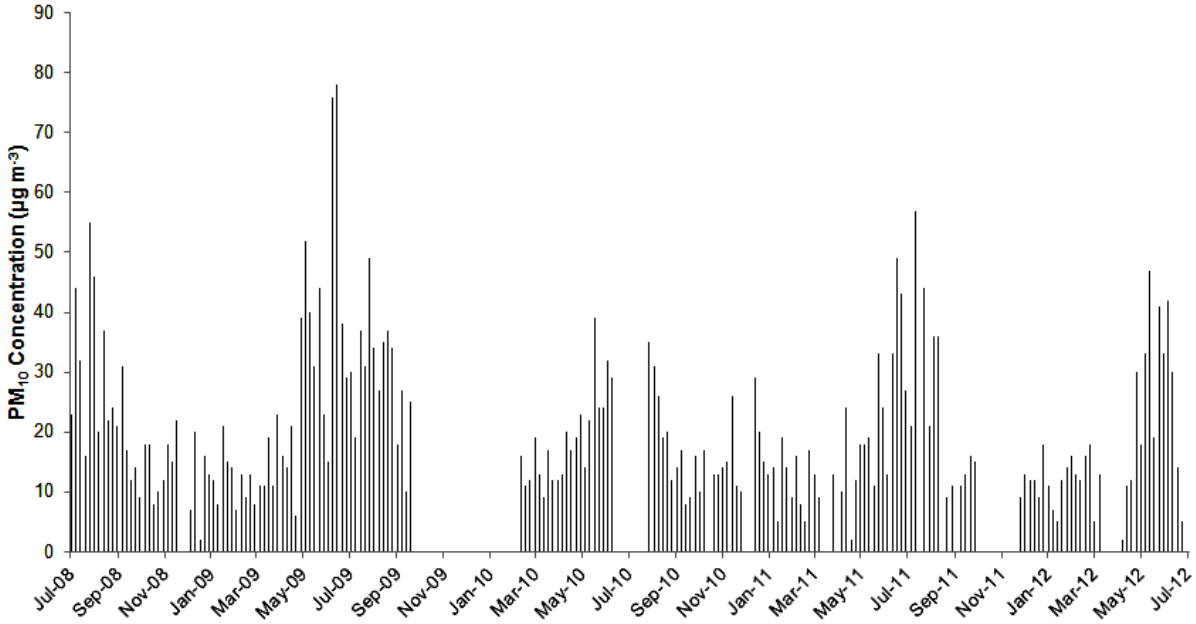

Figure 4.1 Gravimetric PM_{10} results. Gaps are from missed sample days or samples removed as part of the quality assurance process.

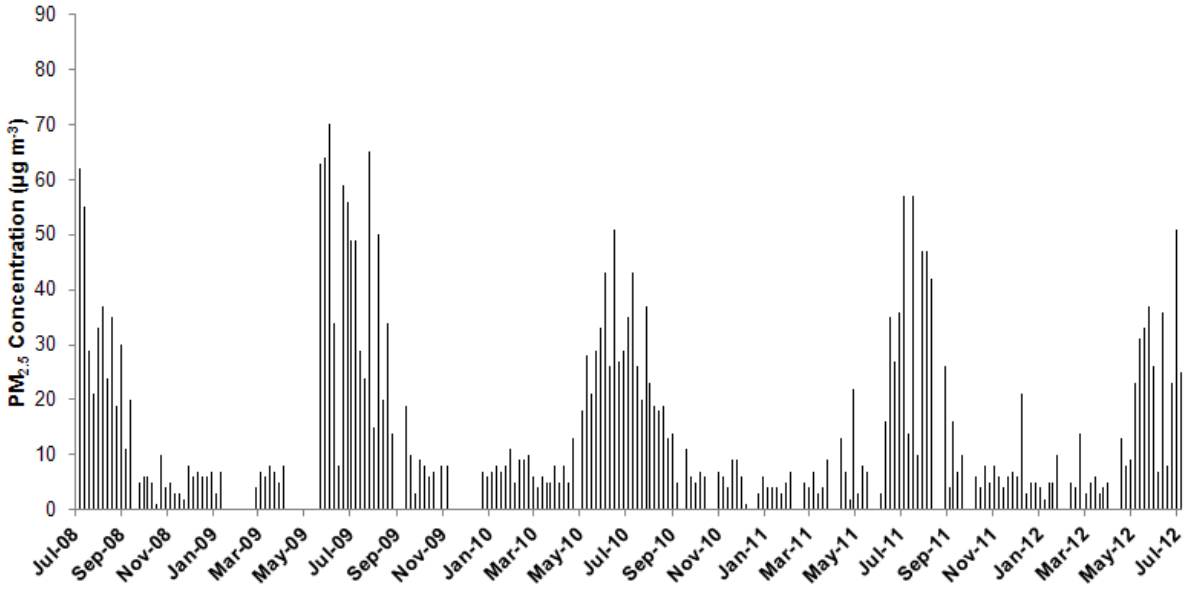

Figure 4.2 Gravimetric $PM_{2.5}$ results. Gaps are from missed sample days or samples removed as part of the quality assurance process.

4.2 COMPOSITION OF PM_{10} AND $PM_{2.5}$ AT ST. VINCENT STREET

Elemental concentrations for PM_{10} and $PM_{2.5}$ at St. Vincent Street are presented in Tables 4.1 and 4.2, respectively. Tables 4.1 and 4.2 indicate that some measured species were close to or below the limits of detection (LOD) in each of the samples. Carbonaceous species, represented by BC, were found to dominate PM_{10} and $PM_{2.5}$ mass concentrations. Along with BC, other important elemental constituents included Na, Cl, Si, Al and S and Na, Cl, S and K in PM_{10} and $PM_{2.5}$, respectively, indicating that combustion sources, marine aerosol, soil and secondary sulphate particles are important contributors to PM_{10} and $PM_{2.5}$ at the monitoring site. Elemental correlation plots for PM_{10} and $PM_{2.5}$ are provided in Figures A2.1 and A2.2, respectively, in Appendix 2.

Table 4.1 Elemental concentrations in PM_{10} collected at St. Vincent Street (190 samples).

	Average (ng m^{-3})	Max (ng m^{-3})	Min (ng m^{-3})	Median (ng m^{-3})	StdDev (ng m^{-3})	Ave Uncert (ng m^{-3})	Ave LOD (ng m^{-3})	#>LOD	%>LOD	Signal to Noise ratio
PM_{10} (µg m^{-3})	**21**	**78**	**2**	**17**	**13**					
BC	2907	11158	8	1803	2680	29	156	187	98	55
H	249	1536	23	139	269	18	41	171	90	10
Na	496	2298	0	396	407	113	221	148	78	3
Mg	99	311	0	86	57	18	27	183	96	3
Al	135	604	5	108	103	10	13	189	99	8
Si	339	1463	27	269	260	12	9	190	100	17
P	23	58	0	21	12	5	8	172	91	2
S	291	781	0	269	141	10	7	188	99	15
Cl	831	4447	0	595	748	20	6	188	99	24
K	219	933	1	163	166	9	7	188	99	15
Ca	125	358	1	112	67	8	7	188	99	9
Sc	3	15	0	2	3	3	9	14	7	0
Ti	21	198	0	14	28	5	7	136	72	3
V	2	16	0	1	3	2	9	21	11	0
Cr	2	19	0	0	3	2	8	14	7	0
Mn	4	19	0	4	4	3	8	50	26	1
Fe	137	540	0	109	102	7	6	188	99	11
Co	1	11	0	0	2	2	11	4	2	0
Ni	2	15	0	1	3	2	9	17	9	0
Cu	4	24	0	3	5	3	11	38	20	0
Zn	22	155	0	17	24	6	11	126	66	2
Ga	3	17	0	0	4	3	17	7	4	0
Ge	4	22	0	0	5	4	21	11	6	0
As	10	66	0	5	14	8	26	35	18	0
Se	7	49	0	0	10	7	35	12	6	0
Br	8	46	0	0	12	9	44	16	8	0
Rb	14	75	0	0	18	15	71	10	5	0
Sr	15	109	0	0	24	16	94	12	6	0
Mo	41	399	0	0	66	46	253	13	7	0
I	16	89	0	12	16	17	28	44	23	0
Ba	13	86	0	8	14	12	30	31	16	0
Hg	10	78	0	0	17	14	61	9	5	0
Pb	17	261	0	0	32	27	80	18	9	0

Table 4.2 Elemental concentrations in $PM_{2.5}$ collected at St. Vincent Street (200 samples).

	Average (ng m-3)	Max (ng m-3)	Min (ng m-3)	Median (ng m-3)	StdDev (ng m-3)	Ave Uncert (ng m-3)	Ave LOD (ng m-3)	#>LOD	%>LOD	Signal to Noise Ratio
PM2.5 (µg m-3)	**16**	**70**	**1**	**8**	**16**					
BC	3208	11310	114	1482	3132	30	156	199	100	55
H	529	3007	16	260	581	21	42	179	90	10
Na	202	1179	0	156	198	89	184	95	48	3
Mg	32	161	0	27	25	15	25	113	57	3
Al	35	186	0	26	28	8	13	178	89	8
Si	72	422	25	58	53	6	9	200	100	17
P	7	27	0	6	6	4	8	85	43	2
S	273	734	25	251	144	9	6	200	100	15
Cl	279	1874	8	207	266	10	6	200	100	24
K	220	989	12	129	219	8	7	200	100	15
Ca	30	108	0	28	14	5	7	196	98	9
Sc	2	10	0	1	2	2	8	10	5	0
Ti	3	19	0	1	4	3	7	34	17	3
V	1	10	0	1	2	2	7	17	9	0
Cr	2	38	0	1	4	2	6	29	15	0
Mn	2	13	0	1	2	2	7	22	11	1
Fe	30	185	1	23	24	4	5	191	96	11
Co	1	10	0	0	2	2	9	13	7	0
Ni	2	15	0	1	3	2	9	15	8	0
Cu	5	197	0	2	15	3	10	38	19	0
Zn	21	131	0	11	25	6	10	112	56	2
Ga	3	24	0	0	5	4	17	16	8	0
Ge	4	29	0	0	6	4	22	14	7	0
As	14	88	0	3	20	8	27	53	27	0
Se	8	40	0	0	10	7	35	23	12	0
Br	8	133	0	0	14	9	45	12	6	0
Rb	13	115	0	0	21	13	74	18	9	0
Sr	18	103	0	9	24	21	90	15	8	0
Mo	60	503	0	0	90	68	2848	24	12	0
I	8	40	0	4	10	11	25	21	11	0
Ba	6	73	0	1	9	8	24	11	6	0
Hg	8	79	0	0	16	11	61	6	3	0
Pb	21	262	0	0	36	32	81	17	9	0

4.3 SOURCE CONTRIBUTIONS TO PM_{10} AND $PM_{2.5}$ AT ST. VINCENT STREET

Five source contributors were identified from PMF receptor modeling analyses of the PM_{10} and $PM_{2.5}$ data at St. Vincent Street. Figures 4.3 and 4.4 present the source profiles extracted from the PMF analyses of PM_{10} and $PM_{2.5}$, respectively. The source contributors identified in Figures 4.3 and 4.4 were found to explain 99 and 93% of the PM_{10} and $PM_{2.5}$ gravimetric mass, respectively. The sources identified were:

- The first factor was identified as sulphate because of the dominance of sulphur in the profile. This source contribution was from secondary sulphate aerosol.
- The second factor was identified as originating from motor vehicle emissions because of the presence of BC, Al, Si, Ca and Fe as significant components representing a combination of tailpipe emissions and re-entrained road dust. Copper present in the profile also indicates emissions from the wear of brake linings.
- The third factor was labelled biomass combustion and contains H (as an indicator of organic compounds), BC and K as primary species along with some S and Cl. Interestingly arsenic was strongly associated with the the biomass combustion profiles , suggesting that residents are burning copper chrome arsenate (CCA)-treated timber in their domestic solid fuel heaters.
- The fourth factor was identified as a marine aerosol source because of the predominance of Na and Cl, along with some Mg, S, K, and Ca.
- The fifth factor was identified as soil and contains Al, Si, S, K, Ca and Fe as primary species.

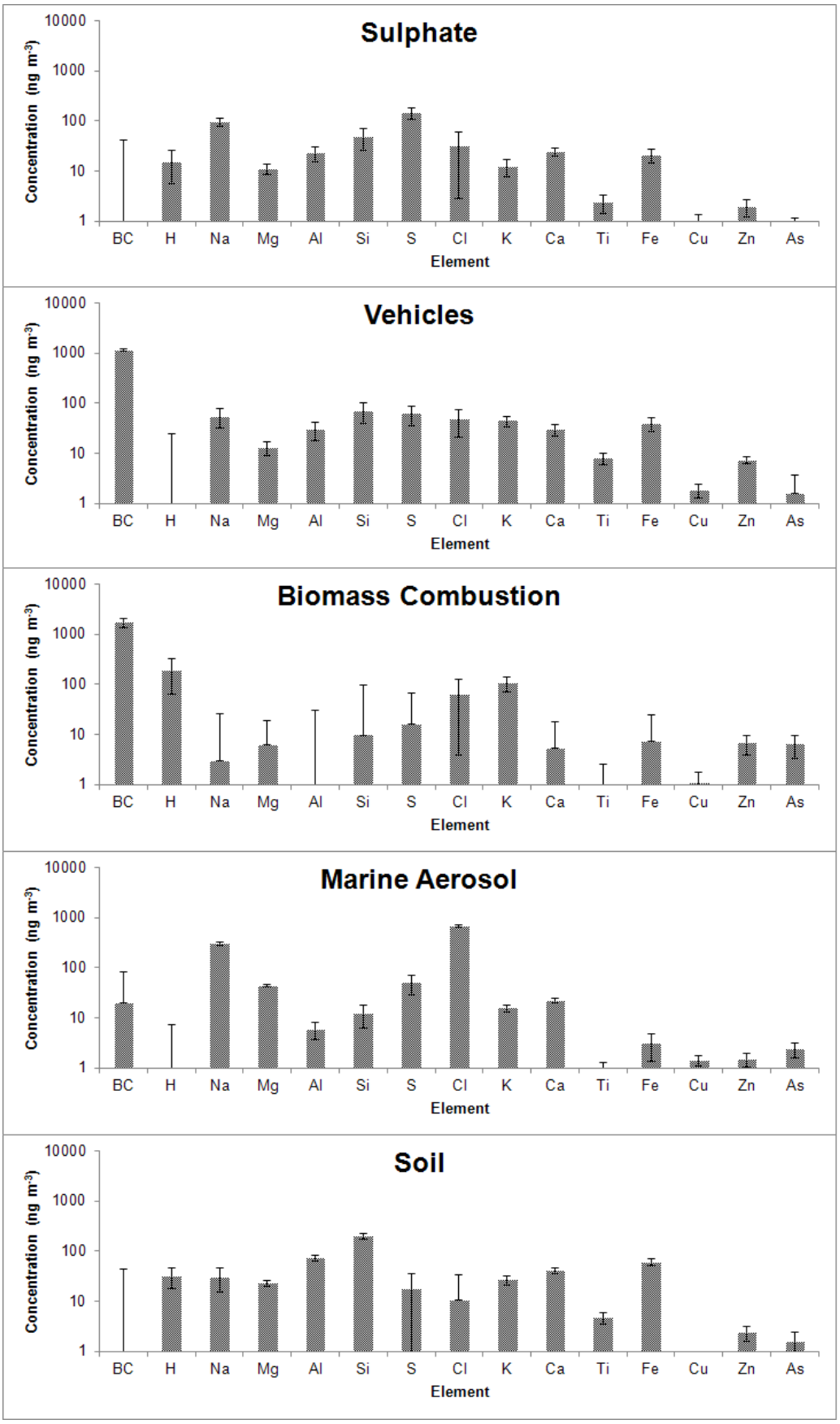

Figure 4.3 PM_{10} source profiles at St. Vincent Street.

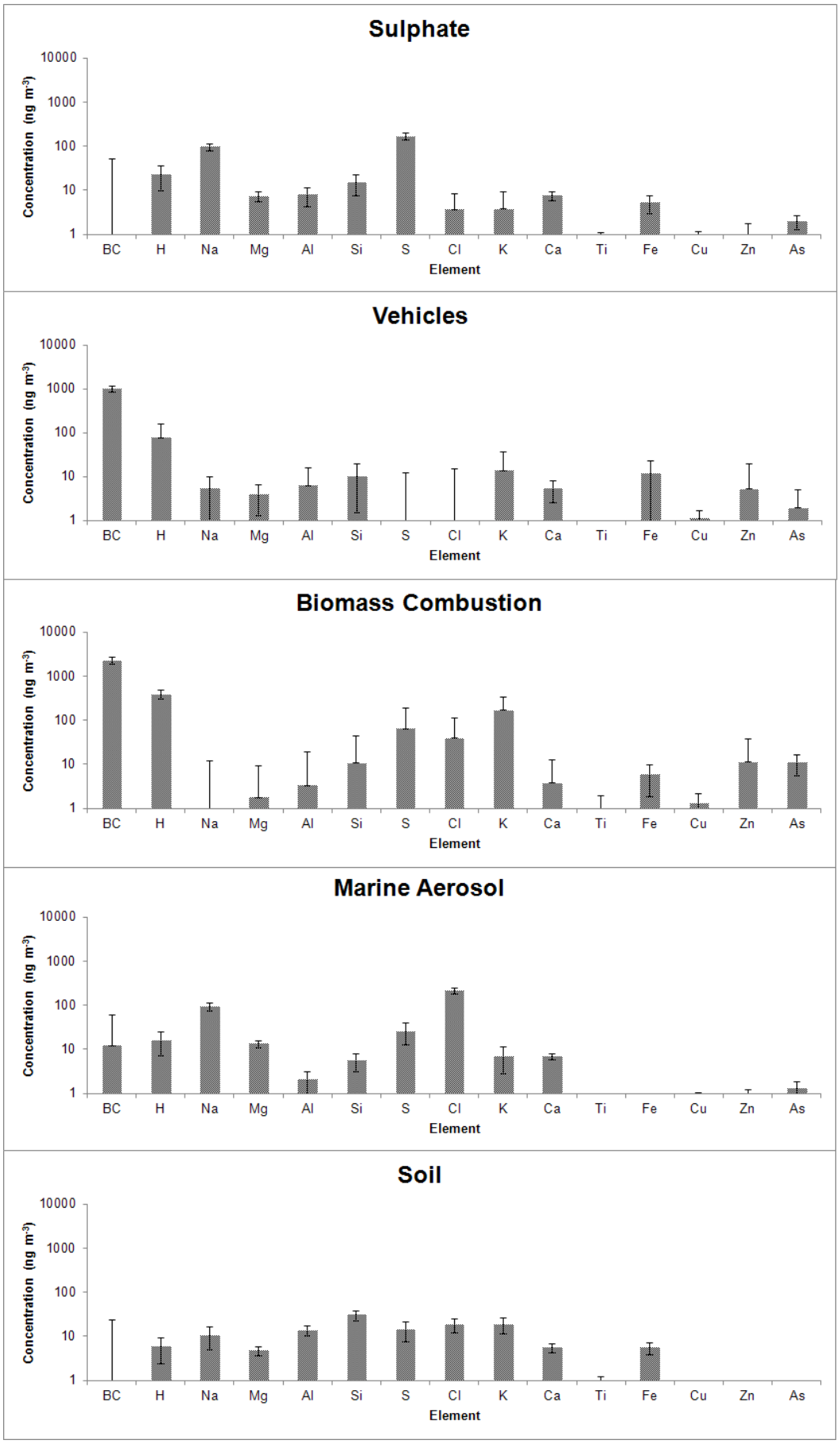

Figure 4.4 $PM_{2.5}$ source profiles at St. Vincent Street.

Figures 4.5 and 4.6 present the relative source contributions to PM_{10} and $PM_{2.5}$ at St. Vincent Street. Also included in Figures 4.5 and 4.6 are the standard deviations in mass contributions for each of the sources, indicating the variability in average mass contributions over the monitoring period.

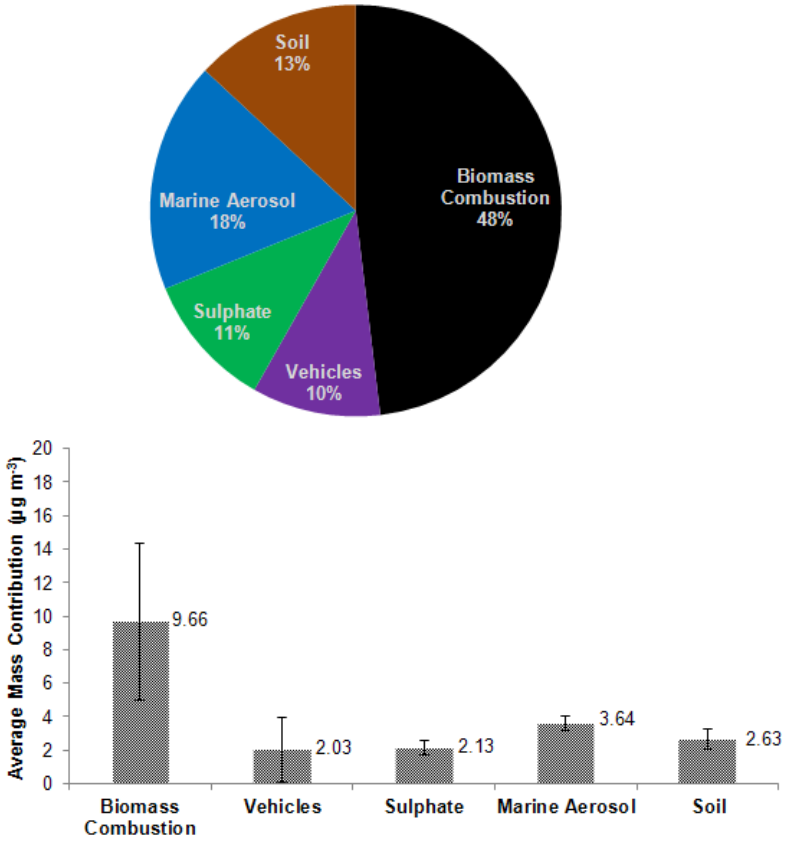

Figure 4.5 Average (2008–2012) relative source contributions to PM_{10} at St. Vincent Street.

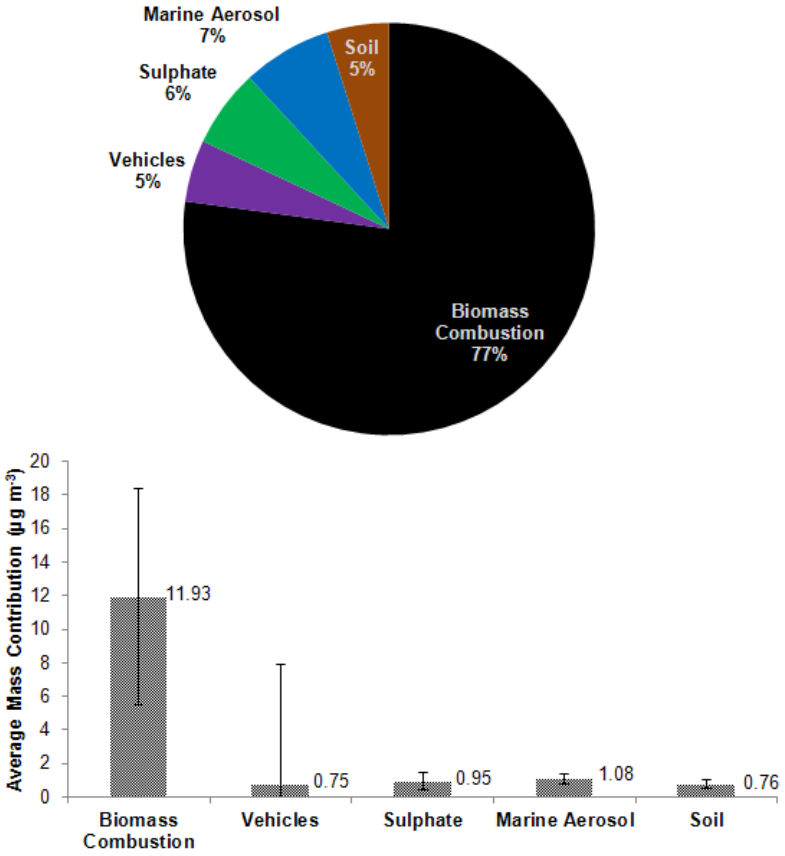

Figure 4.6 Average (2008–2012) relative source contributions to $PM_{2.5}$ at St. Vincent Street.

The average PM_{10} source contributions estimated by PMF indicated that biomass combustion and marine aerosol were the most significant contributors to PM_{10} mass (48 and 18%, respectively), with lesser contributions from soil (13%), secondary sulphate (11%) and motor vehicles (10%). Biomass combustion was by far the most dominant contributor to $PM_{2.5}$ concentrations (77%), with the soil (5%), motor vehicle (5%), secondary sulphate (6%) and marine aerosol (7%) sources having similar contributions to $PM_{2.5}$ mass.

Temporal variations in the PM_{10} and $PM_{2.5}$ source contributions are presented in Figures 4.7 and 4.8, respectively. In both the PM_{10} and $PM_{2.5}$ samples it is evident that PM mass is dominated by the biomass combustion source during winter, which arises primarily from emissions from solid fuel fires used for domestic heating. During other time periods, marine aerosol and soil contributions can be significant.

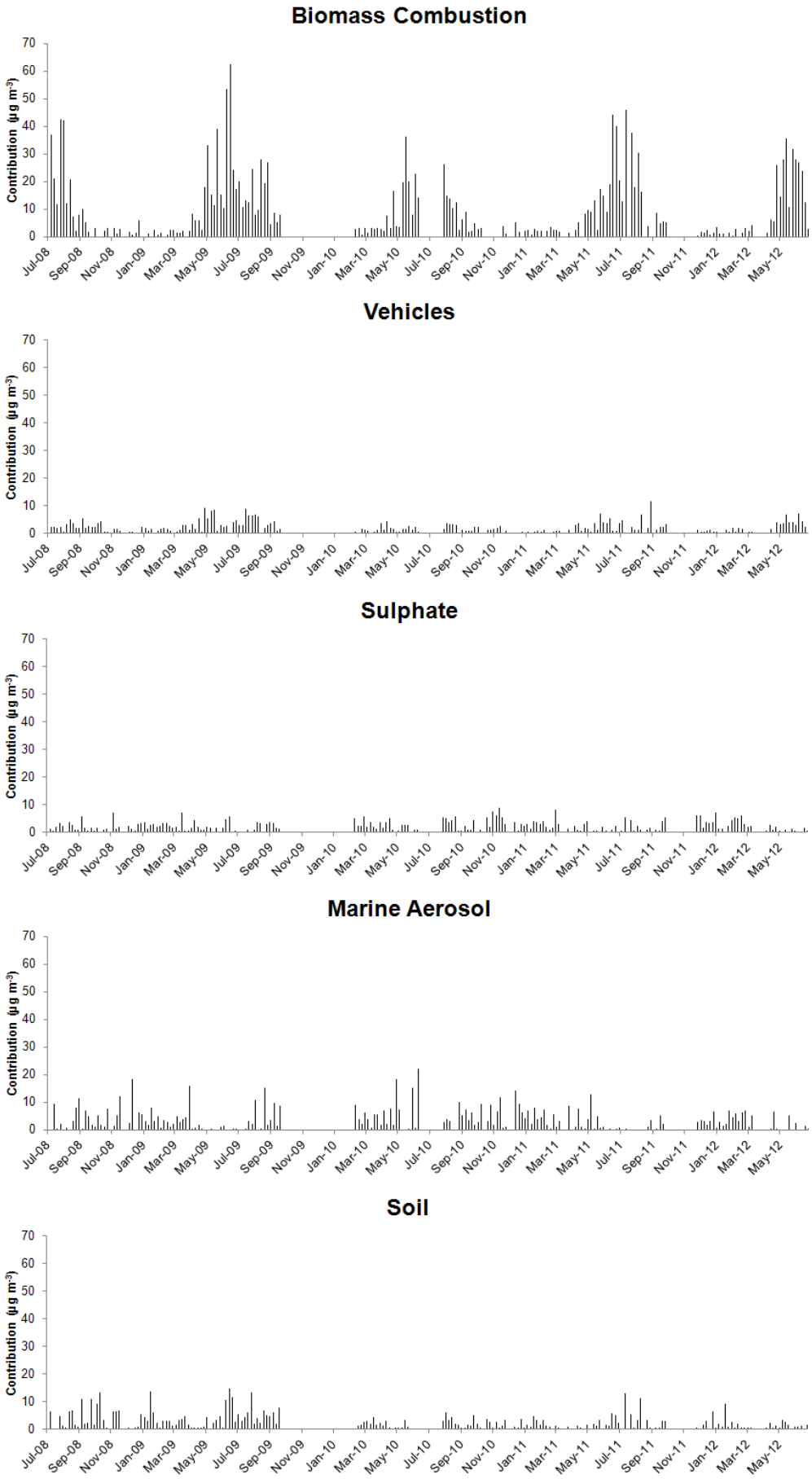

Figure 4.7 Temporal variations in relative source contributions to PM_{10} mass at St. Vincent Street.

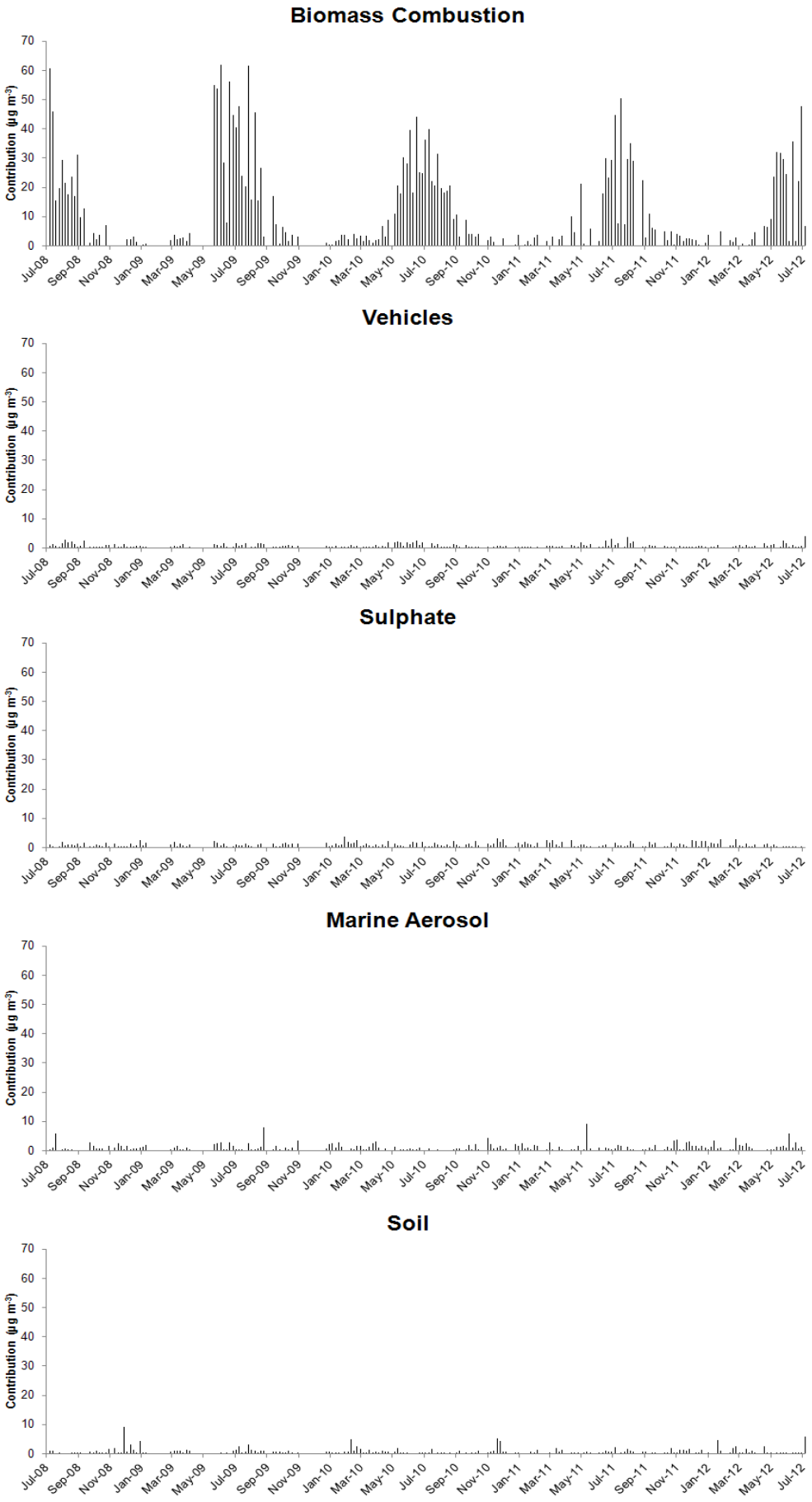

Figure 4.8 Temporal variations in relative source contributions to $PM_{2.5}$ mass at St. Vincent Street.

4.4 SEASONAL VARIATIONS IN PM_{10} AND $PM_{2.5}$ SOURCES

The primary source of PM_{10} and $PM_{2.5}$ during the winter (June–August) at St. Vincent Street was biomass combustion associated with solid fuel fire emissions for domestic heating. Little seasonal variation was apparent in the other $PM_{2.5}$ sources. The marine aerosol PM_{10} source showed some seasonality, with higher contributions during the spring and summer. Wintertime PM_{10} (32 µg m^{-3}) and $PM_{2.5}$ (31 µg m^{-3}) concentrations were also significantly higher than during other seasons. Figures 4.9 and 4.10 present seasonal variations in PM_{10} and $PM_{2.5}$ source contributions, respectively, identified using PMF.

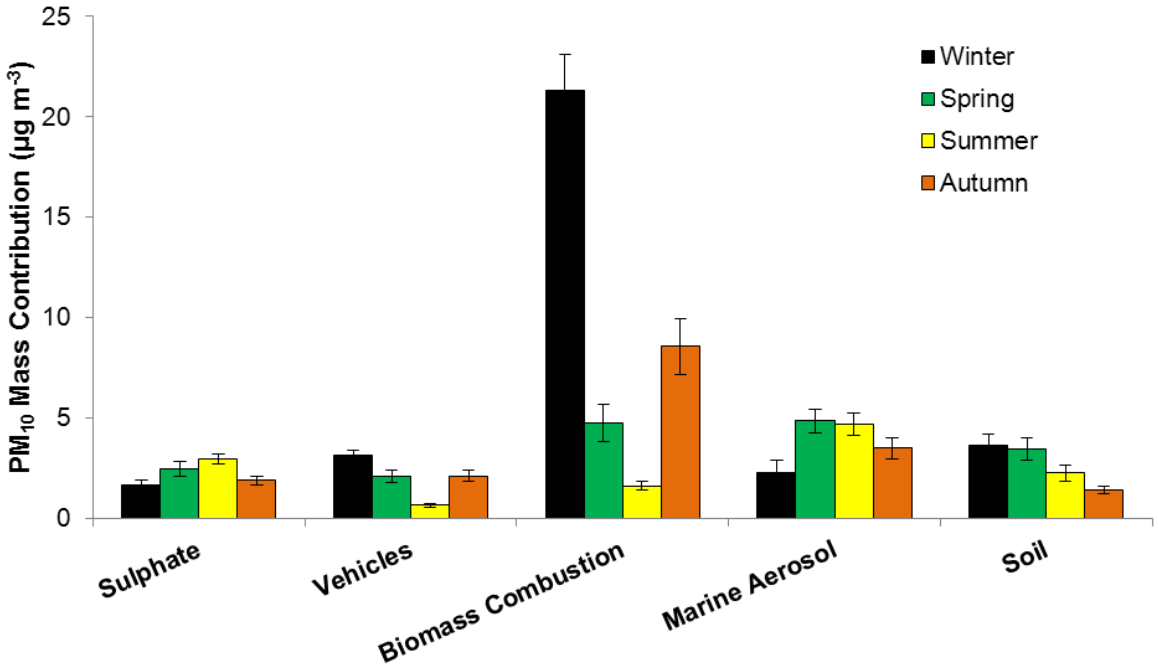

Figure 4.9 2008–2012 seasonal variations in PM_{10} source contributions at St. Vincent Street.

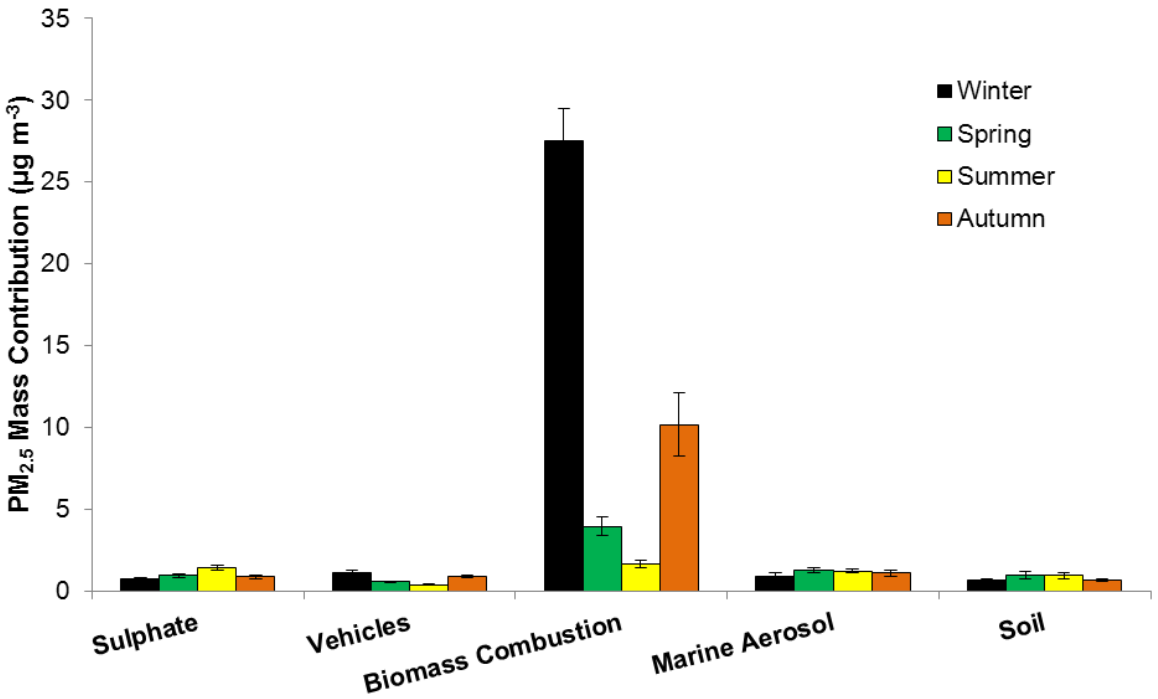

Figure 4.10 2008–2012 seasonal variations in $PM_{2.5}$ source contributions at St. Vincent Street.

4.5 WEEKEND AND WEEKDAY VARIATIONS IN PM_{10} AND $PM_{2.5}$ SOURCES AT ST. VINCENT STREET

Average mass contributions from 2008–2012 from the different sources were divided into weekday (136 PM_{10} and 138 $PM_{2.5}$) and weekend (53 PM_{10} and 60 $PM_{2.5}$) categories to examine any differences in relative contributions. Figures 4.11 and 4.12 present plots of weekday and weekend source mass contributions over the monitoring period.

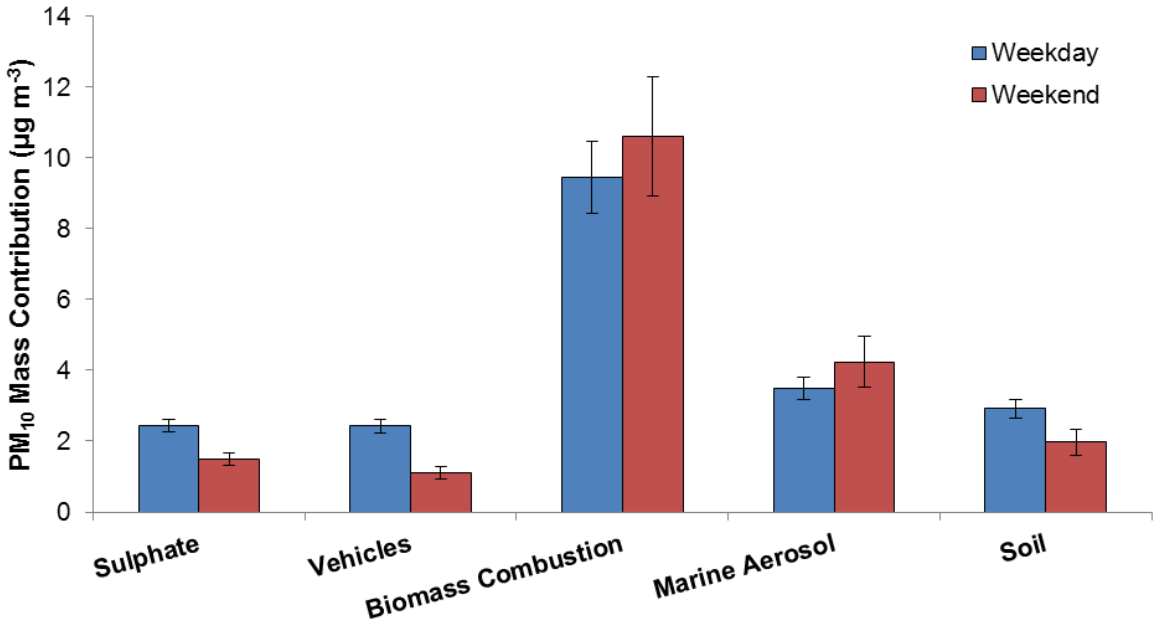

Figure 4.11 2008–2012 weekday/weekend variations in PM_{10} source contributions at St. Vincent Street.

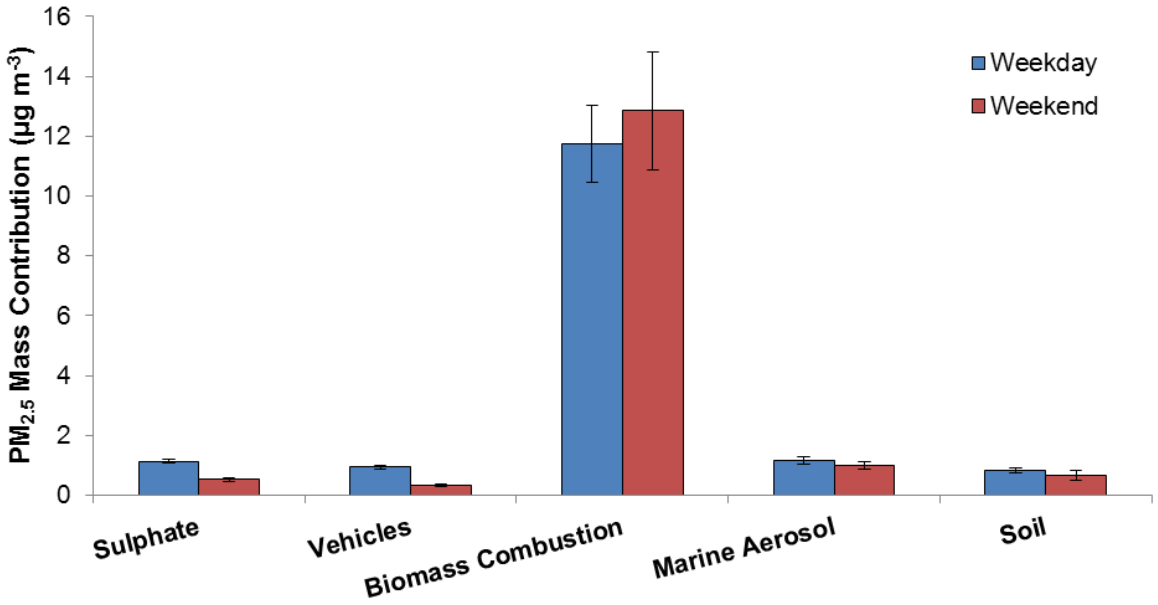

Figure 4.12 2008–2012 weekday/weekend variations in $PM_{2.5}$ source contributions at St. Vincent Street.

For PM_{10}, three sources showed significantly higher (no overlap in the standard errors of their calculated means) contributions during weekdays compared to weekends. The sources were vehicles, soil and secondary sulphate. In $PM_{2.5}$, vehicles and secondary sulphate had significantly higher concentrations during weekdays as well. Motor vehicle contributions

would be expected to be higher during weekdays because of commuter traffic with an associated increase in motor vehicle emissions. The higher weekday contribution from soil in PM_{10} suggests that re-entrainment by motor vehicles and/or local commercial activities such as construction or excavation could have an important influence on soil contributions. The cause for higher weekday contributions from secondary sulphate in PM_{10} and $PM_{2.5}$ is unclear, but could be related to shipping activity at the Port of Nelson. More work would be required to confirm this suggestion.

4.6 VARIATIONS IN PM_{10} AND $PM_{2.5}$ SOURCE CONTRIBUTIONS AT ST. VINCENT STREET WITH WIND DIRECTION

Bivariate polar plots using the source contributions to PM_{10} and $PM_{2.5}$ were produced using R statistical software and the openair package (Carslaw, 2012; Carslaw and Ropkins, 2012; Team, 2011). Using bivariate polar plots, source contributions can be shown as a function of both wind speed and direction, providing invaluable information about potential source regions and how pollution from a specific source builds up. To produce the polar plots, wind speeds and directions were vector averaged using functions available in openair. A full description of the vector averaging process can be found in Carslaw (2012).

4.6.1 Biomass combustion

Biomass combustion source contributions to PM_{10} and $PM_{2.5}$ are considered to be primarily from domestic solid fuel fire emissions. Figures 4.13 and 4.14 present bivariate polar plots of biomass combustion contributions to PM_{10} and $PM_{2.5}$, respectively. Figures 4.13 and 4.14 show that peak biomass combustion contributions occurred under low wind speeds (< 1 m s^{-1}) from the southwest, in line with the downhill slope of the valley in which the sampling site is located. This indicates that katabatic flows under cold and calm anticyclonic synoptic meteorological conditions coupled with domestic fire emissions and poor dispersion were responsible for elevated particle concentrations at the St. Vincent Street site, similar to previous results in other New Zealand locations (Ancelet et al., 2012; Ancelet et al., 2013b). Such meteorological conditions can reasonably be anticipated one or two days ahead of time so that it can be used as a predictor of high concentrations of particulate matter pollution due to domestic fires or to issue warnings of an air pollution risk.

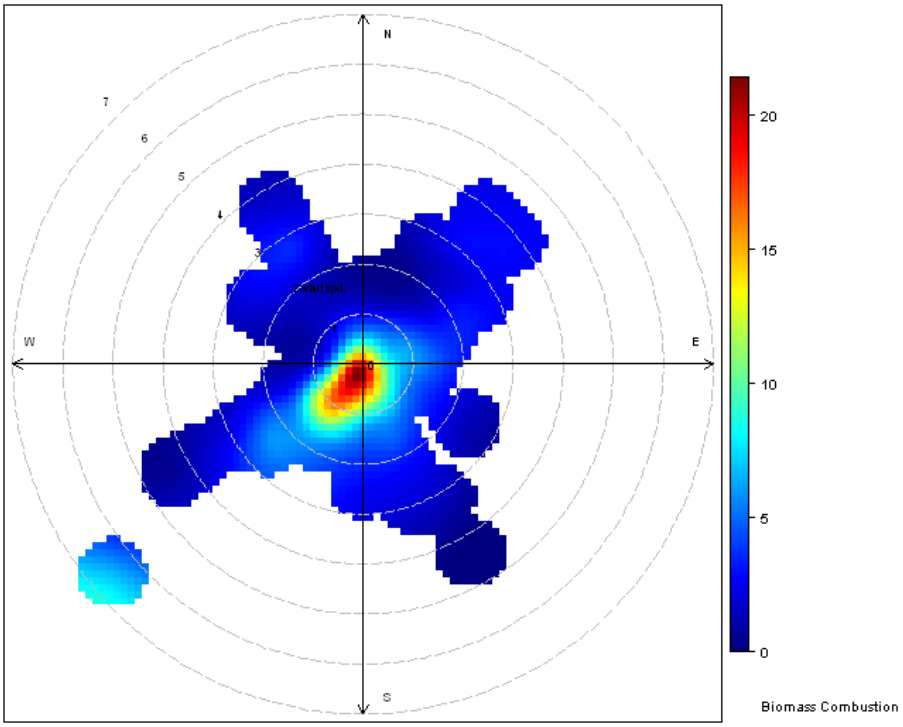

Figure 4.13 Polar plot of biomass combustion contributions to PM_{10} concentrations at St. Vincent Street. The radial dimensions indicate the wind speed in 1 m s^{-1} increments and the color contours indicate the average contribution to each wind direction/speed bin.

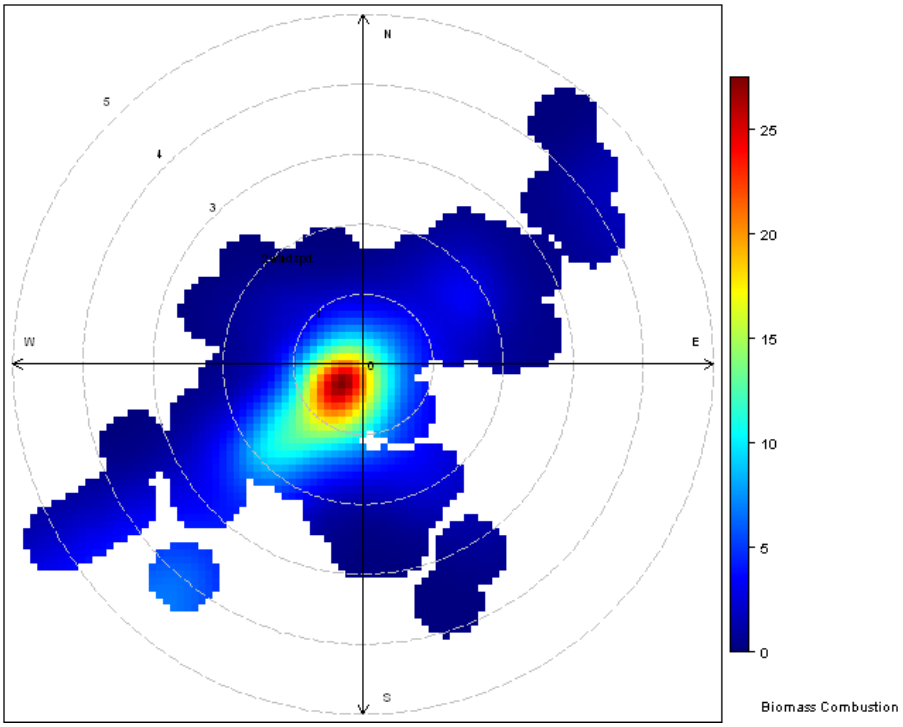

Figure 4.14 Polar plot of biomass combustion contributions to $PM_{2.5}$ concentrations at St. Vincent Street. The radial dimensions indicate the wind speed in 1 m s^{-1} increments and the color contours indicate the average contribution to each wind direction/speed bin.

4.6.2 Vehicles

The motor vehicle source for PM_{10} showed southwest directionality, as shown in Figure 4.15, with peak concentrations occurring under high wind speeds (> 6 m s^{-1}). Motor vehicle $PM_{2.5}$ contributions also showed southwest directionality, but peaked under low wind speeds. Vehicle contributions from the Nelson CBD north of the site were probably responsible for the low wind speed northerly component in the $PM_{2.5}$ polar plot.

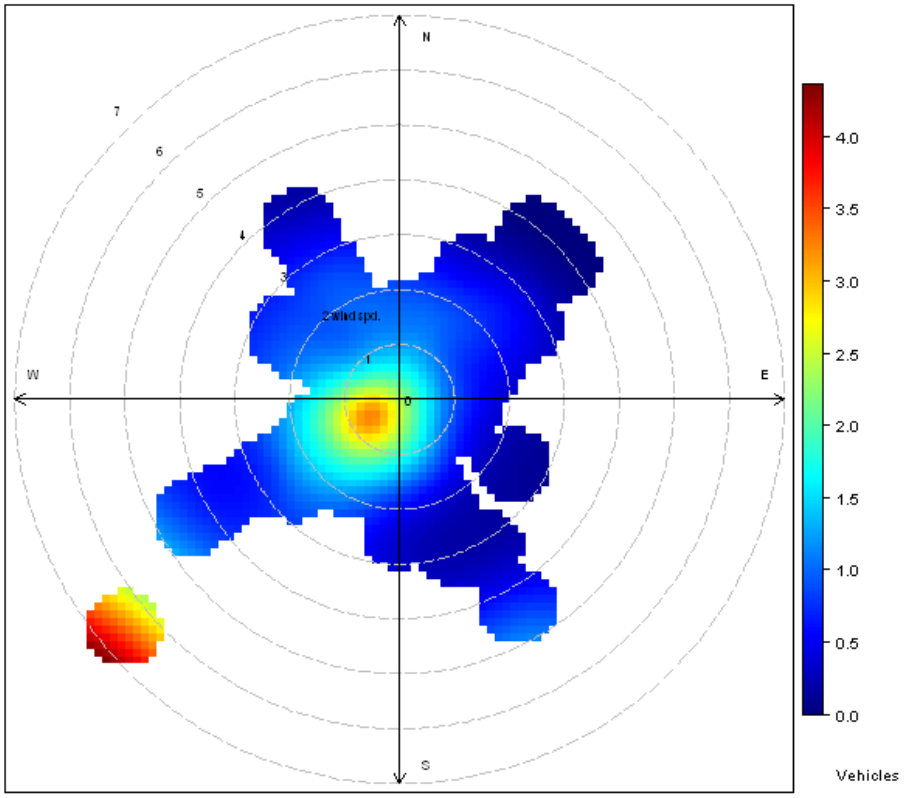

Figure 4.15 Polar plot of vehicle contributions to PM_{10} concentrations at St. Vincent Street. The radial dimensions indicate the wind speed in 1 m s^{-1} increments and the color contours indicate the average contribution to each wind direction/speed bin.

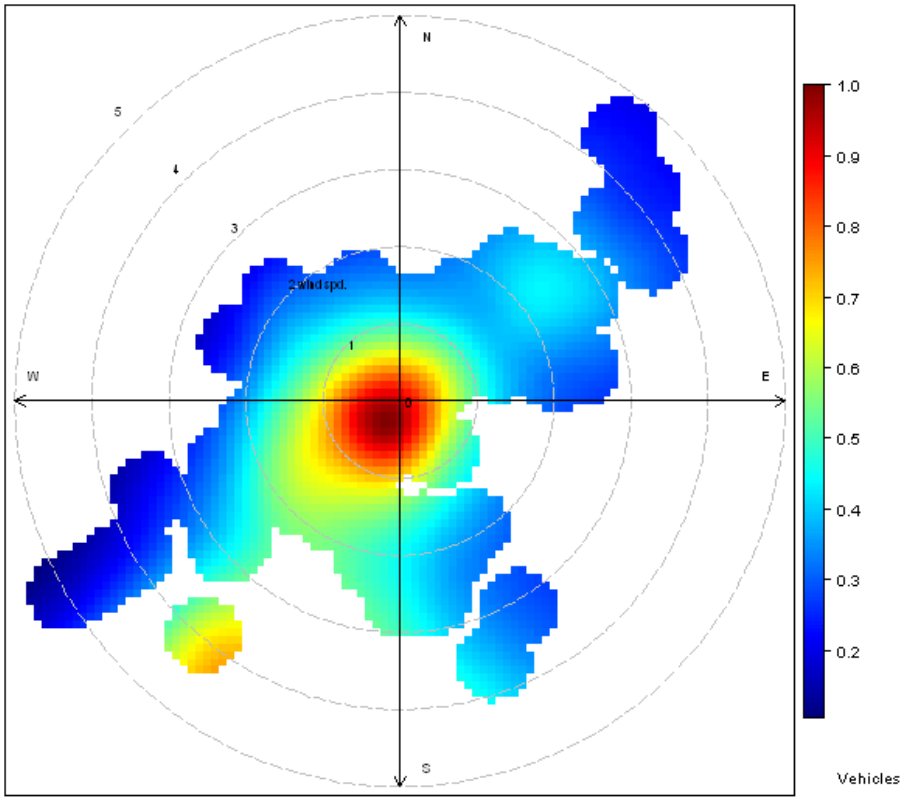

Figure 4.16 Polar plot of vehicle contributions to $PM_{2.5}$ concentrations at St. Vincent Street. The radial dimensions indicate the wind speed in 1 m s^{-1} increments and the color contours indicate the average contribution to each wind direction/speed bin.

4.6.3 Sulphate

The PM_{10} and $PM_{2.5}$ secondary sulphate contributions mostly originated from the north, towards the Port of Nelson. High secondary sulphate contributions from the southwest under high wind speeds for PM_{10} were also apparent.

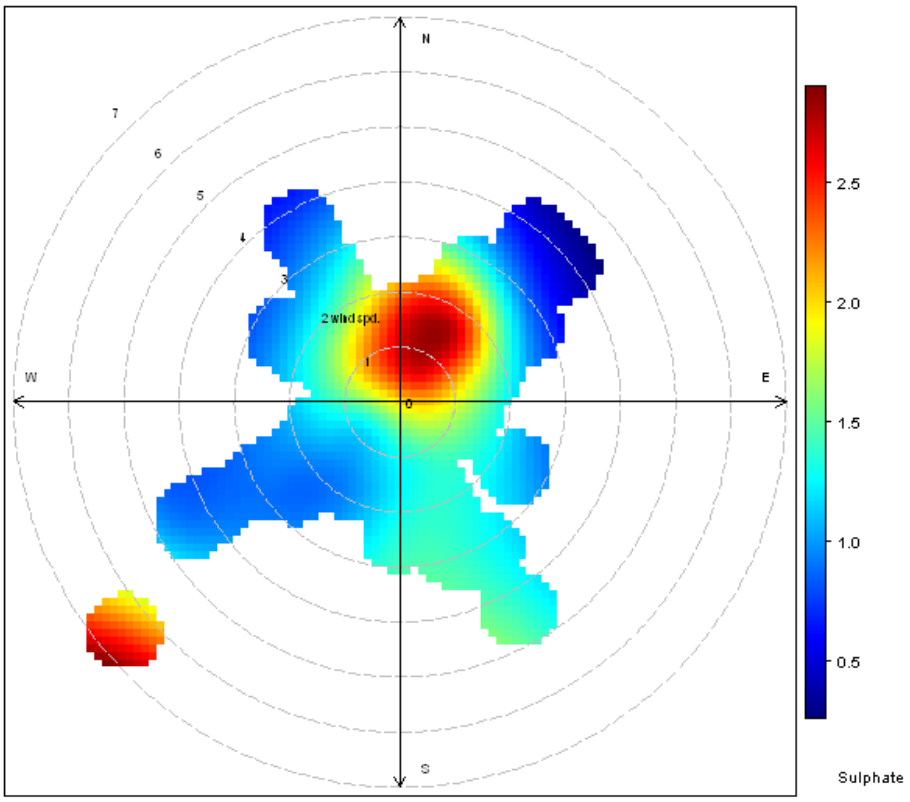

Figure 4.17 Polar plot of sulphate contributions to PM_{10} concentrations at St. Vincent Street. The radial dimensions indicate the wind speed in 1 m s^{-1} increments and the color contours indicate the average contribution to each wind direction/speed bin.

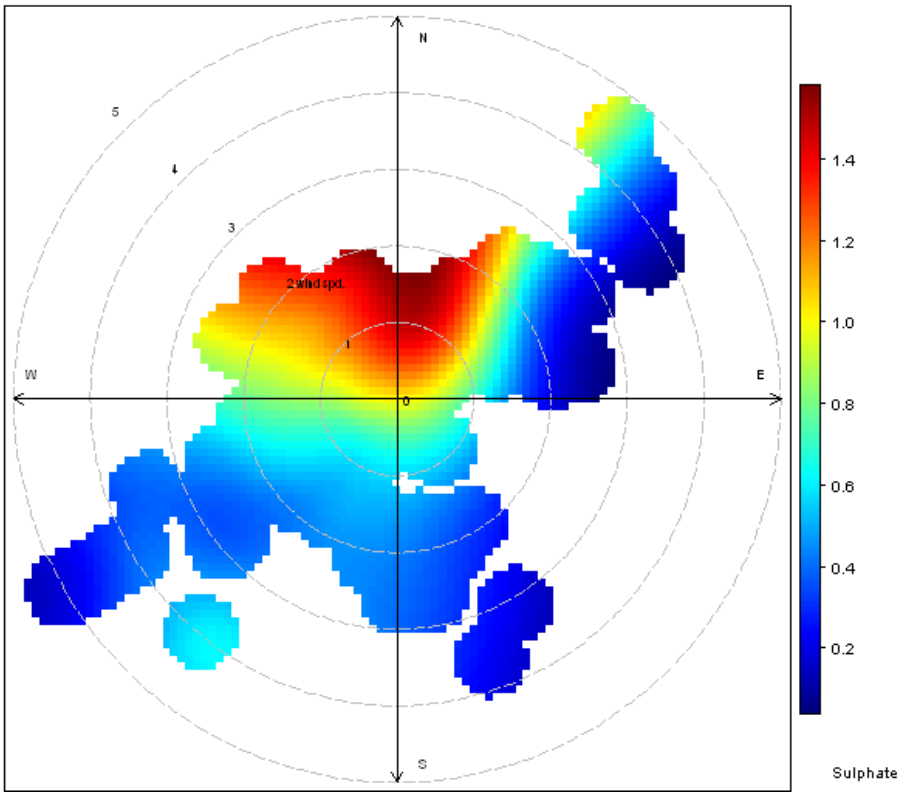

Figure 4.18 Polar plot of sulphate contributions to $PM_{2.5}$ concentrations at St. Vincent Street. The radial dimensions indicate the wind speed in 1 m s^{-1} increments and the color contours indicate the average contribution to each wind direction/speed bin.

4.6.4 Marine aerosol

The PM_{10} marine aerosol contributions largely originated from the northeast and northwest (Figure 4.19), while $PM_{2.5}$ marine aerosol contributions originated from the northeast (Figure 4.20). As expected, marine aerosol contributions increased under higher wind speeds. The most likely sources of marine aerosol were the Tasman Sea and Southern Ocean.

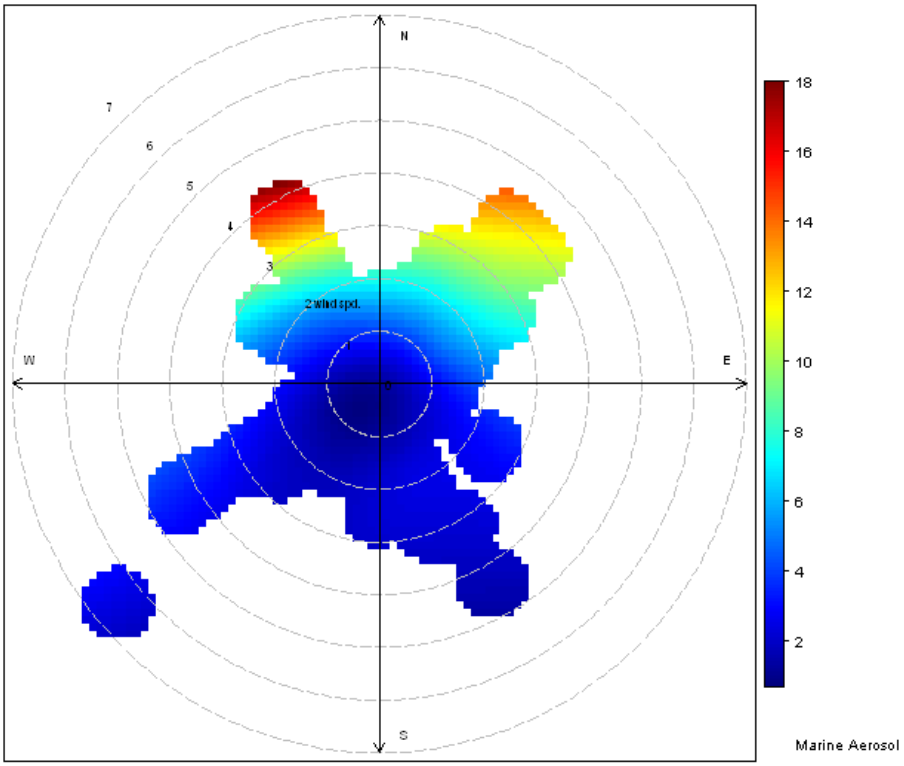

Figure 4.19 Polar plot of marine aerosol contributions to PM_{10} concentrations at St. Vincent Street. The radial dimensions indicate the wind speed in 1 m s^{-1} increments and the color contours indicate the average contribution to each wind direction/speed bin.

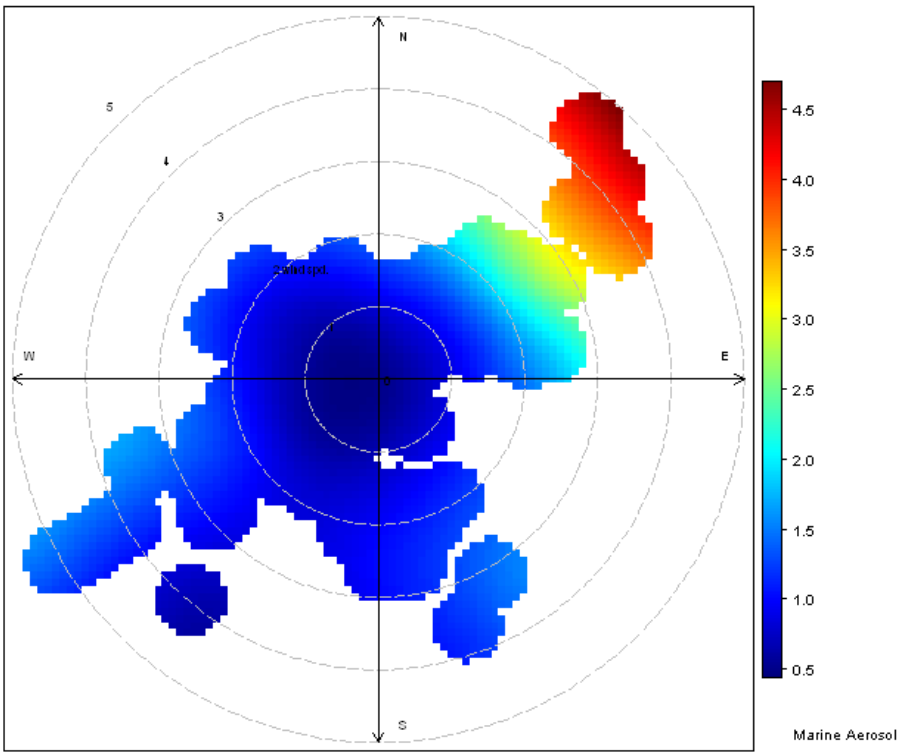

Figure 4.20 Polar plot of marine aerosol contributions to $PM_{2.5}$ concentrations at St. Vincent Street. The radial dimensions indicate the wind speed in 1 m s^{-1} increments and the color contours indicate the average contribution to each wind direction/speed bin.

4.6.5 Soil

Soil contributions to PM_{10} largely originated from the southeast under high wind speeds (> 5 m s^{-1}) (Figure 4.21), while $PM_{2.5}$ contributions originated to the west of the St. Vincent Street site (Figure 4.22). From Figure 4.22, it is likely that $PM_{2.5}$ soil contributions are influenced by the action of high wind speeds, local dust generating activities or the turbulent passage of vehicles along local roads or unsealed yards.

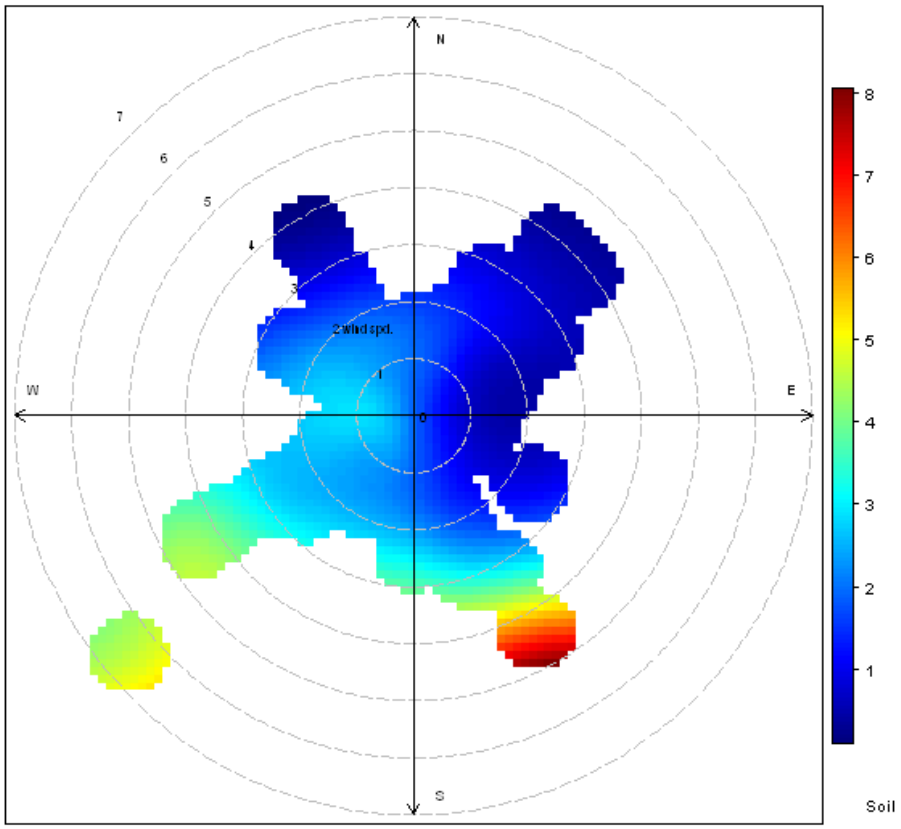

Figure 4.21 Polar plot of soil contributions to PM_{10} concentrations at St. Vincent Street. The radial dimensions indicate the wind speed in 1 m s^{-1} increments and the color contours indicate the average contribution to each wind direction/speed bin.

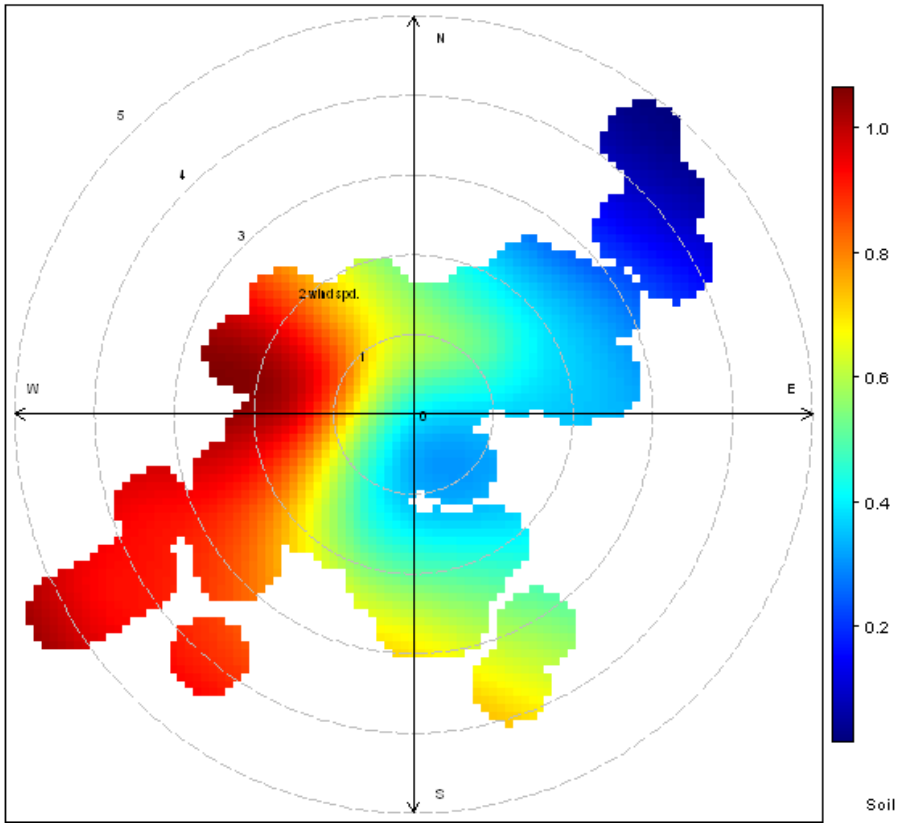

Figure 4.22 Polar plot of soil contributions to $PM_{2.5}$ concentrations at St. Vincent Street. The radial dimensions indicate the wind speed in 1 m s^{-1} increments and the color contours indicate the average contribution to each wind direction/speed bin.

5.0 DISCUSSION OF THE ST. VINCENT STREET PM_{10} RECEPTOR MODELING RESULTS

Monitoring of PM_{10} and $PM_{2.5}$ at St. Vincent Street shows that concentrations of both size fractions peak during the winter and that the NES for PM_{10} is exceeded on several occasions each winter. Five source contributors to PM_{10} and $PM_{2.5}$ at St. Vincent Street were identified from receptor modeling. The receptor modeling analyses show that some source contributors have distinct seasonalities and that PM_{10} and $PM_{2.5}$ concentrations at St. Vincent Street are primarily influenced by local emission sources.

5.1 SOURCES OF PM_{10} AND $PM_{2.5}$ AT ST. VINCENT STREET

5.1.1 Biomass combustion

Temporal and seasonal trends show that PM_{10} and $PM_{2.5}$ from biomass combustion emissions peaked during the winter at St. Vincent Street, as shown in Figures 5.1 and 5.2. Biomass combustion can therefore be considered to be primarily from the emissions of solid fuel fires used for home heating during the winter.

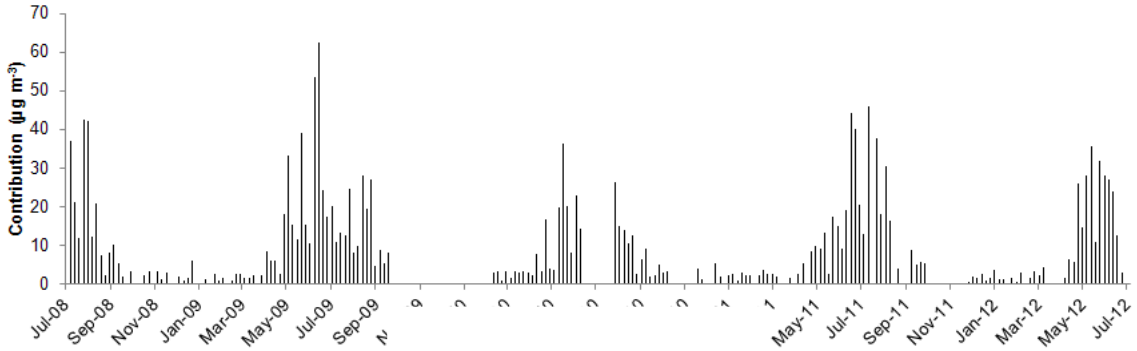

Figure 5.1 Biomass combustion source contributions to PM_{10} at St. Vincent Street.

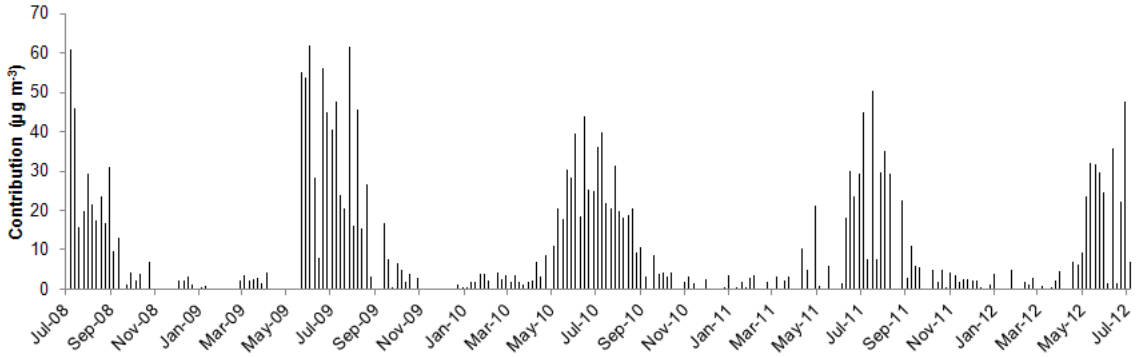

Figure 5.2 Biomass combustion source contributions to $PM_{2.5}$ at St. Vincent Street.

The results indicate that biomass combustion is the emission source responsible for peak PM_{10} and $PM_{2.5}$ concentrations, and for consequent exceedances of the NES. Further discussion on peak events is provided in Section 5.2.

5.1.2 Motor vehicles

Emissions from motor vehicles were found to be minor contributors to PM_{10} and $PM_{2.5}$ concentrations. The temporal and seasonal variations show that the lowest motor vehicle

contributions occurred during the summer, likely because of increased dispersion during the warmer months from convective turbulence and sea breezes. Analysis of polar plots using vehicle contributions to PM_{10} and $PM_{2.5}$ indicated that peak vehicle contributions occurred from the southwest, the most predominant wind direction aligning with the direction of the valley in which the St. Vincent Street site is located. Some influence from the Nelson CBD is also evident based on the analysis of source strengths with wind direction, as indicated in the $PM_{2.5}$ polar plot for motor vehicles.

5.1.3 Sulphate

The PM_{10} and $PM_{2.5}$ secondary sulphate source showed no strong seasonal pattern. Analysis of the sulphate source contributions using polar plots showed that sulphate was transported from north of the sampling site. Sources of secondary sulphate include emissions from shipping activities in the port area (Davy et al., 2008). Longer range sources include marine phytoplankton activity (release of dimethyl sulphide as a gaseous precursor to secondary sulphate) and potentially and emissions of SO_2 gas from the Central Plateau volcanic zone (Davy et al., 2009b). The average secondary sulphate source contribution (2.13 µg m^{-3}) to PM_{10} at St. Vincent Street was higher than for Wellington (1.2 µg m^{-3} at both Seaview and Wainuiomata) and for six Auckland sites (1.3–1.5 µg m^{-3}) suggesting that there was some localised emission source. The average secondary sulphate contribution to $PM_{2.5}$ (1.0 µg m^{-3}) was much closer to those reported for Wellington and Auckland sites. Further discussion of secondary sulphate sources is provided in Chapter 6.

5.1.4 Marine aerosol

The elemental composition for the marine aerosol source closely resembled that of seawater and the source profile is dominated by chlorine and sodium, as shown in Figure 4.3 and 4.4. Analysis of temporal and seasonal variations in marine aerosol showed higher concentrations during spring and summer, indicating that the generation of marine aerosol is dependent on meteorological factors, such as wind and evaporation potential. Analysis of marine aerosol contributions to PM_{10} and $PM_{2.5}$ concentrations showed distinct northeasterly directionality, with some contribution from the northwest for PM_{10}. Interestingly the average marine aerosol contribution to PM_{10} at St. Vincent Street (3.6 µg m^{-3}) was lower than those found for Wainuiomata (5.9 µg m^{-3}) and Seaview (6.3 µg m^{-3}) in Wellington (Davy et al., 2009a; Davy et al., 2008) and at six Auckland sites (6–7 µg m^{-3}) (Davy et al., 2009b). The lower marine aerosol concentrations at St. Vincent Street may reflect a sheltering effect of the surrounding mountain ranges and somewhat calmer meteorological conditions in Nelson. The average marine aerosol contribution to $PM_{2.5}$ concentrations was lower (1 µg m^{-3}) than that for PM_{10} because of the dominance of coarse ($PM_{10-2.5}$) particles in the marine aerosol size distribution.

5.1.5 Soil

The PM_{10} and $PM_{2.5}$ soil source originates from airborne crustal matter particles with coarse particles dominating the size range. Soil particles can be generated by wind action or disturbance of surface dusts by motor vehicles, road works or construction activities. At St. Vincent Street, wind action on bare soil, unsealed yards or the turbulent passage of vehicles on local roads are the most likely sources of crustal matter particles. Seasonal patterns were evident for PM_{10} and $PM_{2.5}$ crustal matter source contributions, with higher contributions during spring and summer because of dryer and windier meteorological conditions.

5.2 ANALYSIS OF CONTRIBUTIONS TO PM_{10} AND $PM_{2.5}$ ON PEAK DAYS

For air quality management purposes, contributions from the various sources to peak PM_{10} events are of most interest. Therefore, the mass contributions of sources to all PM_{10} concentrations over 33 µg m^{-3} (the Ministry for the Environment 'Alert' level as discussed in Section 2.1) are presented in Figure 5.3. It should be noted that the concentrations presented in Figure 5.3 are those from the PMF results. To select concentrations above the 'Alert' level, actual PM_{10} concentrations measured by NCC were used.

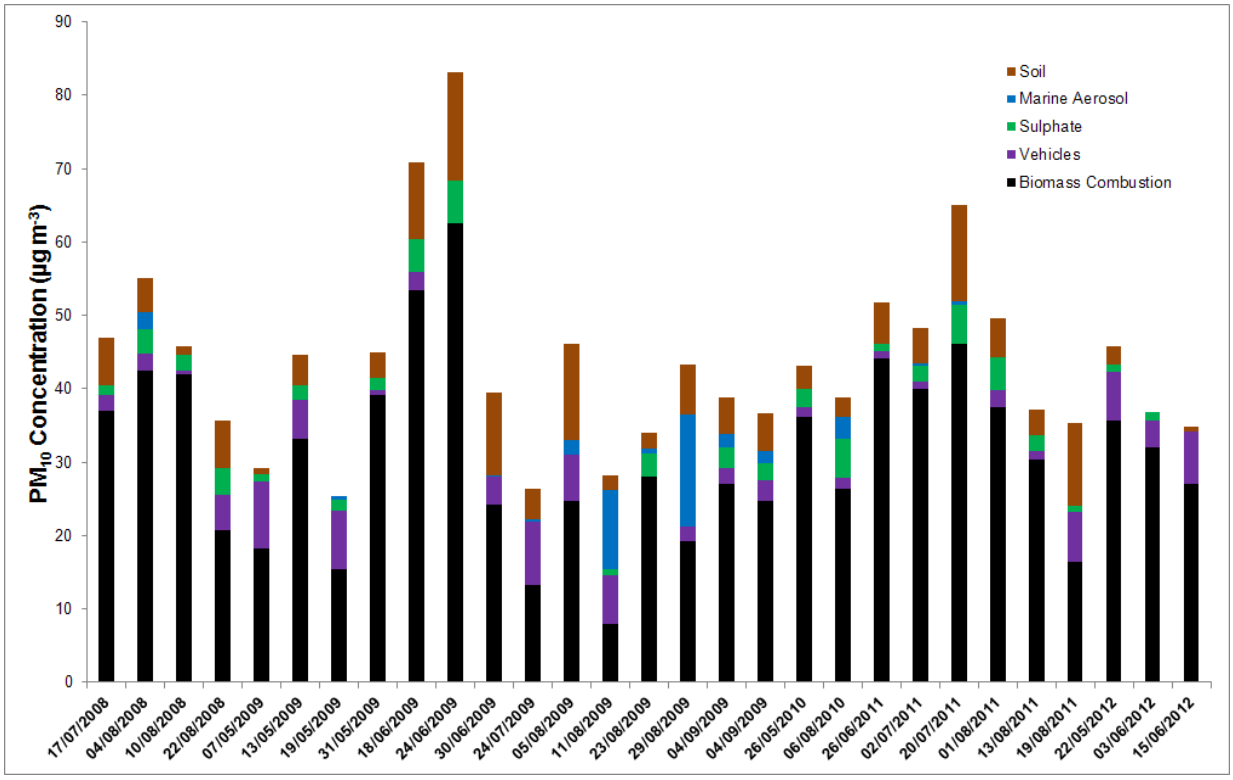

Figure 5.3 Mass contributions to peak PM_{10} events (> 33 µg m^{-3}) at St. Vincent Street.

Figure 5.3 shows that peak PM_{10} events occurred primarily during autumn and winter, and that biomass combustion was responsible for an average of 70 % of PM_{10} mass on high pollution days. On four days, biomass combustion was responsible for more than 90 % (contributing up to 93 %) of PM_{10} mass. There are several days where other, primarily coarse particle sources (marine aerosol, crustal matter), have a significant influence on PM_{10} concentrations, but none contributed sufficient PM_{10} concentrations on their own to result in an exceedance of the NES. It is likely that domestic fire emissions will continue to be primarily responsible for NES exceedances out to the 2020 full compliance date.

In a similar fashion, mass contributions of sources to all $PM_{2.5}$ concentrations over 17 µg m^{-3} ('Alert level) are presented in Figure 5.4. Two items of note are readily apparent from Figure 5.4. First, biomass combustion is the most significant source responsible for elevated $PM_{2.5}$ concentrations. Second, significantly more 'Alert' events are apparent for $PM_{2.5}$ concentrations. This is perhaps not surprising, given that biomass combustion (a fine particle source) dominates PM_{10} concentrations as well, but does highlight that if a $PM_{2.5}$ standard is introduced in New Zealand, the St. Vincent Street site in Nelson would have some difficulty complying with the standard. This is highlighted even more so by the fact that the St. Vincent Street monitoring site exceeded the New Zealand ambient air quality guideline for $PM_{2.5}$ 48 times during the course of this study (note that this is based only on a 1-day-in-6 sampling

regime and therefore, the true number is likely to be six times this value; ie. the $PM_{2.5}$ NZAAQG would have been exceeded 300 times over 4 years).

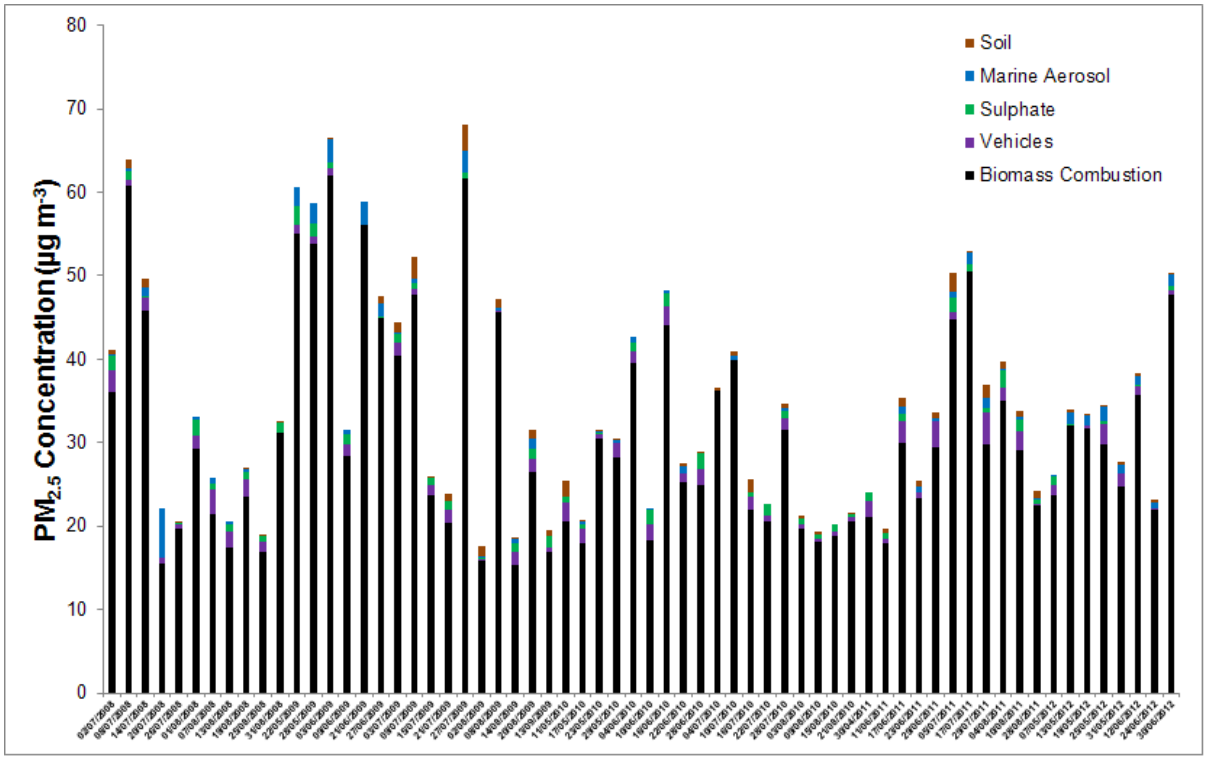

Figure 5.4 Mass contributions to peak $PM_{2.5}$ events (> 17 µg m^{-3}) at St. Vincent Street.

6.0 HOURLY PARTICULATE MATTER STUDY

During the 2011 winter, an intensive PM monitoring campaign was undertaken in Nelson Airshed A that incorporated the St. Vincent Street site. The aim of the campaign was to identify the sources and factors contributing to measured PM concentrations on an hourly time-scale. The results of this study have been used for the production of a manuscript that has been submitted to the international journal *Urban Climate*. This chapter reports the results of the hourly PM sampling campaign as they have been prepared in the manuscript. Overviews of the techniques used and information about the monitoring sites have also been included for clarity.

6.1 INTRODUCTION

We have recently reported the first PM source apportionment study using hourly data obtained from two sampling sites in the rural community of Masterton, New Zealand (Ancelet et al., 2012). A similar study undertaken in Alexandra has also been reported (Ancelet et al., 2013a). In the current study, hourly coarse ($PM_{10-2.5}$) and fine ($PM_{2.5}$) samples were collected from four sites in Nelson and were analyzed for elemental content and black carbon (BC). Hourly PM_{10} concentrations were determined using continuous PM_{10} (BAM) monitors and positive matrix factorization (PMF) was used to determine the PM sources and their contributions on an hourly time-scale at each site using the hourly elemental, BC and PM_{10} data

Using hourly source contributions and meteorological data from each of the sites, potential PM transport mechanisms were also identified. High-temporal resolution source apportionment studies can provide unique and highly relevant information for the implementation of PM mitigation strategies.

6.2 EXPERIMENTAL

6.2.1 Sample collection

Ambient air monitoring was conducted at four locations in an urban valley in Nelson. Three of the sites were located along the general katabatic flow pathway (upwind, central and downwind). The fourth site (Aloft) was located alongside the central site, but was raised to a height of 26 m above the ground level site using a knuckleboom (when wind conditions permitted). This type of experimental setup has recently been reported (Ancelet et al., 2013a), and Figure 6.1 presents a schematic illustration of the sampling site locations. The sampling site locations were designed to provide an indication of PM transport horizontally and vertically within the Nelson South airshed.

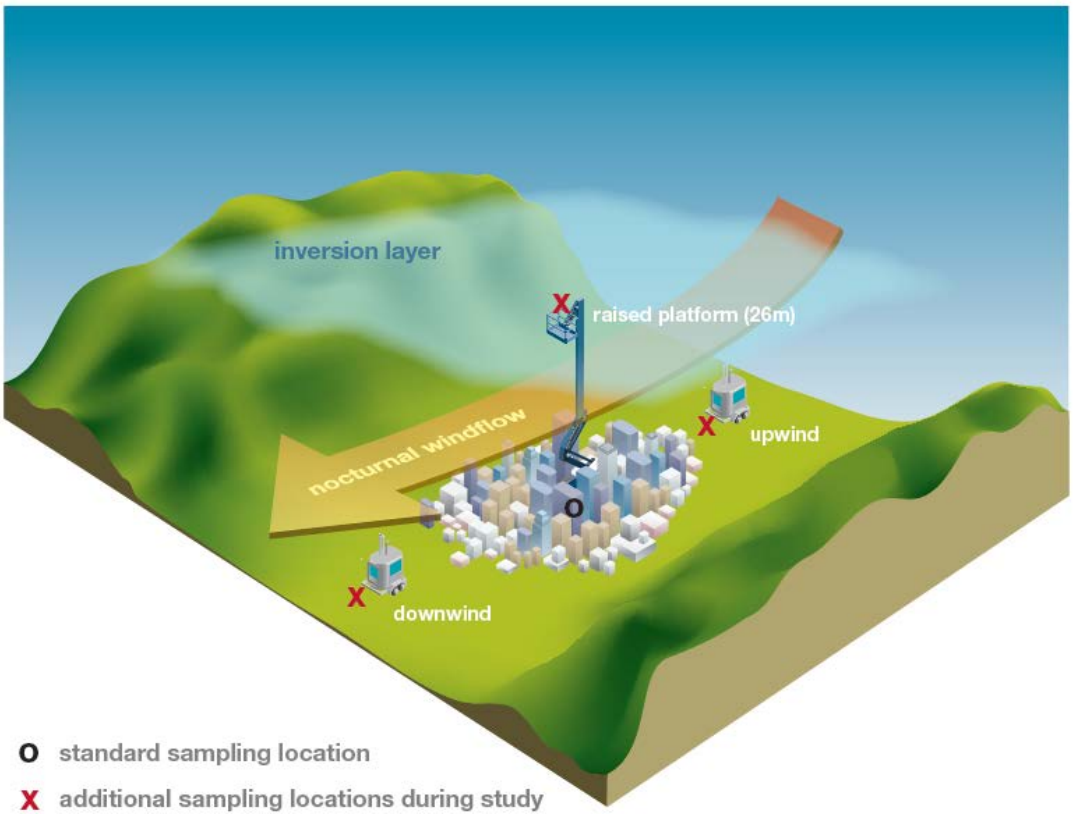

Figure 6.1 Schematic illustration of the sampling site locations in Nelson Airshed A.

The upwind site was located on the grounds of the Nelson Intermediate School (NIS) (latitude –41.172266°, longitude 173.260500°). The NIS site was situated approximately 1.4 km southwest of the central site and 90 m from the nearest road. The central (NCC) and elevated (Aloft) sites were co-located with a Nelson City Council ambient air quality monitoring station used for compliance monitoring (latitude –41.164150°, latitude 173.162447°) and were approximately 90 m from the nearest road. The downwind site was located within the Nelson Fire Station compound (NFS) (latitude –41.162241°, longitude 173.164400°) and was approximately 600 m north of the NCC site and 60 m from the nearest road. The land around each of the sites was flat and surrounded by open space or buildings no more than two stories high. Figure 6.2 presents the locations of each of the sampling sites.

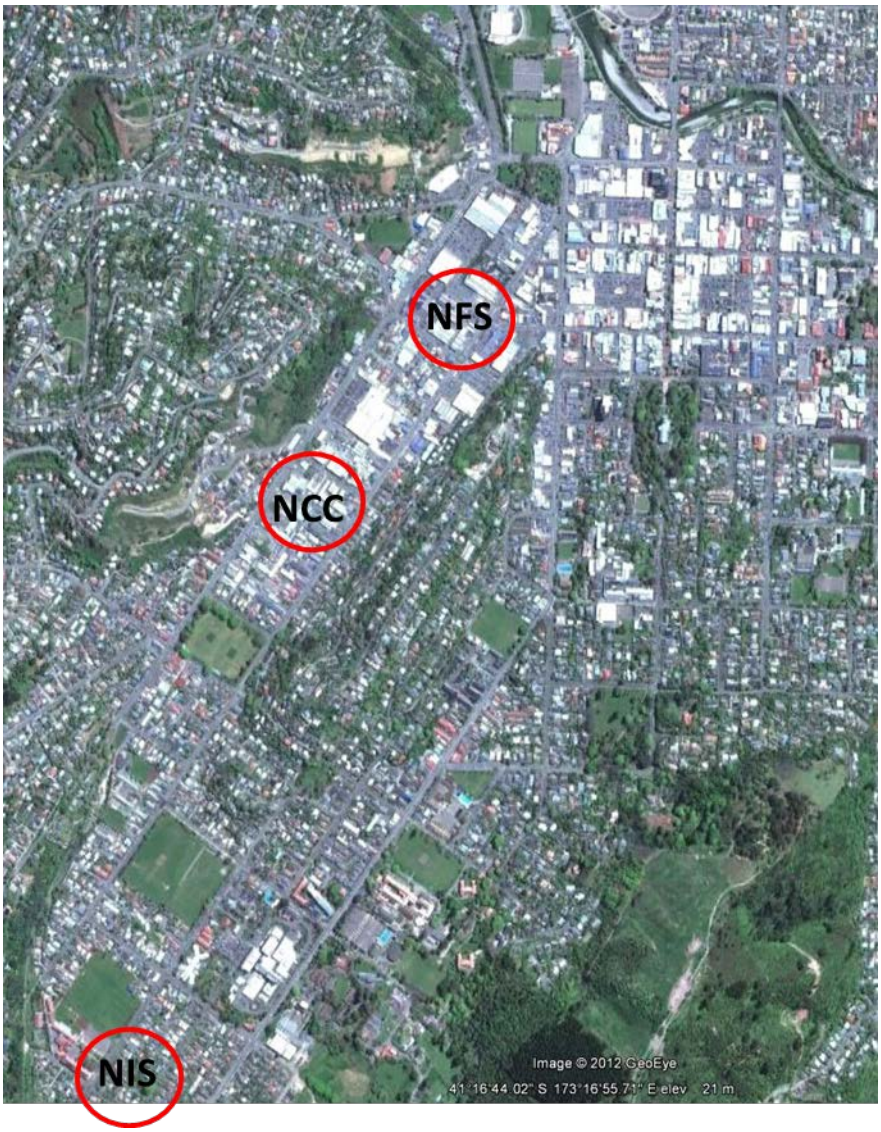

Figure 6.2 Locations of the sampling sites within Nelson (NIS: Nelson Intermediate School; NCC: Nelson City Council; NFS: Nelson Fire Station). The Aloft site was co-located with the NCC site.

Each site was equipped with a Streaker sampler (PIXE International Corporation, USA), an E-BAM (Met One Instruments, Inc.) and a meteorological station (Vaisala WXT520) in the same fashion as previously reported (Ancelet et al., 2012). In this study, a total of 47 samples, or 47 hours, were collected on each set of size-resolved ($PM_{10–2.5}$ and $PM_{2.5}$) filters. The monitoring program ran from June–August 2011 and a total of 6896 samples were collected among the four sites (2162 from NIS, 2068 from NCC, 1632 from NFS and 1034 (414 when raised to 26 m) from the Aloft site). Differences in the number of samples collected at each site were the result of equipment failures.

6.2.2 Elemental analysis

Ion beam analysis (IBA) was used to measure the concentrations of elements with atomic numbers above neon in the PM collected. IBA measurements were carried out at the New Zealand Ion Beam Analysis Facility operated by the Institute of Geological and Nuclear Sciences (GNS) in Gracefield, Lower Hutt, New Zealand (Trompetter et al., 2005). Further details on the IBA techniques used, analytical uncertainties and limits of detection have been reported previously (Ancelet et al., 2012). Black carbon was measured using a M43D Digital Smoke Stain Reflectometer (Ancelet et al., 2011). Prior to the PMF analyses, data and

uncertainty matrices were prepared for each site in the same manner as previous studies (Polissar et al., 1998; Song et al., 2001).

6.2.3 Receptor modeling

Receptor modeling and apportionment of PM mass by PMF was performed using the EPAPMF version 3.0.2.2 program in accordance with the User's Guide (USEPA, 2008). With PMF, sources are constrained to have non-negative species concentrations, no sample can have a negative source contribution and error estimates for each observed point are used as point-by-point weights. This is a distinct advantage of PMF, since it can accommodate missing or below detection limit data that is a common feature of environmental monitoring (Song et al., 2001). Data screening and the source apportionment were performed in the same manner as previously reported (Ancelet et al., 2012).

6.3 RESULTS AND DISCUSSION

6.3.1 PM_{10} concentrations

PM_{10} concentrations at each of the sites displayed distinct diurnal cycles. Figure 6.3(a) presents the average hourly PM_{10} concentrations at the NIS, NCC and NFS sites over the entire sampling period. A number of features are apparent from Figure 6.3(a). First, the diurnal profiles of the three sites are very similar, with peak PM_{10} concentrations occurring between 7–11 pm and 9–10 am. Second, PM_{10} concentrations at each of the sites decreased in similar fashions, suggesting a common PM sink or dispersion mechanism among the sites. Finally, hourly PM_{10} concentrations during peak hours at NCC were higher than at NIS and NFS.

Figure 6.3(b) presents the average hourly PM_{10} concentrations at the NCC and Aloft sites during periods when the knuckleboom was raised (212 hours total). Since the knuckleboom was only raised when wind speeds were low (during anticyclonic atmospheric conditions), PM_{10} concentrations measured at the NCC site were higher than during periods when the knuckleboom was not raised. Average hourly PM_{10} concentrations at both sites featured peak PM_{10} concentrations occurring between 8 pm–midnight. A small morning peak (8 am) in PM_{10} concentrations at the Aloft site was apparent, while the NCC site featured a much larger morning peak in PM_{10} concentrations between 9–10 am. The higher concentrations measured, particularly during the morning, at the ground level NCC site indicated the formation of a shallow inversion layer that limited the vertical dispersion of PM_{10}. Supporting this conclusion, average wind speeds and air temperatures at the Aloft site were higher than at the ground-based NCC site during hours with peak PM_{10} concentrations. A separate study in Nelson during the same time period also found a similar phenomenon (Grange et al., 2013).

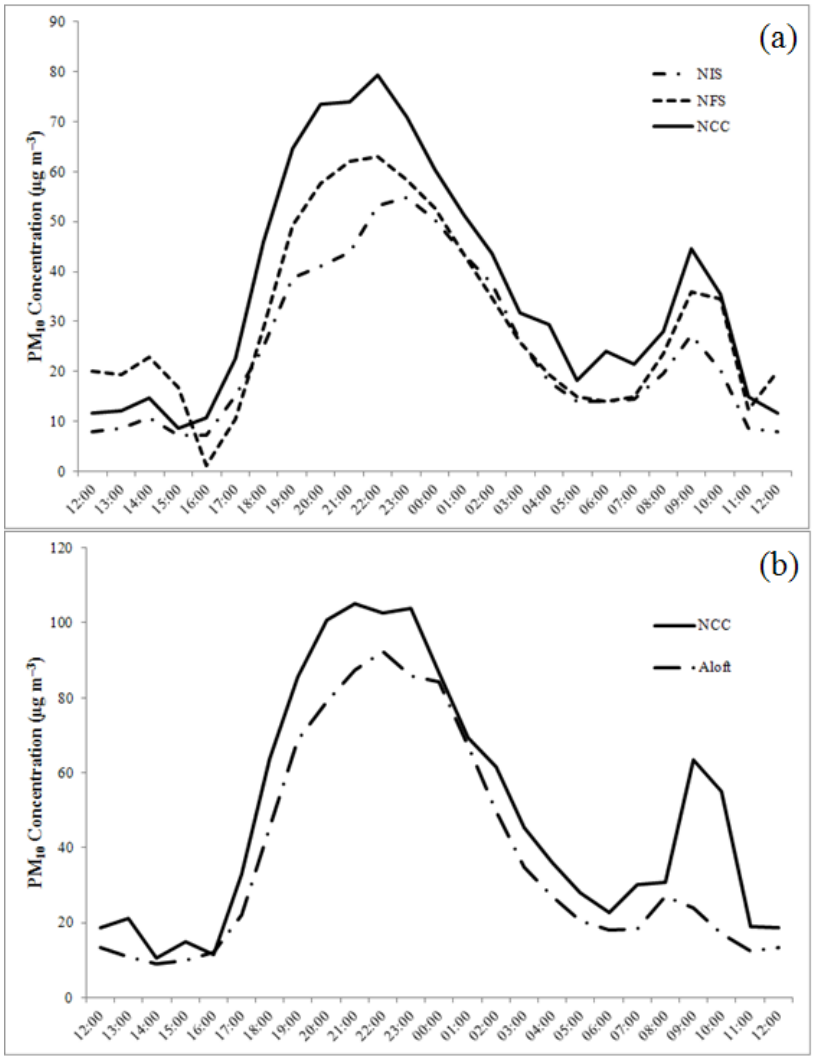

Figure 6.3 Average hourly PM_{10} concentrations at (a) the Nelson Intermediate School, Nelson City Council and Nelson Fire Station sites and (b) at the Nelson City Council and Aloft sites during periods when the knuckleboom was raised.

Comparisons of daily average PM_{10} concentrations among the four sites revealed that NIS did not exceed the New Zealand NES for PM_{10} of 50 µg m^{-3} on any day during the study period, while the NFS, Aloft and NCC sites had 5, 2 and 15 exceedances, respectively, during this study. It is important to note that E-BAMs are not certified for air quality compliance monitoring, but it is clear that the sampling location, both horizontally and vertically, can have a significant impact on measured PM_{10} concentrations in Nelson.

The local meteorology in Nelson was investigated on an hourly basis to gain a better understanding of PM transport. Figure 6.4 presents a wind rose plot over the entire sampling period from NCC. Wind rose plots for the other sites were nearly identical to that from NCC. Figure 6.4 shows that winds during the sampling period were predominantly from the southwest, with smaller contributions from the northeast, in line with the direction of the valley.

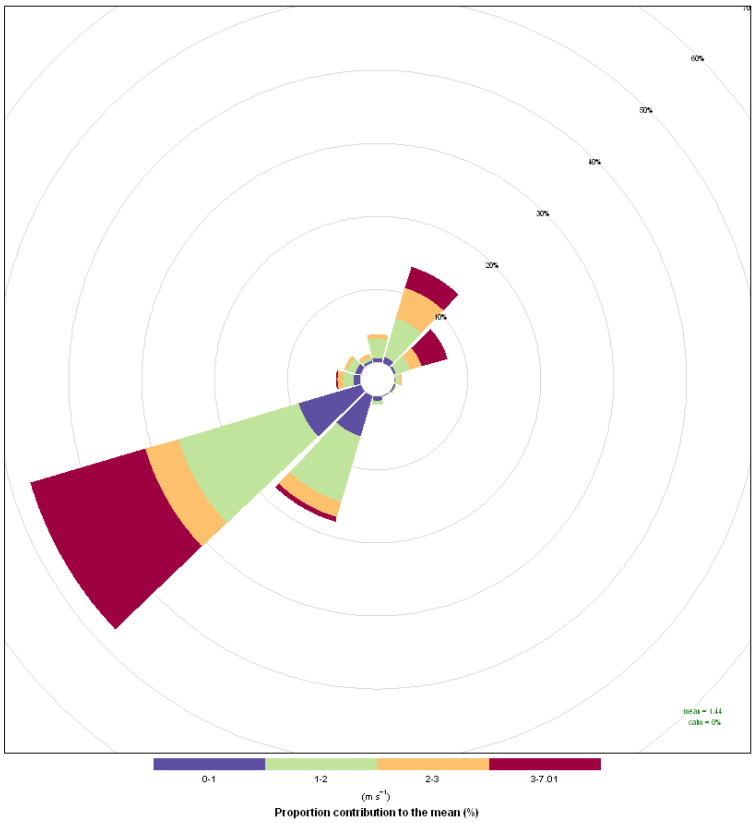

Figure 6.4 Wind rose plots over the entire sampling period from the Nelson City Council site. The radial dimensions indicate the frequency (%) of winds from each direction.

Using the high temporal resolution data available in this study, hourly pollution roses for each of the sites were developed using R statistical software and the openair package (Carslaw, 2012; Carslaw and Ropkins, 2012; Team, 2011). Figure 6.5 presents hourly PM_{10} pollution roses for the NCC site. Figure 6.5 suggests that the elevated PM_{10} concentrations measured at NCC were the result of the transport of PM_{10} by katabatic flows from the southwest along the downslope contour of the valley. According to this mechanism, it would be expected that PM_{10} concentrations at the NFS site, which was further downwind than the NCC site, would be the highest of all the sites. From Figure 6.3(a) it is clear that this is not the case. We suggest that this results from both the urban valley opening up just before the NFS site, allowing for more effective dispersion conditions that result in lower PM_{10} concentrations and a reduction in the number of local emission sources as largely residential areas turn into commercial areas near the NFS site.

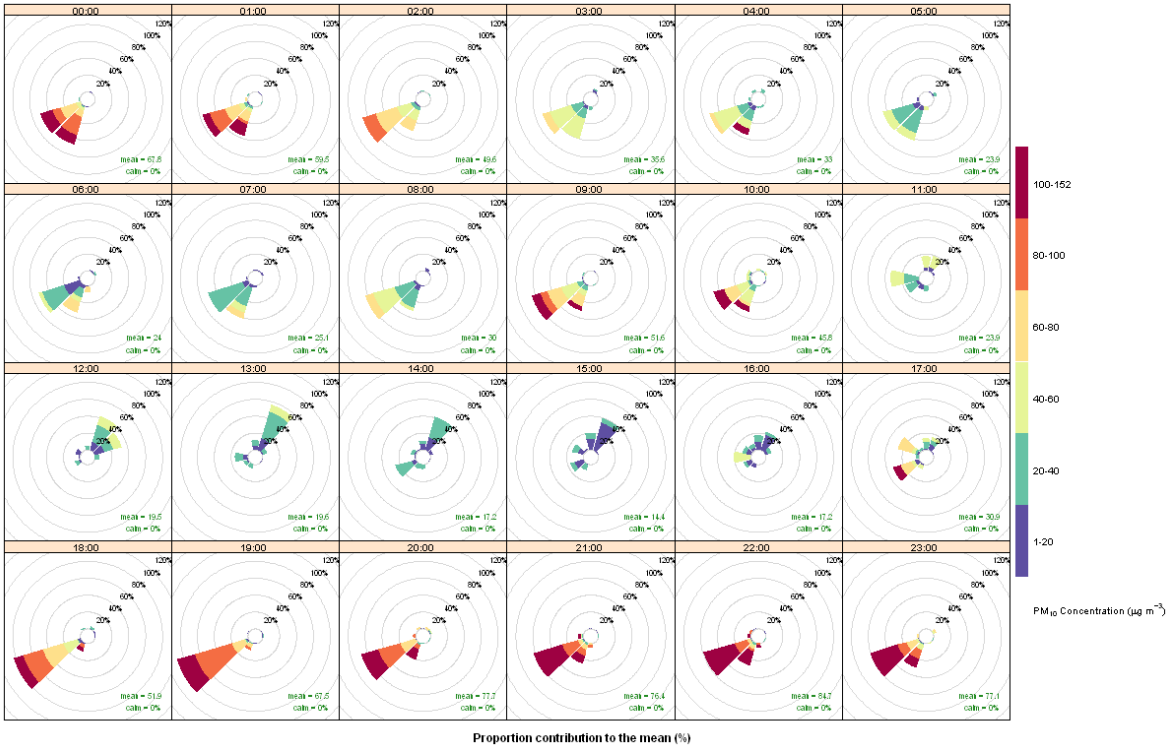

Figure 6.5 Hourly pollution roses from the Nelson City Council site (produced using the Openair package (Carlslaw and Ropkins, 2011)) indicating wind directions contributing the most to average hourly PM_{10} concentrations. The radial dimensions indicate the percentage of the total pollution that arrives from each wind sector during each one-hour period.

6.3.2 Sources of ambient PM_{10}

Reconstructed masses (RCMs) determined using the elemental PM data accounted for 19, 21, 19 and 18% of the PM_{10} mass at the NIS, NCC, NFS and Aloft sites, respectively (Malm et al., 1994). Because numerous species, including organic carbon (OC) were not quantified and shipping sulphate was not accounted for, the relatively low RCMs are not surprising. Fine ($PM_{2.5}$) Al and Si were quantified, but the values were not used because the filters, used as received, were unevenly contaminated with Al and Si, so a background correction could not be performed without unintentionally affecting species variance within the dataset. Marine aerosol (a source featuring little contribution from unmeasured species) RCMs were close to those identified from PMF.

The application of PMF to hourly elemental data from each of the sites revealed five PM_{10} sources at each of the sites. The source profiles obtained for NCC are presented in Figure 6.6 and are representative of the source profiles obtained at the other three sites. The error bars shown in the source profiles indicate standard deviations determined from bootstrapping in the EPAPMF program. Limitations in the bootstrapping technique have previously been discussed (Ancelet et al., 2012).

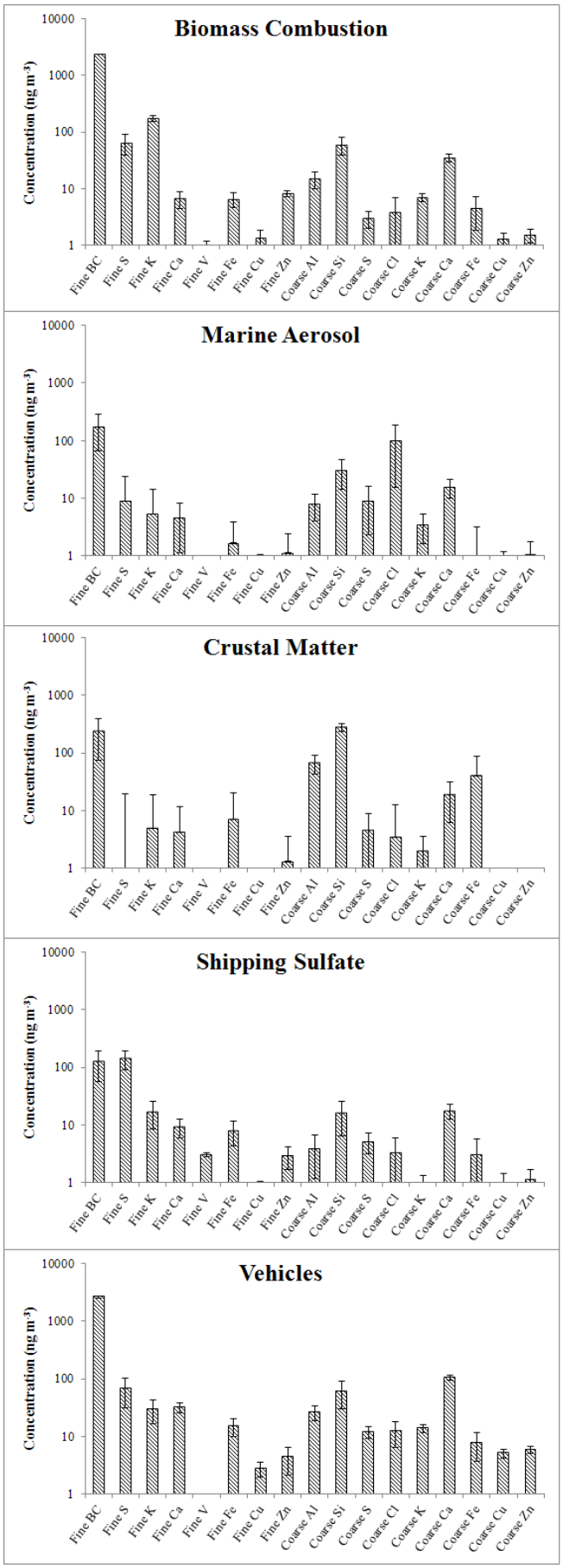

Figure 6.6 Source profiles obtained at the St. Vincent Street site.

The sources presented in Figure 6.6 were found to explain 97, 96, 98 and 98% of the PM_{10} mass measured by the E-BAMS at NIS, NCC, NFS and Aloft, respectively, after regression using PM_{10} concentrations. Factor one contributed to 86, 87, 89 and 85% of the PM_{10} mass at NIS, NCC, NFS and Aloft, respectively. It was identified as a biomass combustion source because of high BC and fine K loadings. Potassium is usually used alongside BC as a marker for biomass burning, and wood combustion in particular (Fine et al., 2002; Khalil and Rasmussen, 2003).

Factor two accounted for 9, 3, 5 and 8% of the PM_{10} mass at NIS, NCC, NFS and Aloft, respectively. This factor was characterised as a vehicular source, which included vehicular exhaust and non-exhaust emissions, such as road dust and brake wear. Road dust is generated by the turbulent passage of vehicles over local roads and the source profiles feature crustal elements (Al and Si) enriched with BC, Ca and Fe. The vehicle source profiles reported here are consistent with those reported previously (Garg et al., 2000; Schauer et al., 2006). Black carbon in the vehicle profiles can be associated with exhaust emissions, deposited tailpipe emissions and the abrasion of tar-sealed surfaces. Iron and copper are typically present in brake wear dust (Thorpe and Harrison, 2008).

The third factor was characterised as marine aerosol because of high Cl concentrations. The marine aerosol contribution to PM_{10} concentrations was 1, 2, 1 and 2% at NIS, NCC, NFS and Aloft, respectively. Marine aerosol is a common component in PM_{10} throughout New Zealand. The fourth factor was characterized as residual oil combustion based on the presence of S and V in the source profile (Ault et al., 2009; Kim and Hopke, 2008; Qin et al., 2006). This source contribution likely resulted from shipping traffic at the Port of Nelson (discussed further in section 6.3.3), and was therefore termed shipping sulfate. Shipping sulphate contributed 1, 3, 4 and 4% to PM_{10} concentrations at NIS, NCC, NFS and Aloft, respectively. The low shipping sulphate contribution at NIS is not surprising, since it was the furthest away from the port. Prior to this study, shipping had not been identified as a potential source of PM_{10}, and is therefore never accounted for in local emission inventories. These results indicate that emissions from ship traffic at the port constitute a significant portion of measured PM_{10} and should be accounted for in future emissions inventories.

The fifth factor was identified as crustal matter based on the presence of Al, Si, K, Ca and Fe in the source profile. Crustal matter accounted for 3, 5, 1 and 1% of the PM_{10} mass at NIS, NCC, NFS and Aloft, respectively.

The average hourly source contributions at each site were calculated to assess variations in source contributions on an hourly time-scale. Figure 6.7 presents the average hourly source contributions at NCC and Figures 6.8, 6.9 and 6.10 present the average hourly source contributions at NIS, NFS and Aloft, respectively.

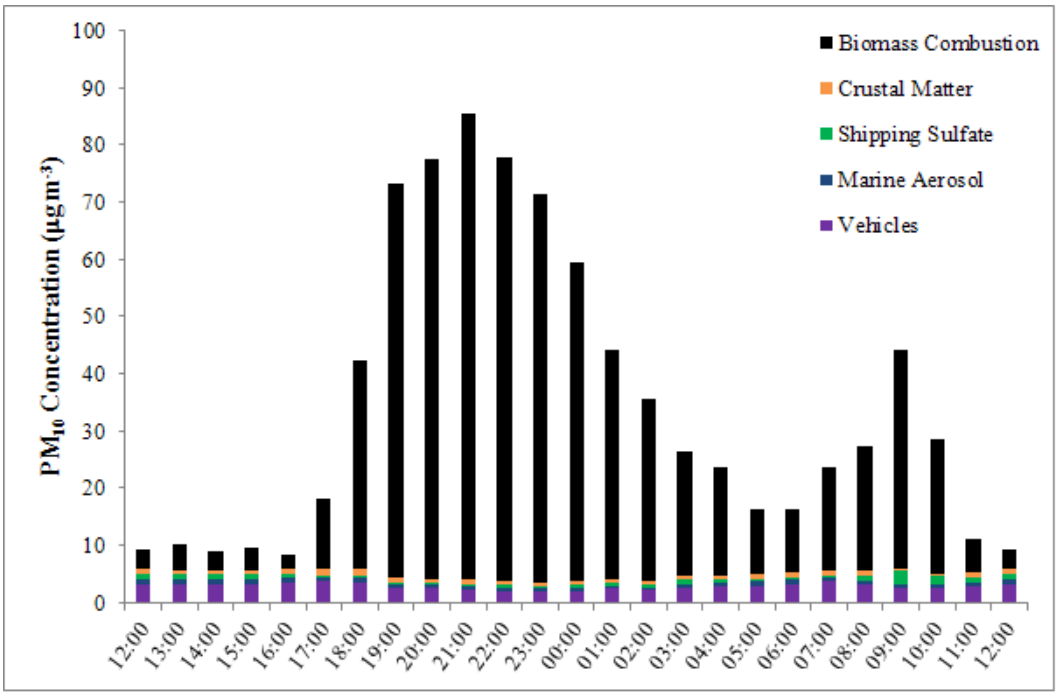

Figure 6.7 Average hourly source contributions at the St. Vincent Street site.

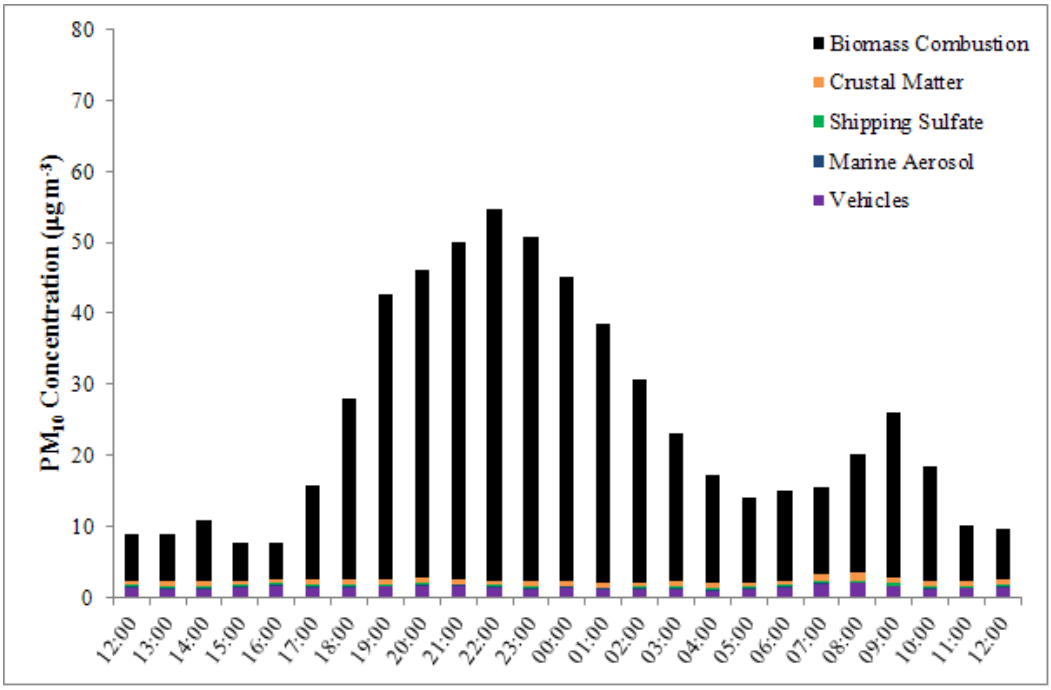

Figure 6.8 Average hourly source contributions at the Nelson Intermediate School site.

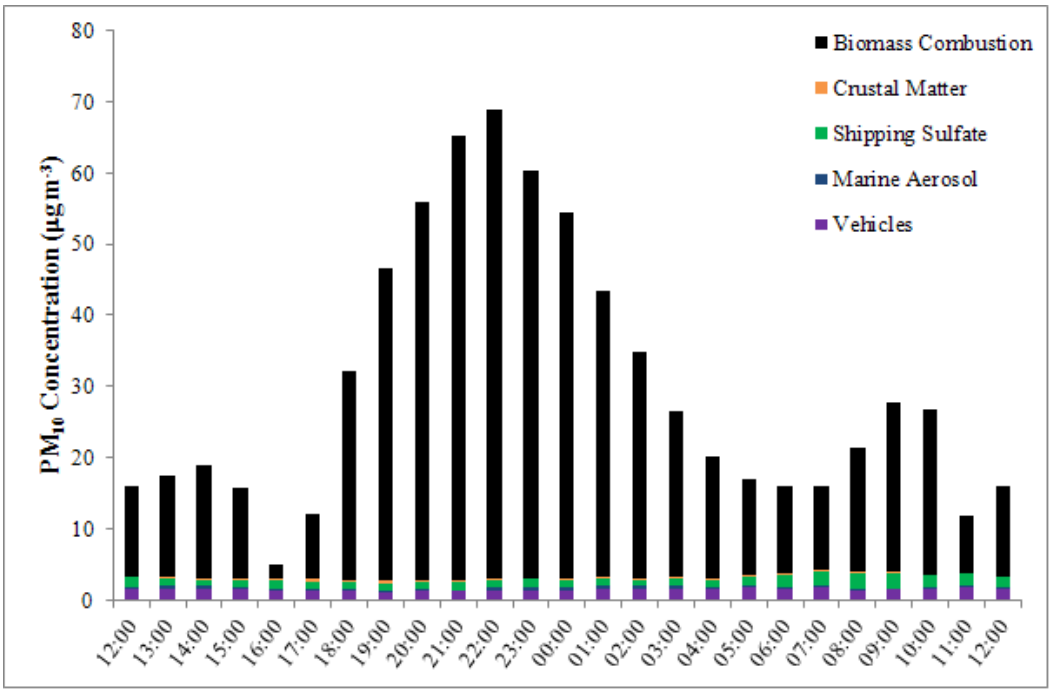

Figure 6.9 Average hourly source contributions at the Nelson Fire Station site.

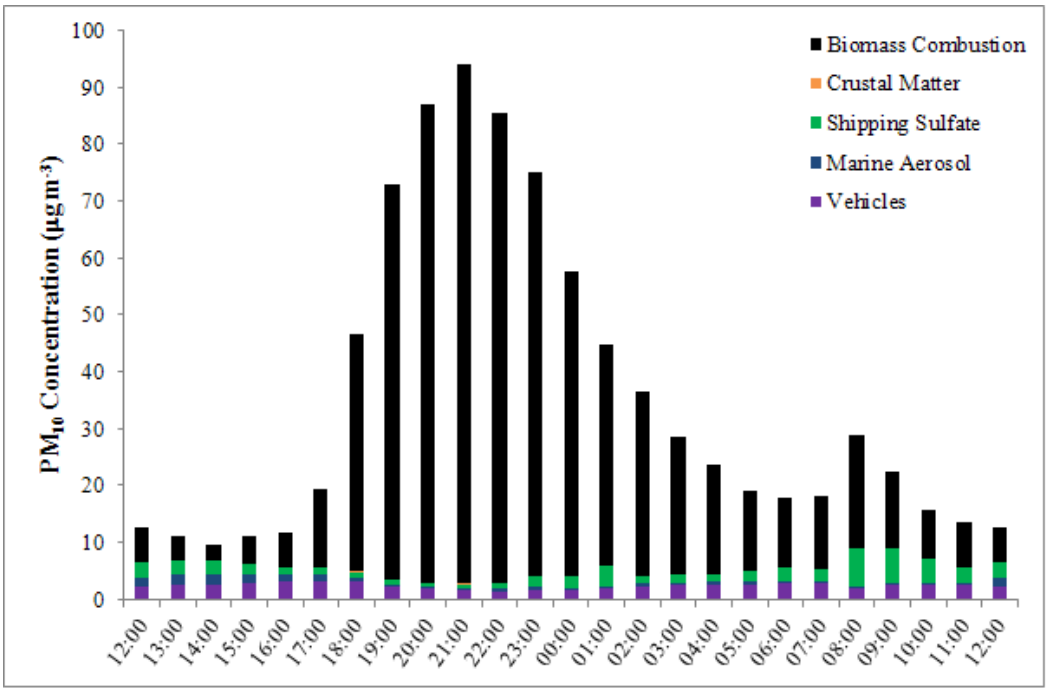

Figure 6.10 Average hourly source contributions at the Aloft site.

A number of notable features are apparent from Figures 6.7, 6.8, 6.9 and 6.10. First, biomass combustion is a significant PM source almost every hour during the winter. Biomass combustion was responsible for both peaks (evening and morning) observed in the PM_{10} diurnal cycle. It is not surprising that biomass combustion dominated the evening peak, since on cold winter evenings home heating is necessary and in Nelson, many households are reliant on wood burners as their main heating source. Interestingly, biomass combustion also dominated the morning PM peak at each of the sites. This phenomenon was also observed in Masterton and Alexandra, New Zealand (Ancelet et al., 2012; Ancelet et al., 2013b), and suggests that Nelson residents are relighting their fires when they rise in the morning. It was suggested by Trompetter *et al.* [6] that the morning peak could also result from built-up PM_{10}

above the inversion layer being re-entrained to ground level by atmospheric mixing upon the break-up of the inversion, which has been reported previously (Aryal et al., 2009). Based on measurements from the Aloft site, ground observations (clear visibility during the early morning) and an associated study in Nelson (Grange et al., 2013) (Appendix 3), this mechanism was ruled out. We therefore suggest that katabatic flows result in dispersion and a consequent decrease in PM_{10} concentrations during the early morning when there are fewer new particle emissions from biomass combustion. The morning peak then arises from fires that are lit or re-stoked in the morning.

Vehicle contributions at each of the sites increased during peak traffic hours. Marine aerosol and crustal matter contributions were generally highest when hourly wind speeds were high. Shipping sulphate contributions decreased during the evening and early morning, probably because of limited up-valley transport. Large increases in shipping sulphate contributions were apparent at the Aloft site during a number of hours and we suggest this was the result of the Aloft site being more exposed to shipping plumes than the ground level sites.

6.3.3 Arsenic concentrations

Because of poor signal-to-noise ratios, arsenic concentrations were not used in the receptor modeling analyses. Despite this, average hourly arsenic concentrations also show the same diurnal cycle as PM_{10} concentrations (Figure 6.11). This suggests that elevated arsenic concentrations are associated with increased biomass combustion contributions, indicating that Nelson residents are burning copper chrome arsenate (CCA)-treated timber in their fires. This behaviour is, however, likely to be intermittent and opportunistic. A more detailed discussion of arsenic concentrations can be found in Chapter 8.

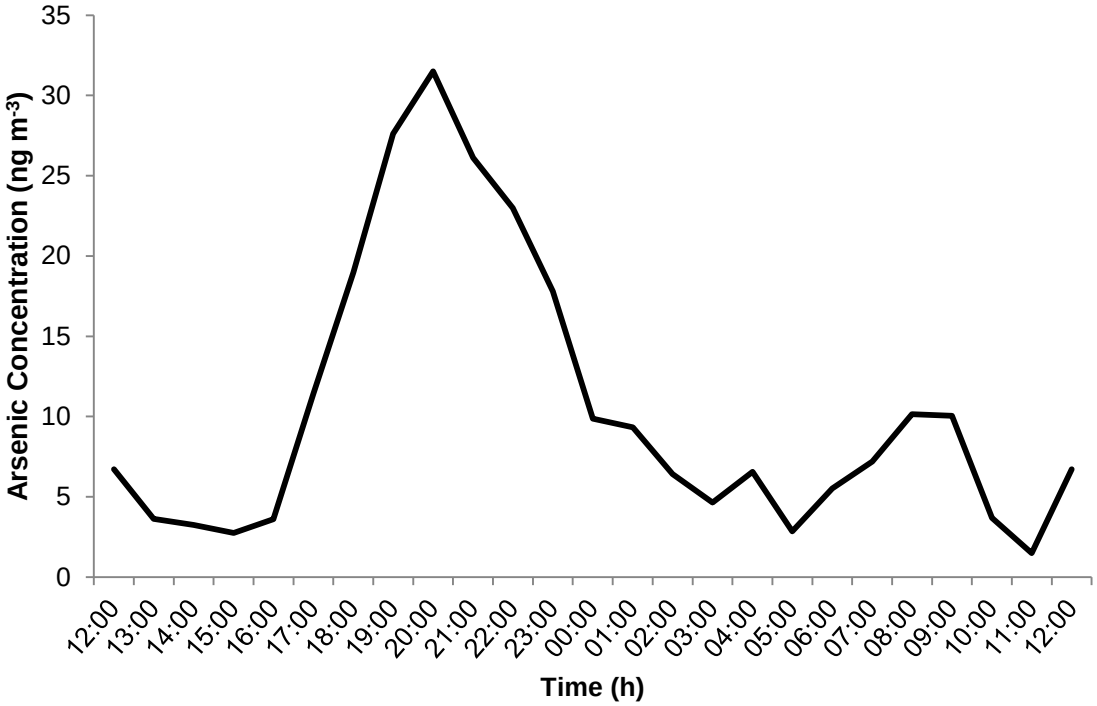

Figure 6.11 Average hourly arsenic concentrations at the St. Vincent Street site.

6.3.4 Source transport

Polar plots using the hourly source contributions were prepared to further investigate the transport mechanism and potential source locations (Carslaw, 2012; Carslaw and Ropkins, 2012; Team, 2011). Using polar plots, the source contributions can be plotted as a function of both wind speed and direction, making them more effective than pollution roses that can only indicate directionality. To provide insight into the observed diurnal variations in source contributions, the hourly source contribution data were divided into night (6 pm–8 am) and day (9 am–5 pm). The source contributions (in µg m^{-3}) shown on the polar plots should not be taken as actual concentrations. The values actually indicate the average concentration for each wind speed/direction bin.

Figure 6.12(a) and (b) presents biomass combustion polar plots obtained using data from the night and day, respectively, at the NCC site. Figure 6.12 indicates that biomass combustion contributions were highest under low wind speeds and southwesterly winds, consistent with the suggestion in section 6.3.1 that katabatic flows northeast along the downslope contour of the valley were responsible for the elevated PM_{10} concentrations observed at the NCC site.

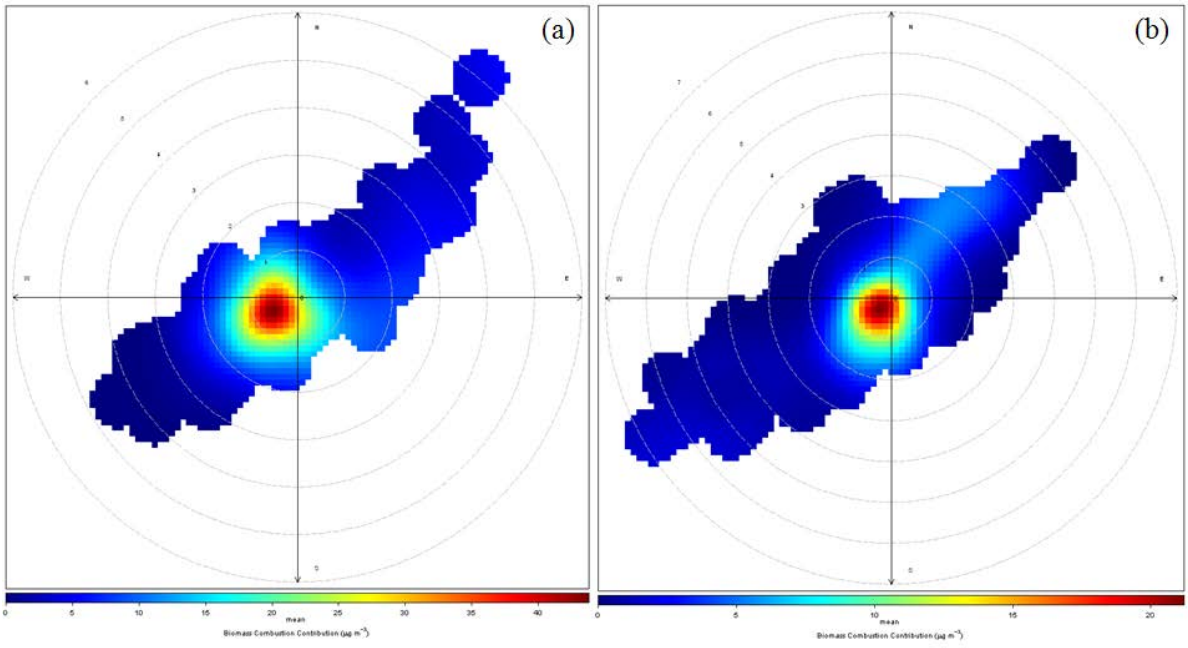

Figure 6.12 Polar plots of biomass combustion contributions during the night (a) and day (b) at the NCC site. The radial dimensions indicate the wind speed in 1 ms^{-1} increments and the color contours indicate the average contribution to each wind direction/speed bin.

Contributions from vehicular sources at each of the sites increased during peak traffic hours, but vehicle contributions were also apparent during hours when traffic flows would be expected to be minimal. Since Nelson is a small city, it is likely that vehicle traffic (heavy-duty diesel vehicles in particular) provides a consistent PM_{10} source throughout the day. Figure 6.13 (a) and (b) presents polar plots of vehicle contributions during the night and day, respectively. During the night, vehicle contributions at NCC were transported to the site by the predominant southwesterly flows experienced within the valley. During the day (Figure 6.13(b)), vehicle contributions were largely from the southwest and high contributions from the city center located northeast of the site were also apparent.

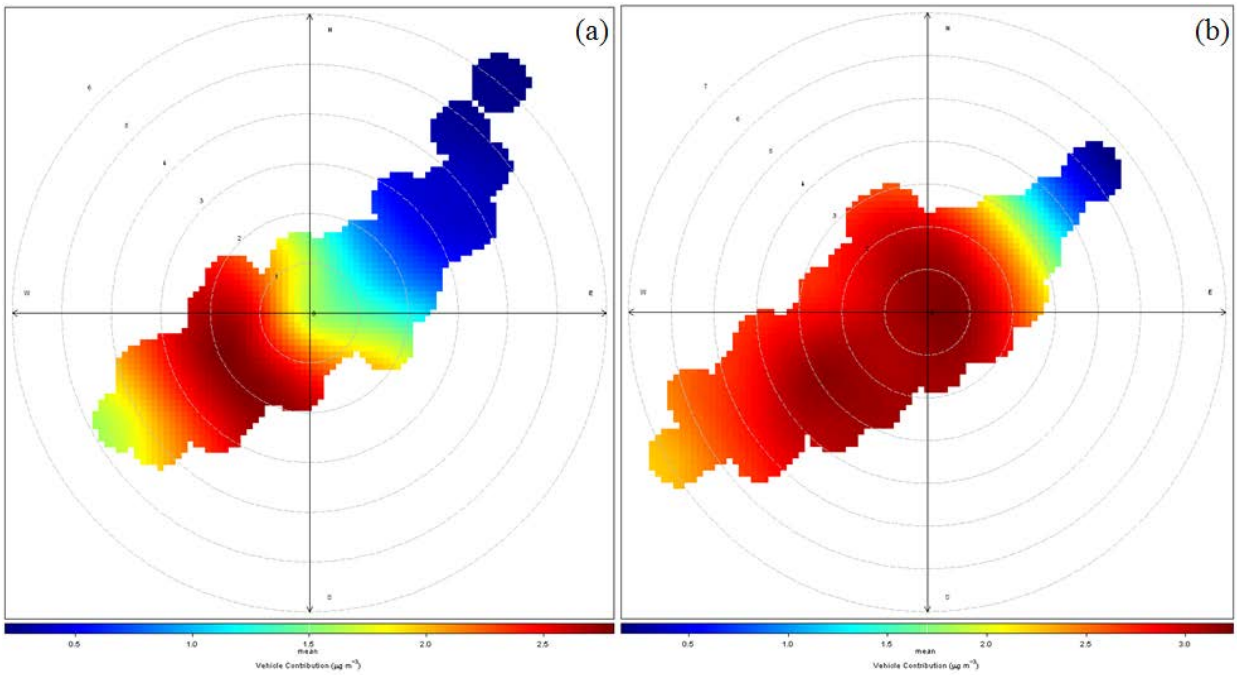

Figure 6.13 Polar plots of vehicle contributions during the night (a) and day (b) at the NCC site. The radial dimensions indicate the wind speed and the contributions indicate the average contribution to each wind direction/speed bin.

Marine aerosol contributions were more pronounced when hourly wind speeds were highest. It is well-known that marine aerosol concentrations increase under increased wind speeds (Fitzgerald, 1991). Night and day polar plots of marine aerosol contributions at NCC were in agreement with this and are presented in Figure 6.14 (a) and (b). Figure 6.14 indicates that marine aerosol contributions were highest under elevated wind speeds from the northeast, in the direction of the Pacific Ocean.

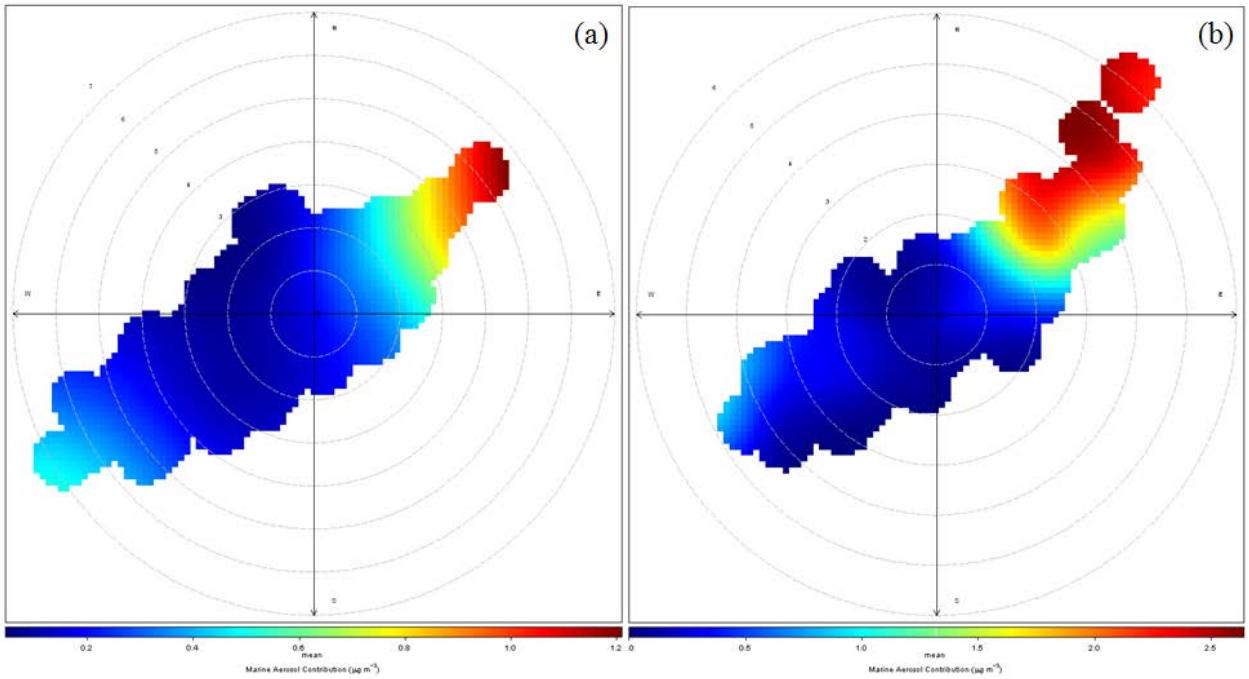

Figure 6.14 Polar plots of marine aerosol contributions during the night (a) and day (b) at the NCC site. The radial dimensions indicate the wind speed and the contributions indicate the average contribution to each wind direction/speed bin.

Figure 6.15 (a) and (b) present night and day polar plots, respectively, of shipping sulphate contributions. The polar plots confirm that this source is the result of shipping emissions and not another residual oil combustion source because shipping sulphate contributions during the day and night were the result of transport from the Port of Nelson area.

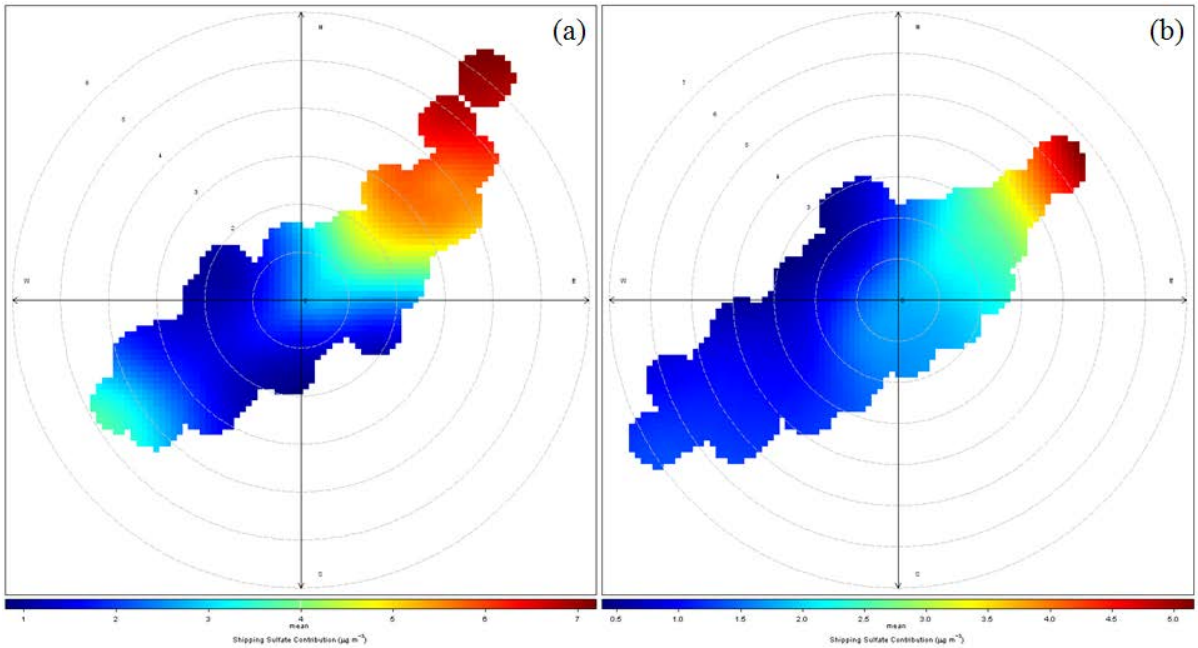

Figure 6.15 Polar plots of shipping sulfate contributions during the night (a) and day (b) at the NCC site. The radial dimensions indicate the wind speed in 1 ms^{-1} increments and the color contours indicate the average contribution to each wind direction/speed bin.

Night and day polar plots of crustal matter contributions at NCC are presented in Figure 6.16 (a) and (b), respectively. Crustal matter contributions were greatest under high wind speeds from the southwest. Low wind speed crustal matter contributions from the north, particularly during the day, were likely from land adjacent to NCC where construction activities were taking place.

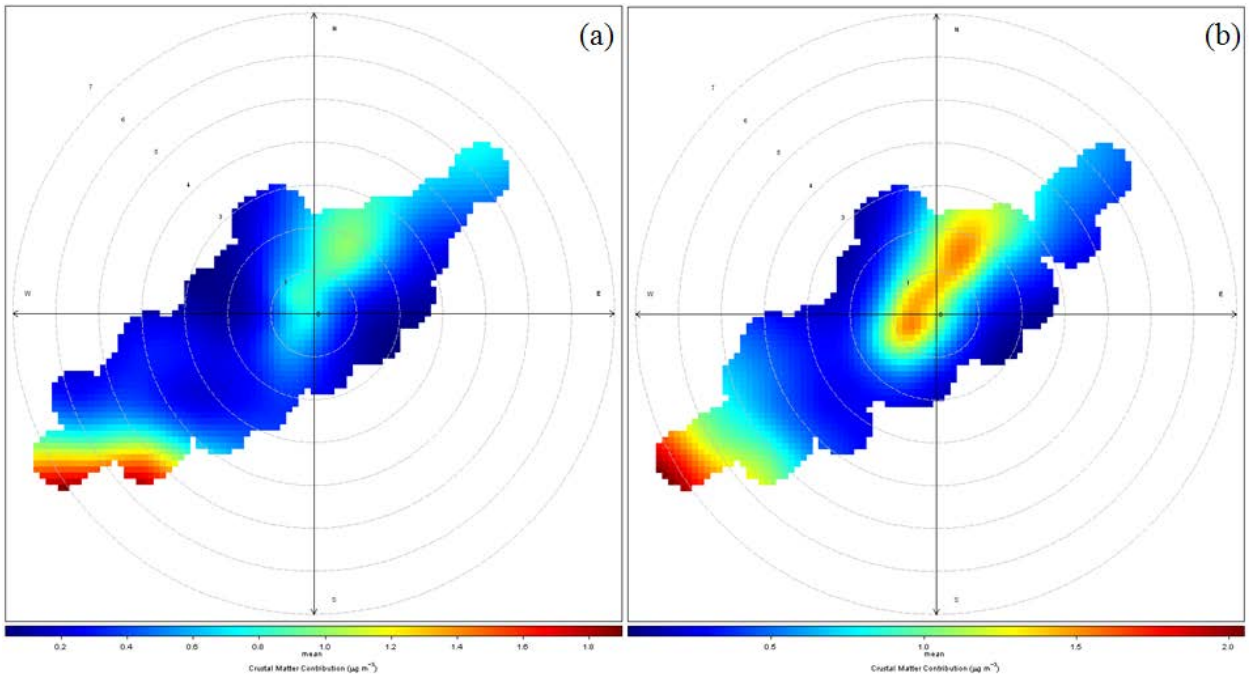

Figure 6.16 Polar plots of crustal matter contributions during the night (a) and day (b) at the NCC site. The radial dimensions indicate the wind speed and the contributions indicate the average contribution to each wind direction/speed bin.

6.4 CONCLUSIONS

This study aimed to identify the sources and factors contributing to PM_{10} concentrations on an hourly time-scale at four locations within Nelson, New Zealand. Three of the locations were located on a horizontal transect, upwind, central and downwind, of general katabatic flows. The fourth site was located centrally, but elevated to a height of 26 m when wind conditions permitted. PM_{10} concentrations among the sites varied, but the central site (NCC) was found to have consistently higher PM_{10} concentrations than the other sites. Katabatic drainage was identified as the main reason for the elevated PM_{10} concentrations and it is likely that PM_{10} concentrations at the downwind site (NFS) were not highest because the urban valley opened up just before the site and the number of upwind PM sources decreased as the valley opened up. PM_{10} concentrations at the elevated site were lower than those measured at ground level, and combined with higher temperatures and wind speeds, suggested that the elevated site was located above a shallow inversion layer (< 26 m). Figure 6.16 presents a general schematic of the drainage flows with relative concentration of PM_{10} super imposed.

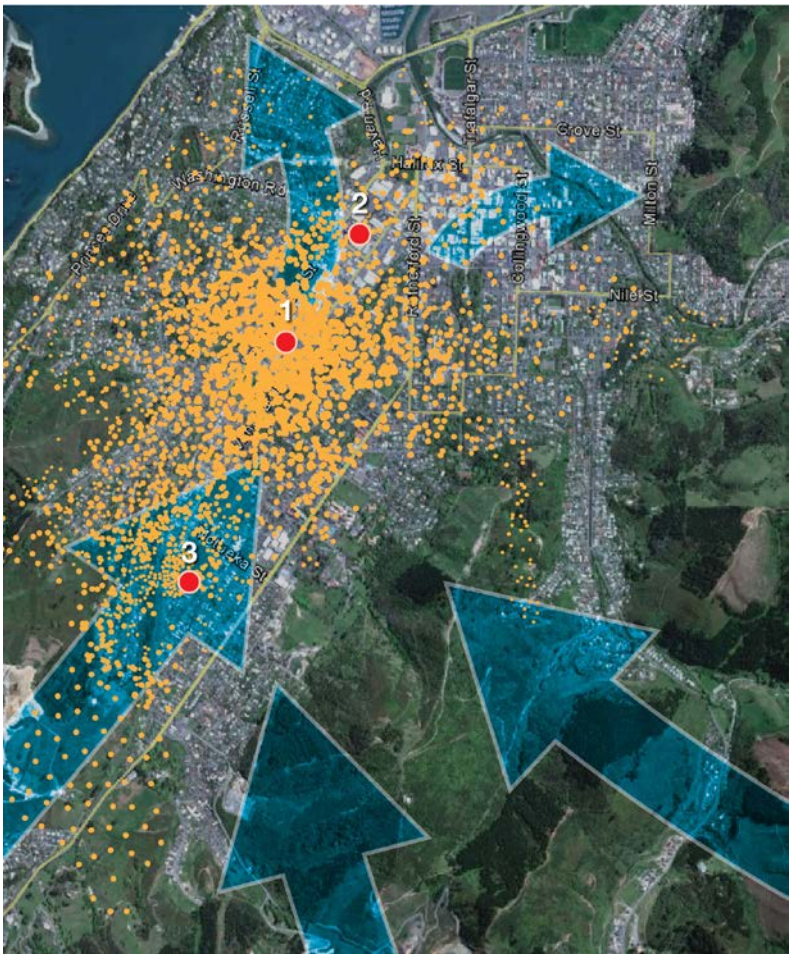

Figure 6.17 Schematic of general katabatic drainage flows (blue arrows) in the Nelson South airshed overlaid with PM_{10} concentration density (orange dots) with the ground based monitoring stations marked (1 = NCC, 2 = NFS, 3 = NIS).

Five PM_{10} sources were identified in Nelson: biomass combustion, motor vehicles, crustal matter, marine aerosol and shipping sulphate. Biomass combustion was the dominant source of PM_{10} during all hours and was responsible for the observed evening and morning peaks in PM_{10} concentrations, suggesting that Nelson residents relight their fires in the morning. Prior to this study, shipping emissions had not been identified as a source of PM in Nelson. Contributions from shipping sulphate were highest at the elevated site and we suggest that this was because the elevated site was situated more within the plume than the ground level sites. The ability to identify PM sources on an hourly time-scale can provide unique and highly relevant information for the management of air quality.

7.0 BLACK CARBON ANALYSIS

7.1 BLACK CARBON CONCENTRATIONS

The receptor modeling for PM_{10} and $PM_{2.5}$ samples collected (2008–2012) at the St Vincent Street site and reported so far have only included those filters (i.e. Teflon) that were able to be analysed using IBA techniques. However, the filter based monitoring programme at the site initially began in 2006 with PM_{10} sampled onto quartz filters. The PM_{10} quartz filter set have been analysed for black carbon (BC) concentrations and, because the results are comparable with the BC determination on $PM_{2.5}$ and PM_{10} Teflon filters, the datasets have been combined to produce a BC time-series from 2006–2012 (Figure 7.1). Gaps in the data are due to missing sample periods.

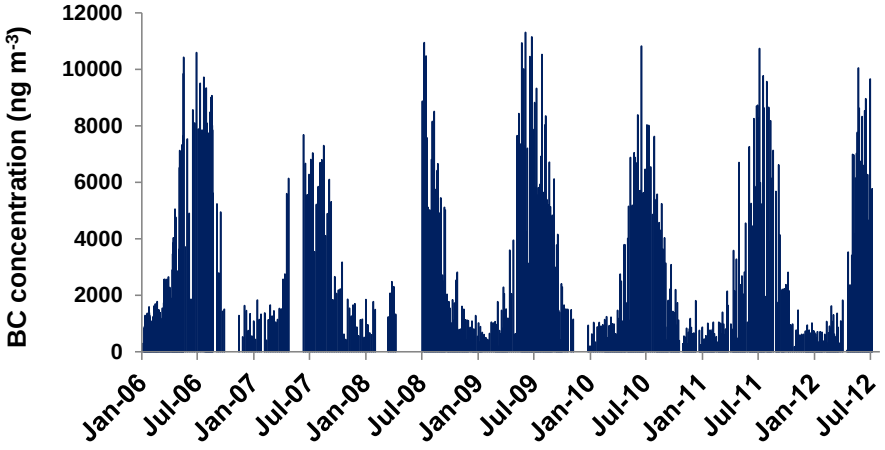

Figure 7.1 Black carbon concentrations at the St. Vincent Street site.

The longer BC dataset provides the opportunity to examine the relative influence of combustion sources on PM_{10} over the same time period, since BC is primarily produced by combustion processes (biomass burning, motor vehicles and industrial installations). The relationship between PM_{10} and BC is strong because peak PM_{10} concentrations in the Nelson A airshed are driven by local combustion source activity (emissions from motor vehicles and biomass burning), as shown by the scatterplot presented in Figure 7.2.

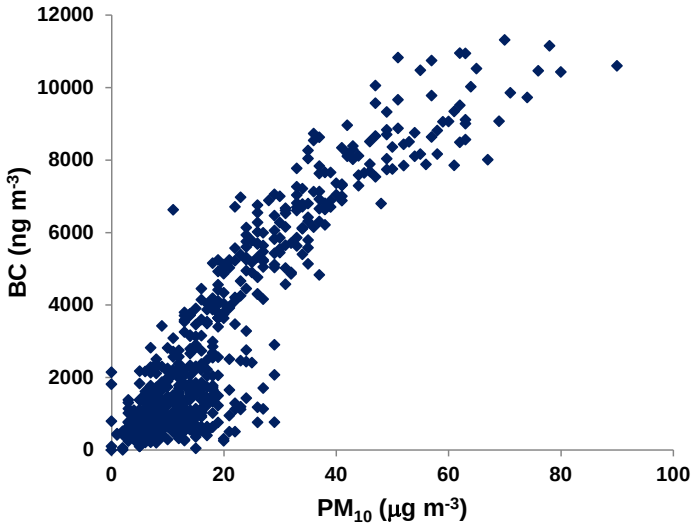

Figure 7.2 Scatterplot of black carbon concentrations (ng m^{-3}) versus PM_{10} concentrations (µg m^{-3}) at St. Vincent Street.

Interestingly, the plot presented in Figure 7.2 shows some curvature at peak BC concentrations. This effect is from self-absorption within the sample during the light reflectance measurements as the thickness of the BC layer on the filter increases.

7.2 BLACK CARBON TREND ANALYSIS

The analysis of trends in air pollutant concentrations is critical for assessing source activity and the effects of pollution mitigation strategies and policy intervention measures to reduce air pollution concentrations. Since particulate matter concentrations in Nelson have exceeded the NES during the winter for many years, the Nelson Air Plan contains an air quality target of 50 µg m^{-3} (24-hour average). The Nelson City Council operative air plan also includes measures to reduce emissions of PM_{10} into the local airshed, such as a ban on the outdoor burning of rubbish, a ban on the use of open fires, the phasing out of older burners and restrictions on the installation of solid fuel burners to achieve compliance with the NES.

The openair package based on 'R' statistical software has been used to analyse the Nelson data for trends (Carslaw, 2012; Carslaw and Ropkins, 2012; Team, 2011). For the trend analysis, the TheilSen function in openair was used (Carslaw, 2012). The analysis of trends in the BC concentration data (2006–2012) shows that year-on-year BC concentrations are decreasing (Figure 7.3), but that this trend is not statistically significant to the 90th percentile confidence limits. The same analysis applied to the PM_{10} data is shown alongside that of BC for comparison.

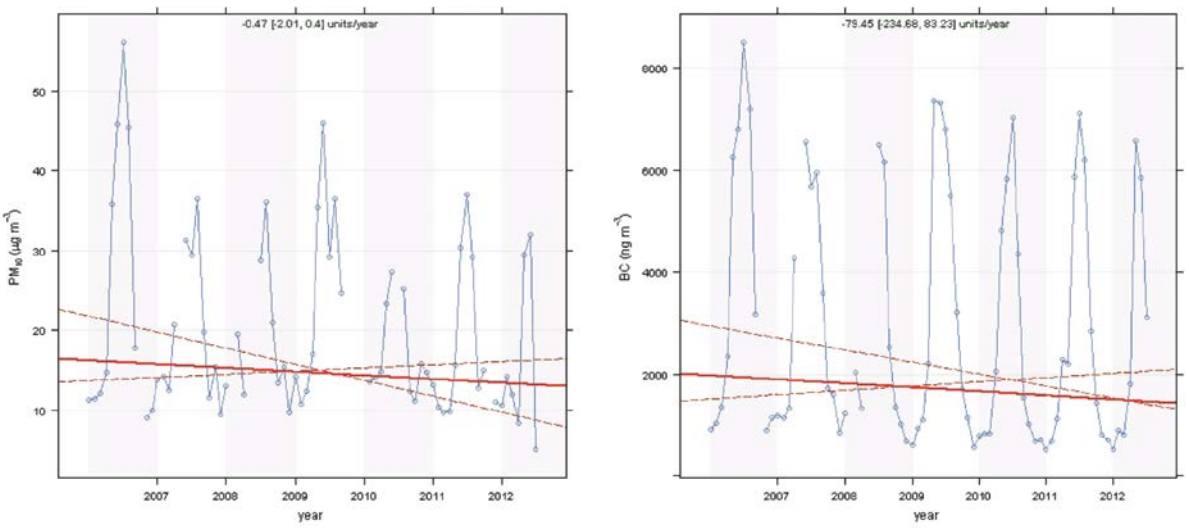

Figure 7.3 Trend analysis for PM_{10} (left) and Black Carbon concentrations (right) at the St Vincent Street site. The solid red line indicates the trend estimate, while the dashed red lines indicate the 95 % confidence intervals for the trend based on data resampling methods.

Strongly seasonal cycles for both PM_{10} and BC concentrations can affect the results of the trend analysis because it is not only the quantity and rate of emissions that dictate ambient concentrations, but meteorology and longer-term climate can also have significant influences on local pollutant concentrations (Trompetter et al., 2010). When the data were deseasonalised the trends were more strongly evident, with PM_{10} decreasing at an average rate of 0.5 µg m^{-3} per year (90% confidence limits) and BC decreasing at 113 ng m^{-3} per year (99.9 % confidence limits), as shown in Figure 7.4.

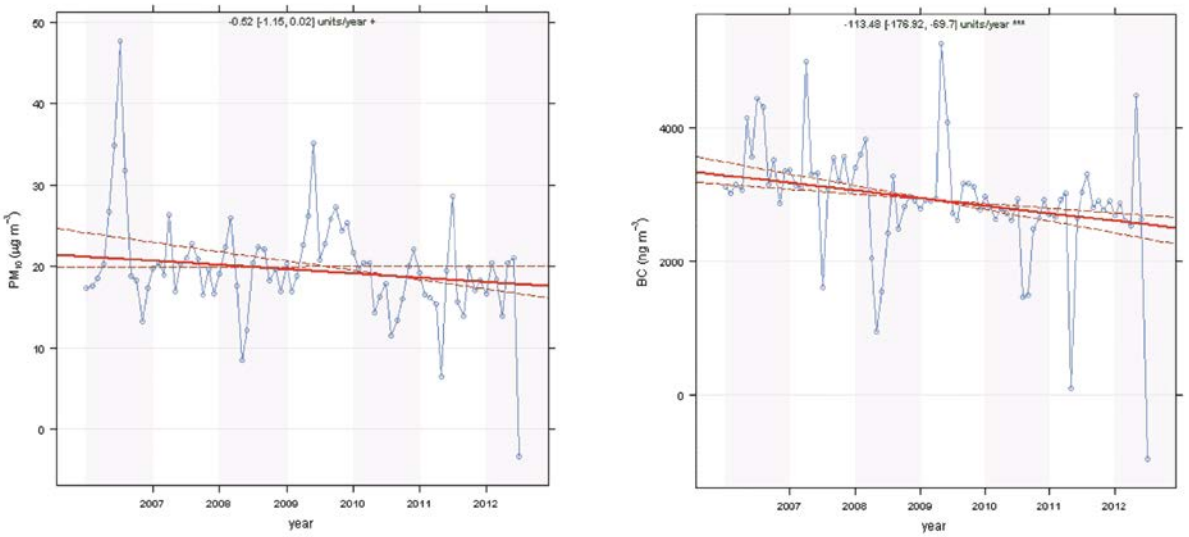

Figure 7.4 Trend analysis for PM_{10} (left) and Black Carbon (right) deseasonalised concentrations at the St Vincent Street site. The solid red lines indicate the trend estimates, while the dashed red lines indicate the 95 % confidence intervals based on data resampling methods.

The trends in PM_{10} and BC were explored further by examining the average seasonal trends, which show (Figure 7.5) that much of the decrease in concentrations for PM_{10} (3 µg m^{-3} per year, 95 % confidence limits) and BC (242 ng m^{-3} per year, 95 % confidence limits) has occurred during winter months (June, July and August).

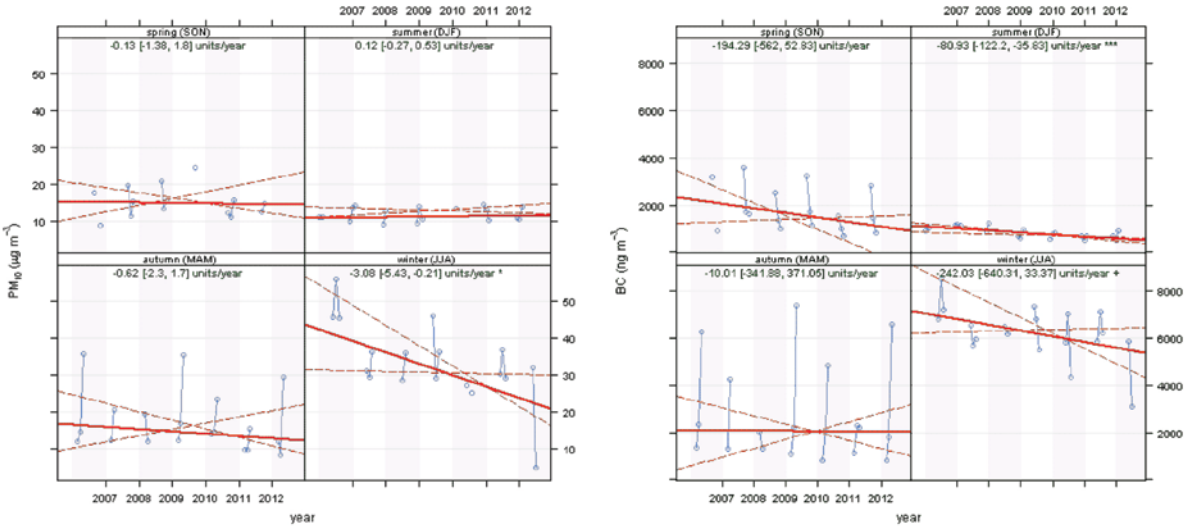

Figure 7.5 Seasonal trend analysis for PM_{10} (left) and Black Carbon (right) concentrations at the St Vincent Street site. The solid red lines indicate the trend estimates, while the dashed red lines indicate the 95 % confidence intervals based on data resampling methods.

Interestingly, the data suggests that there has also been a strongly significant (99.9 % confidence limits) decrease in summer BC concentrations and this may reflect the introduction of outdoor burning restrictions in the Nelson A airshed and further afield.

The data shows that both PM_{10} and BC concentrations have been decreasing over the years 2006–2012, indicating that it was most likely to be a reduction in combustion source emissions affecting PM_{10} concentrations with the most significant reductions occurring during winter months.

The receptor modeling analyses for PM_{10} and $PM_{2.5}$ sources presented in Chapter 4, found that biomass combustion and motor vehicle emissions were the primary sources of combustion related particulate matter in the Nelson A Airshed. The receptor modeling data was recompiled to provide source contributions to BC rather than PM_{10} or $PM_{2.5}$ because of the contribution of coarse particle road dust to motor vehicle related particulate matter concentrations. While BC concentrations related to biomass combustion or motor vehicle emissions may change with a reduction in domestic fire use or improved engine emissions respectively, the road dust component is likely to behave independently (depending on road type, traffic density, etc.) and therefore confound any trend analysis. When the trend analysis was applied to the source apportionment data for motor vehicle and biomass combustion source contributions to BC, it was found that the reduction in biomass combustion-related BC was primarily responsible for the BC reductions (90 % confidence limits) during winter (Figure 7.6). The analysis also suggests that there was a reduction in motor vehicle-related BC during spring months, though the reasons for this are unclear. The data also suggests that motor vehicle-related BC is increasing during winter and could reflect a growth in traffic and/or an increase in the diesel powered fleet. It should be noted that the source related trend analysis was limited to 4 years of data and should be treated as provisional at this stage.

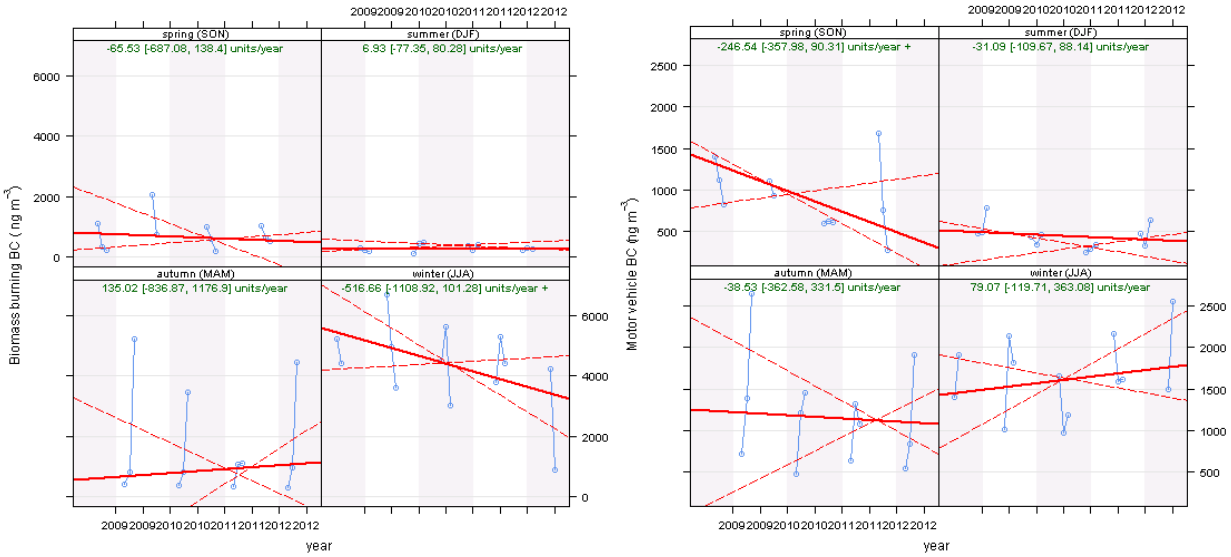

Figure 7.6 Seasonal trend analysis for biomass combustion (left) and motor vehicle-related (right) black carbon concentrations at the St Vincent Street site. The solid red lines indicate the trend estimates, while the dashed red lines indicate the 95 % confidence intervals based on data resampling methods.

7.3 SUMMARY OF BLACK CARBON TREND ANALYSES

The analysis of 6.5 years of BC data has shown that combustion-related particulate matter is decreasing in Nelson Airshed A, and that decrease was most significant during winter months. When the biomass combustion and motor vehicle source contributions to BC derived from receptor modeling were examined, the results suggest that reductions in biomass combustion related BC concentrations (and by inference domestic fire emissions) during winter are the primary driver of the decreasing trend in PM_{10} concentrations. While BC, and by extension PM_{10} concentrations, are decreasing year-on-year, it is impossible to assess whether NCC is likely to comply with 1 breach of the NES by 2020. This is because although PM_{10} concentrations on a yearly time-scale are decreasing, human behaviour and local meteorology play critical roles in exceedances of the PM_{10} standard as well. If, for example, a large high pressure system caused strong temperature inversions in Nelson over a number of days, it would result in cold, calm days with insufficient pollutant dispersion when residents are more likely to use their fires (or for longer periods), then this may lead to exceedances of the NES. Over the course of a year, these exceedances would likely have little effect on the annual average, but would have important implications for air quality management for NCC.

8.0 ARSENIC ANALYSIS

8.1 ARSENIC CONCENTRATIONS AT ST. VINCENT STREET

The receptor modeling results for PM_{10} and $PM_{2.5}$ samples collected (2008–2012) at the St. Vincent Street site (Chapters 4 and 5) have shown that arsenic was strongly associated with the biomass burning source because of the use of copper chrome arsenate (CCA)-treated timber as part of the fuel stream in domestic fires. The data here, and from other studies in New Zealand (Davy et al., 2012; Davy et al., 2011c), indicate that the As is confined to the $PM_{2.5}$ size fraction. The As elemental concentration results for the $PM_{2.5}$ and PM_{10} Teflon filters measured by IBA have therefore been combined to produce an As time-series from 2008–2012 (Figure 8.1). Gaps in the data are from missing sample periods.

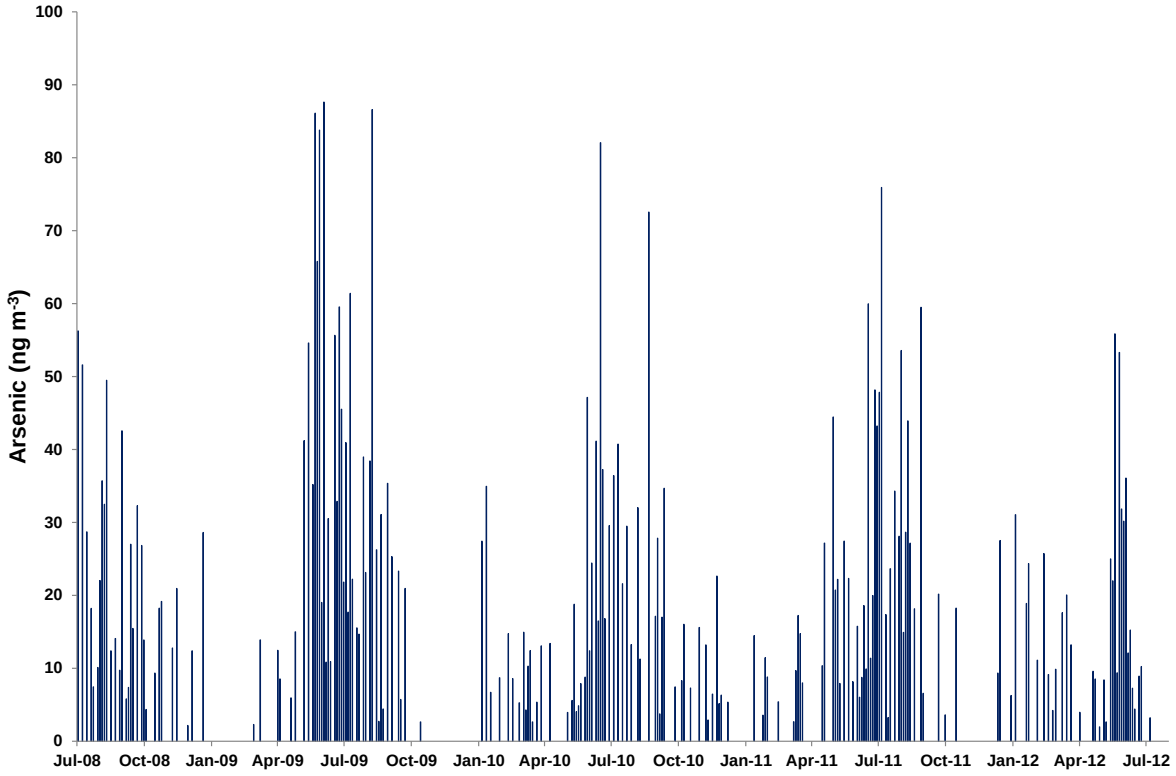

Figure 8.1 Arsenic concentrations at the St. Vincent Street site.

8.2 SOURCES OF ARSENIC IN THE ENVIRONMENT

Arsenic occurs naturally in many soils and parent rock in New Zealand, with concentrations typically in the 2–6 ppm range, although this can be considerably more (50 ppm) in geothermal zones (Craw et al., 2000; Craw et al., 2003; Robinson et al., 2004; Simmons and Browne, 2000). Other sources of arsenic in the New Zealand environment are primarily anthropogenic in origin, for example timber treatment and use of treated timber, pesticides, herbicides, fertilisers and mining operations (gold, coal) (Robinson et al., 2004).

8.3 ARSENIC AND AIR POLLUTION

Arsenic associated with air particulate matter pollution is primarily from the combustion of arsenic-containing fuels, such as coal and CCA-treated timber. Research on emissions from

coal-fired power plants indicates that arsenic is released as particle associated arsenic oxides, mostly as the fully oxidised arsenate (As in 5+ oxidation state) (Shah et al., 2006). Combustion of treated timber in wood burners (or open burning) is at lower temperatures (with a certain amount of pyrolysis) compared to coal fired power plants. An analysis by Helsen and co-workers suggests both the 3+ and 4+ oxidation states are released, and that low temperature pyrolosis (< 327 °C) may retain arsenic in the ash (Helsen and van den Bulck, 2003). It has also been shown that the copper and chromium components are preferentially retained in the ash during combustion of CCA-treated timber.

8.4 AIR QUALITY GUIDELINES FOR ARSENIC

The New Zealand Ambient Air Quality Guidelines (NZAAQG) contain inhalation based health risk guidelines for arsenic species (MfE, 2002). The guideline value for inorganic arsenic is 0.0055 μg m^{-3} (annual average) and for arsine (AsH_3) the guideline value is 0.055 μg m^{-3} (annual average). At temperatures above 230 °C arsine decomposes to arsenic oxides (Lide, 1992), therefore arsine is unlikely to be present in combustion emissions. For the purposes of this discussion we assume that arsenic emitted from combustion processes is present as inorganic oxides, although further work is required to examine the exact nature of arsenic speciation and oxidation state in aerosol samples. The NZAAQG recommend determination of arsenic by PM_{10} sampling in accordance with 40 CFR Part 50, Appendix J (i.e. high-volume sampling), followed by analysis using atomic absorption spectroscopy or an equivalent method. Recent research work on the comparison of arsenic concentrations determined by IBA and the NZAAQG methodology indicates the relationship is linear and the slope is close to unity but that the minimum detection limits for IBA are higher (Mitchell et al., 2013). Thus As concentrations (determined using IBA on Teflon filters) lower than about 20 ng m^{-3} are somewhat uncertain. However, the long-term As concentration averages produce similar results for both analytical methods and the true value lies within the uncertainty estimates (standard error in the mean) for the IBA methodology. With the above caveats on the As results, the annual average arsenic concentrations have been calculated for the three complete years of data (2009, 2010 and 2011) and are presented in Figure 8.2.

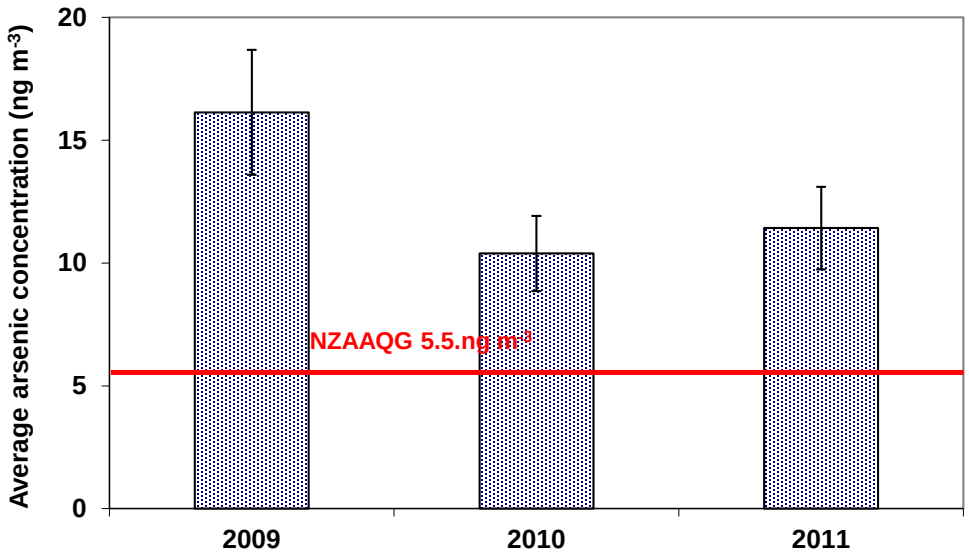

Figure 8.2 Annual average arsenic concentrations at the St. Vincent Street site.

8.5 IMPLICATIONS FOR AIR QUALITY MANAGEMENT

Nelson City Council is responsible for air quality management in the Nelson region. Rules prescribed in the Nelson Air Quality Plan prohibit the discharge of contaminants to air from the burning of CCA-treated timber on any small-scale fuel burning appliance or by deliberate outdoor burning (AQr.20). Therefore, the problem for Nelson City Council is one of enforcement and public education. Similar regulations apply at all other locations in New Zealand. In terms of inhalation health risk, the NZAAQG stipulate a mean annual concentration of 5.5 ng m^{-3} for inorganic arsenic to protect public health. A critical result from the Wainuiomata study was that arsenic exceeded the NZAAQG even though the airshed complied with the PM_{10} NES and $PM_{2.5}$ NZAAQG (Mitchell, 2013). Therefore compliance with the NZAAQG for arsenic in the Nelson A Airshed may not occur even if PM_{10} concentrations meet the NES.

The use of CCA-treated timber as fuel for domestic fires is probably widespread in New Zealand urban areas but only as and when waste timber is at hand. The data suggests that sufficient quantities are being burned to have an acute localised effect, but repeated exposure year-to-year during winter may also include a chronic exposure that is close to or exceeds ambient air quality guidelines at urban locations in New Zealand. The problem presents itself as one of enforcement of air quality regulations or a need for more extensive public education. A further issue is the disposal of the ash from domestic fires that is likely to be contaminated with residual arsenic, as well as copper and chromium. If this is used in gardens it may pose an addition exposure pathway through the ingestion of any vegetables grown in contaminated soils.

9.0 COMPARISON OF RECEPTOR MODELING RESULTS WITH NCC EMISSIONS INVENTORY

The receptor modeling for PM_{10} and $PM_{2.5}$ samples collected (2008–2012) at the St. Vincent Street site provides the opportunity to compare and discuss the relative magnitudes of the source contributions to particulate matter concentrations with emissions inventory estimates. Emissions inventories estimate the rate of emissions (kg/day, tonnes/year) from different source categories, while receptor modeling infers source contributions to actual ambient concentrations as measured at a monitoring site (mass per unit volume basis (µg m^{-3})). The results are therefore not directly comparable, though both are useful tools for examining different aspects of air quality management. Broad comparisons can be made between the results from emissions inventories and receptor modeling with respect to the primary sources of air pollutants, future projections and trends.

An emissions inventory for PM_{10} was prepared for Nelson City Council by Environet Ltd., with 2006 as the baseline year for calculating emissions to the atmosphere from various sector categories (Wilton, 2006). The inventory calculated emissions for domestic heating, motor vehicles and industrial sources, but not for natural and secondary particulate matter sources such as marine, crustal matter and secondary sulphate aerosol, because it is not possible to generate sensible emissions data for those sources. Figure 9.1 presents the emissions inventory estimates for Nelson Airshed A (adapted from (Wilton, 2006)).

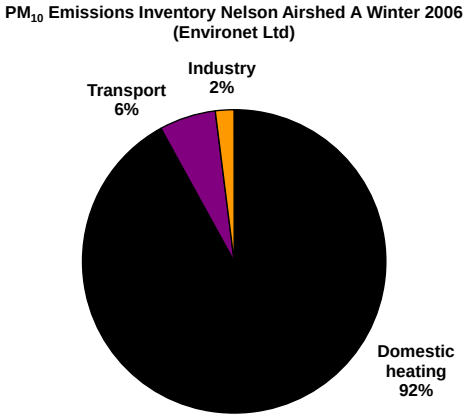

Figure 9.1 Relative contribution of inventoried sources to daily winter PM_{10} emissions (2006) in Nelson Airshed A (adapted from Wilton, 2006).

The PM_{10} receptor modeling data from the St. Vincent Street site has been recompiled to present average winter (June–August) source contributions to PM_{10} concentrations for 2009, 2010 and 2011 (winter periods with complete data records) as shown in Figure 9.2. It can be seen that un-inventoried sources (sulphate, marine aerosol and soil) can have a significant, but somewhat variable influence (17–37 %) on average winter PM_{10} concentrations. No specific industrial source signature or contribution was identified from the receptor modeling and it is likely that such emissions are mixed in with the primary combustion sources (vehicles and biomass burning). In any case, the emissions inventory results suggest that industrial emissions are a minor contributor (2 %).

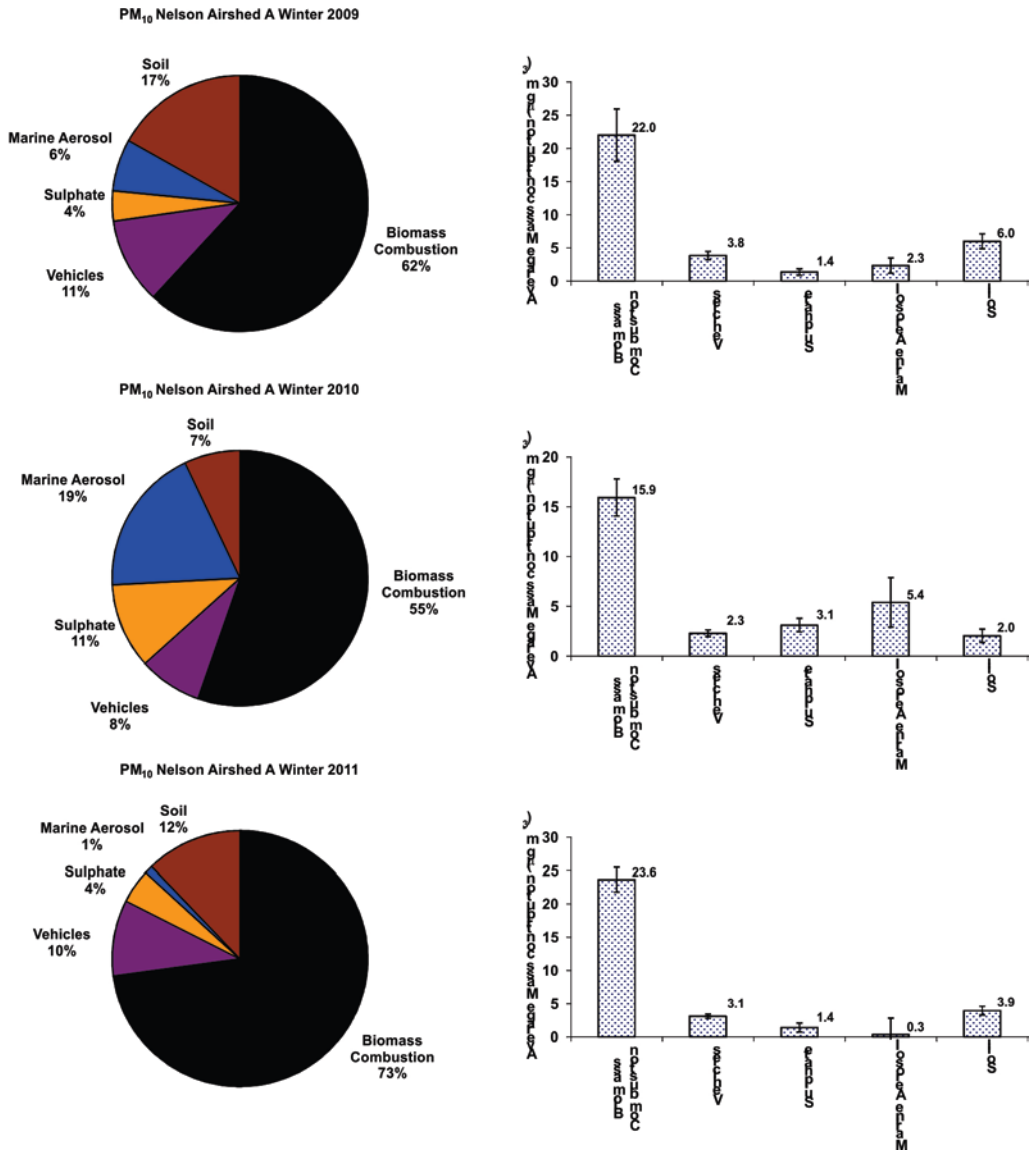

Figure 9.2 Source contributions to average daily winter PM_{10} concentrations (2009–2011) in Nelson Airshed A.

The average concentrations calculated from receptor modeling results include all winter days sampled, but for air quality management purposes, the primary interest lies in those days with peak $PM_{2.5}$ (>17 µg m^{-3}) and PM_{10} concentrations (>33 µg m^{-3}). Further to the analysis provided in Section 5.2, the average contributions to peak $PM_{2.5}$ and PM_{10} are presented in Figure 9.3.

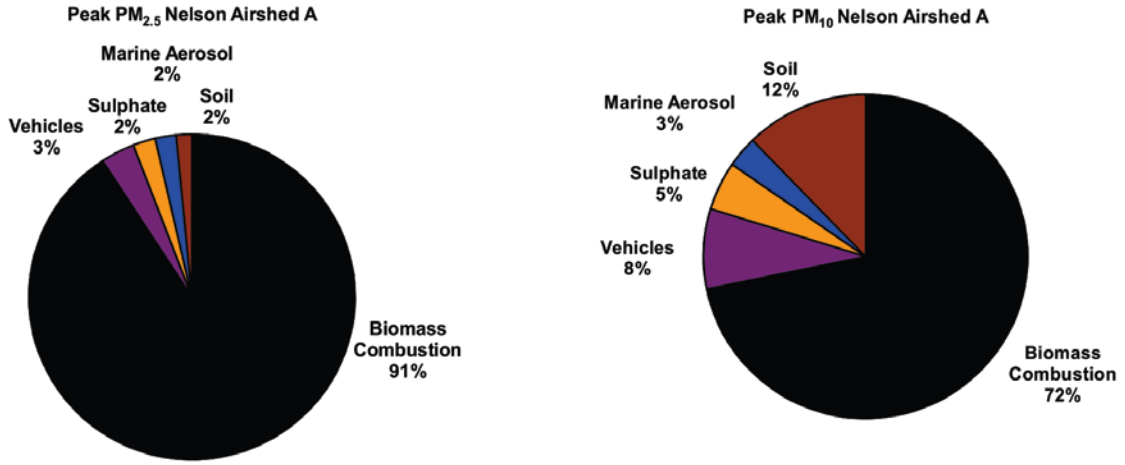

Figure 9.3 Average source contributions to peak $PM_{2.5}$ (left) and peak PM_{10} (right) concentrations (2009-2011) in Nelson Airshed A.

The data show that peak $PM_{2.5}$ is dominated by biomass combustion, but that peak PM_{10} still has a significant proportion (20 %) from natural and secondary sources, which should be factored into any PM_{10} pollution reduction strategy because nothing can be done with regard to emissions from these sources. In fact, the PM_{10} emissions inventory estimates for motor vehicles and domestic heating are more representative of a $PM_{2.5}$ emissions inventory, since combustion-related particulate emissions are generally less than 1 µm (PM_1). In any case, it is clear that any measure to reduce domestic heating emissions will result in a reduction of peak $PM_{2.5}$ and PM_{10} concentrations. However, for the Nelson A airshed, the many more days where $PM_{2.5}$ exceeds the NZAAQG compared to PM_{10} NES exceedances suggests that it will take longer to comply with the $PM_{2.5}$ monitoring guideline.

Interestingly, motor vehicle contributions to $PM_{2.5}$ were about half those for PM_{10}, with the difference being the contribution from coarse particle ($PM_{10-2.5}$) resuspended road dust that includes abraded road surface material, wear of brake linings and tyres, and any other fine particulate material deposited on the road surface. The emissions inventory has assumed a road dust contribution of around 15 %, but the results from this study and research carried out elsewhere in New Zealand suggest that the road dust contribution can be significantly higher (25–60 %) of the total PM_{10} contribution from motor vehicles, depending on factors such as road surface composition, traffic density, vehicle speeds and local dust generating activities where material ends up on the roadway (Davy et al., 2011a; Davy et al., 2011b; Davy et al., 2011c).

When non-inventoried sources are excluded from the PM_{10} receptor modeling results for the winter period (i.e. we are left with motor vehicle and biomass burning source contributions), then the results suggest that the emissions inventory estimates for those specific sources are probably in the right ball park (Figure 9.4). The higher motor vehicle source contribution (12–15 %) compared to the emissions inventory (6 %) is likely from significant underestimation of the resuspended road dust component.

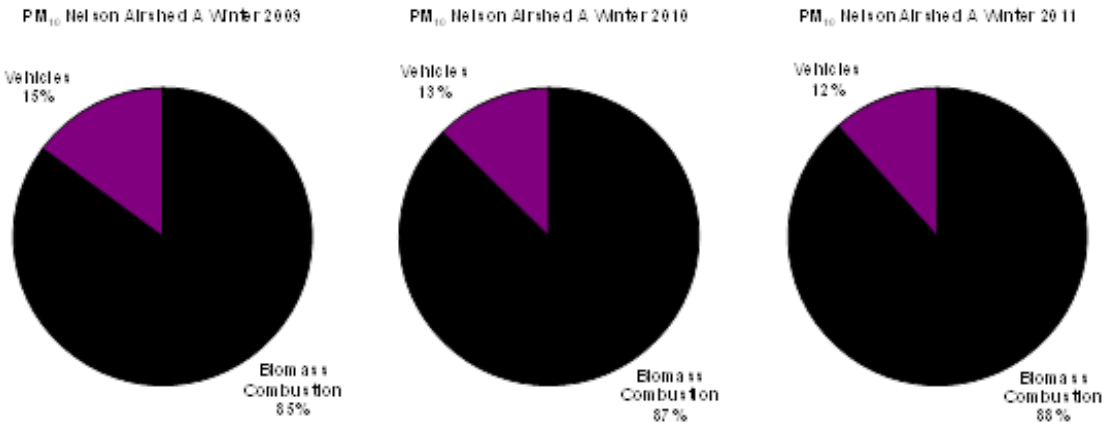

Figure 9.4 Motor vehicle and biomass combustion source contributions to average daily winter PM_{10} concentrations (2009–2011) in Nelson Airshed A.

10.0 COMPARISON OF ST. VINCENT STREET RECEPTOR MODELING RESULTS WITH THE TAHUNANUI STUDY

The receptor modeling of PM_{10} and $PM_{2.5}$ samples collected (2008–2012) at the St. Vincent Street site provides the opportunity to compare with the results from the Tahunanui PM_{10} study (2008–2009) based on samples collected at the Blackwood Street air quality monitoring site, which has previously been reported (Davy et al., 2010). The Tahunanui source apportionment results were date-matched with the Nelson South data to provide 60 concurrent PM_{10} sample days for both sites, ranging from the beginning of September 2008 to the end of September 2009. Source contributions for common sources were cross correlated to examine their relationships, if any existed. Figure 10.1 presents the matched PM_{10} and source data from the two monitoring sites.

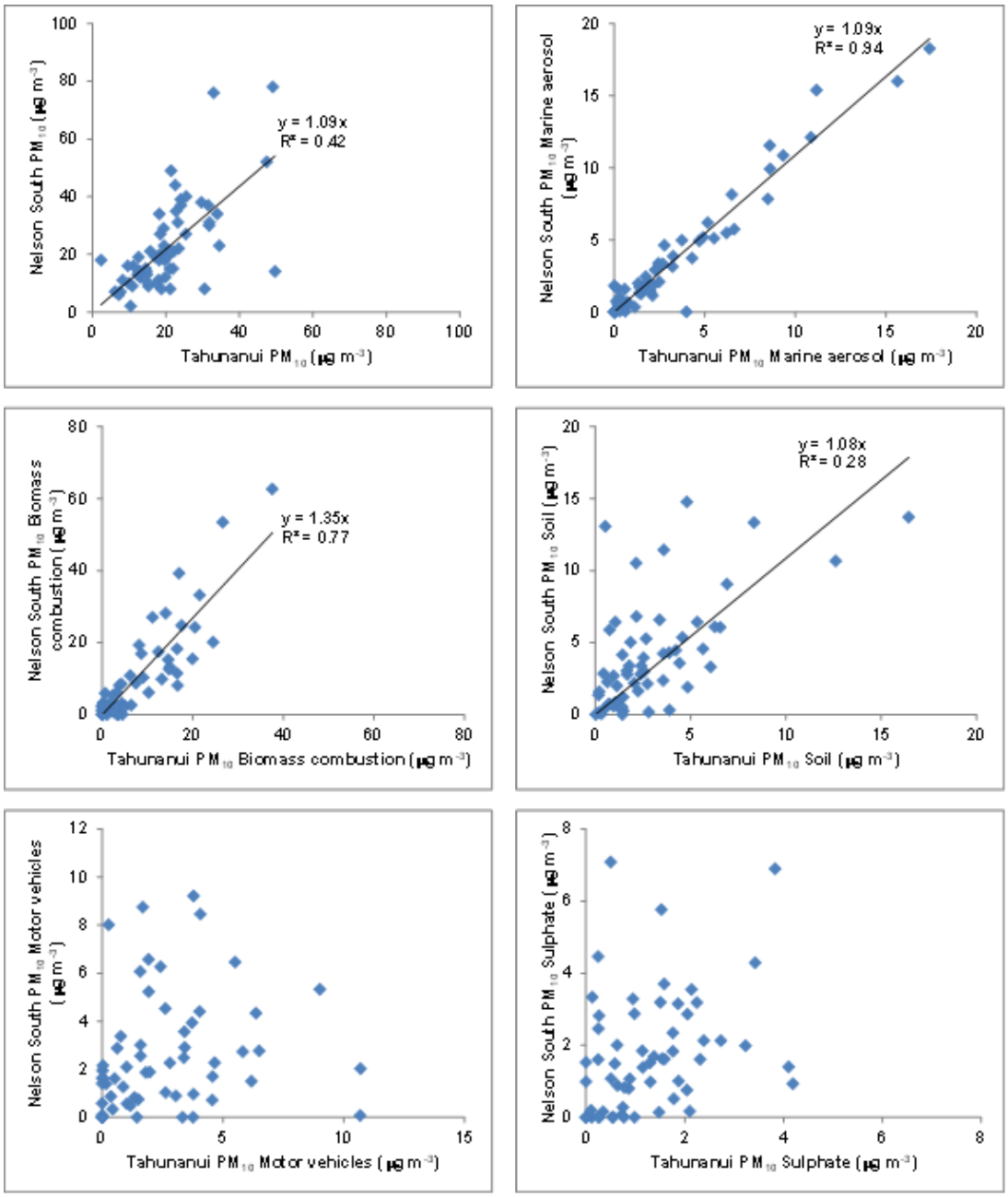

Figure 10.1 Matched PM_{10} source contributions for the Nelson South and Tahunanui receptor modeling studies.

Figure 10.1 shows that PM_{10} concentrations at each site tend to increase together and there were several factors likely to be driving this relationship. The first is the matched biomass combustion sources (r = 0.88), which were found to be responsible for peak PM_{10} concentrations at each site. However, it is unlikely biomass combustion emissions from one airshed are influencing PM_{10} concentrations in the other because they are largely decoupled by the intervening hills, but rather that the common mechanism is the prevailing meteorological conditions. That is, particulate matter concentrations from biomass combustion emissions peak on cold, calm winter days in both airsheds because of the number of domestic solid fuel fires in use and the lack of dispersion. The biomass combustion concentrations in Nelson South were about 35 % higher on average than Tahunanui, probably because of the density of residential properties (and therefore emissions from domestic solid fuel fires) and the confinement of the Nelson South valley.

The second common driver for PM_{10} in the two airsheds is the highly correlated one-to-one marine aerosol contributions (r = 0.97) which is a true regional source, such that atmospheric concentrations of marine aerosol at one site are exactly matched at the other site. Similar highly correlated and one-to-one relationships for marine aerosol were observed across six monitoring sites in Auckland (Davy et al., 2011). Our research has shown that marine aerosol arriving at New Zealand is primarily generated in the Tasman Sea and Southern Ocean and that the concentrations are dependent on the wind field strength, the fetch across the sea surface and the time taken for the aerosol to arrive at a monitoring site from the point of generation (Davy et al., 2011;Fitzgerald, 1991). The only other PM_{10} source common to both locations that demonstrates a moderate correlation are the crustal matter (soil) contributions (r = 0.62). Peak crustal matter contributions at both sites were found to occur under moderate to strong southwest winds and, while it is unlikely that crustal matter from one airshed is affecting PM_{10} concentrations in the other (i.e. it is not a regional source), the common mechanism is most probably re-entrained local dusts due to wind action.

The motor vehicle sources do not show any correlation which is consistent with other studies since motor vehicle emissions tend to have a localised influence and concentrations of motor vehicle-related particulate matter drop off rapidly as the distance of a monitoring site from nearby roadways increases. Some auto-correlation between sites is possible because of commuter behaviour. That is, peak traffic conditions (and therefore maximum emissions) tend to occur at the same time of day in most urban locations. The secondary sulphate sources do not correlate either and it is suspected that the greatest influence on secondary sulphate in each of the airsheds is emissions from shipping sources in the Port Nelson area and shipping lane approaches. The influence of shipping emissions was clearly evident in the high resolution (hourly) sampling and source apportionment analysis presented in Chapter 6.

11.0 SUMMARY OF NELSON SOUTH RECEPTOR MODELLING STUDIES

The elemental analysis and source apportionment of $PM_{2.5}$ and PM_{10} samples from the Nelson A airshed has provided a wealth of information for air quality management purposes and key findings have been summarised in the following sections.

11.1 SOURCES OF PM_{10} AND $PM_{2.5}$

Both $PM_{2.5}$ and PM_{10} were found to have the same primary contributing sources, but with a varying influence on each size fraction depending the relative amounts of coarse particulate matter ($PM_{10-2.5}$) associated with each source type. The sources identified and relative contributions to $PM_{2.5}$ and PM_{10} in the Nelson South airshed are shown in Table 11.1:

Table 11.1 Sources of particulate matter in the Nelson South Airshed

Source name	Primary emission source	Main size fraction	Average contribution to PM_{10} (2008-2012) $\mu g\ m^{-3}$	Average winter contribution to PM_{10} (JJA) $\mu g\ m^{-3}$
Biomass combustion	Domestic solid fuel fires	$PM_{2.5}$	9.7	21
Motor vehicles	Tailpipe and re-suspended road dust	$PM_{2.5}$ and $PM_{10-2.5}$	2.0	3.1
Secondary sulphate	Shipping, marine phytoplankton, coal combustion, volcanic emissions	$PM_{2.5}$ and $PM_{10-2.5}$	2.1	1.6
Marine aerosol	Generated in open ocean (Tasman Sea, Sothern Ocean)	$PM_{10-2.5}$	3.6	2.3
Soil	Wind blown dust, re-suspension by motor vehicles	$PM_{10-2.5}$	2.6	3.7

It was found that there were many more days where $PM_{2.5}$ exceeds the NZAAQG compared to PM_{10} NES exceedances because of the primarily $PM_{2.5}$ biomass combustion source. The data suggests that it will take longer to comply with the $PM_{2.5}$ monitoring guideline than the PM_{10} NES.

11.2 TEMPORAL PATTERNS IN SOURCE CONTRIBUTIONS

The biomass combustion source was found to have a strong seasonal cycle with peak concentrations during winter from the use of solid fuel fires for home heating. Seasonal cycles in PM_{10} concentrations for other sources were also evident and these were likely to be meteorologically driven. Diurnal patterns in source contributions derived from high resolution (hourly) sampling showed that biomass combustion is the primary driver of the mid-evening and mid-morning peaks observed in the PM_{10} data, with a minimum from 5–6 am. Analysis of multi-site data indicates the mid-morning peak is due to the relighting of domestic fires and critically, the mid-morning peak can push the 24-hour PM_{10} average over the NES. PM_{10}

associated with motor vehicle sources were observed to have a distinct weekday-weekend difference in contributions because of the normal working week patterns in commuter behaviour and traffic density.

11.3 SPATIAL PATTERNS IN SOURCE CONTRIBUTIONS

The multi-site monitoring campaign undertaken during the 2011 winter showed that the St. Vincent Street site regularly records the highest PM_{10} concentrations in the Nelson South airshed, with down-valley katabatic drainage the main particulate matter transport mechanism observed during peak PM_{10} events.

11.4 TRENDS IN BLACK CARBON CONCENTRATIONS AND SOURCE CONTRIBUTIONS

A seven year record (2006–2012) of black carbon concentrations provided sufficient data for a trend analysis for combustion sources. It was found that black carbon concentrations and PM_{10} were decreasing year-on-year, with the primary decrease occurring during winter months at a rate of 242 ng m^{-3}/winter/year for black carbon, and 3 μg m^{-3}/winter/year for PM_{10}. When the sources of BC were accounted for, the winter decrease was found to be entirely from reductions in biomass combustion-associated black carbon.

11.5 ARSENIC CONCENTRATIONS AT ST. VINCENT STREET

Arsenic contamination in particulate matter has been found in urban air across New Zealand and the Nelson South airshed is no exception. Average annual concentrations calculated from the Ion Beam Analysis elemental data indicates that the New Zealand Ambient Air Quality Guideline for arsenic (5.5 ng m^{-3} annual average) is substantially exceeded every year, with the highest concentrations during winter (maxima around 90 ng m^{-3}). The arsenic was strongly associated with the biomass combustion source and therefore, the arsenic contamination is considered to be from the use of copper chrome arsenate (CCA)-treated timber as fuel for domestic fires. The use of CCA-treated timber as fuel for domestic fires is probably widespread in New Zealand urban areas but only as and when waste timber is at hand. The data suggests that sufficient quantities are being burned to have an acute localised effect, but repeated exposure year-to-year during winter may also include chronic exposure. The primary health concern for inhalation exposure to arsenic is that it is a known carcinogen.

11.6 COMPARISON OF THE RECEPTOR MODELLING RESULTS WITH EMISSIONS INVENTORY ESTIMATES

The receptor modeling provided the opportunity to compare the relative magnitudes of the source contributions to particulate matter concentrations with emissions inventory estimates. Emissions inventories estimate the rate of emissions (kg/day, tonnes/year) from different source categories, while receptor modeling infers source contributions to actual ambient concentrations as measured at a monitoring site (mass per unit volume basis (μg m^{-3})). The results are therefore not directly comparable, though both are useful tools for examining different aspects of air quality management. A broad comparison of receptor modelling results with emissions inventory estimates found that around 20 % of peak PM_{10} concentrations (> 33 μg m^{-3}) was from non-inventoried sources. It was also found that motor vehicle emissions were significantly underestimated because of the substantial road dust contribution to motor vehicle-associated PM_{10}. However, this is mainly due to the difficulty of obtaining sensible emission factors for the re-suspended road dust component.

11.7 COMPARISON OF THE NELSON SOUTH WITH THE TAHUNANUI RECEPTOR MODELLING STUDY

The receptor modeling of PM_{10} and $PM_{2.5}$ samples collected (2008–2012) at the St. Vincent Street site provided the opportunity to compare with the results from the Tahunanui PM_{10} study (2008–2009) based on samples collected at the Blackwood Street air quality monitoring site. The Tahunanui source apportionment results were date-matched with the Nelson South data to provide 60 concurrent PM_{10} sample days for both sites, ranging from the beginning of September 2008 to the end of September 2009. It was found that the biomass combustion sources were well-correlated, but rather than biomass combustion emissions from one airshed influencing PM_{10} concentrations in the other, the common mechanism was likely to be the prevailing meteorological conditions. That is, particulate matter concentrations from biomass combustion emissions peak on cold, calm winter days in both airsheds because of the number of domestic solid fuel fires in use and the lack of dispersion. The biomass combustion concentrations in Nelson South were about 35 % higher on average than Tahunanui, probably because of the density of residential properties (and therefore emissions from domestic solid fuel fires) and the confinement of the Nelson South valley restricting dispersion of air pollution.

Marine aerosol contributions to PM_{10} were also highly correlated on a one-to-one basis in the two airsheds because marine aerosol is a true regional source, such that atmospheric concentrations at one site are exactly matched at the other site. Peak crustal matter contributions at both sites were found to occur under moderate to strong southwest winds and, while it is unlikely that crustal matter from one airshed is affecting PM_{10} concentrations in the other (not a regional source), the common mechanism is most probably re-entrained local dusts from wind action. Motor vehicle associated PM_{10} was not correlated because of the localised effect of motor vehicle emissions related to the proximity of a monitoring site to nearby roads. The secondary sulphate sources do not correlate either and it is suspected that the greatest influence on secondary sulphate in each of the airsheds is emissions from shipping sources in the Port Nelson area and shipping lane approaches.

12.0 REFERENCES

Ancelet, T., Davy, P.K., Mitchell, T., Trompetter, W.J., Markwitz, A., Weatherburn, D.C., 2012. Identification of particulate matter sources on an hourly time-scale in a wood burning community. Environmental Science and Technology 46, 4767-4774.

Ancelet, T., Davy, P.K., Trompetter, W.J., Markwitz, A., Weatherburn, D.C., 2011. Carbonaceous aerosols in an urban tunnel. Atmospheric Environment 45, 4463-4469.

Ancelet, T., Davy, P.K., Trompetter, W.J., Markwitz, A., Weatherburn, D.C., 2013a. Particulate matter sources on an hourly time-scale in a rural community during the winter. Journal of the Air & Waste Management Association.

Ancelet, T., Davy, P.K., Trompetter, W.J., Markwitz, A., Weatherburn, D.C., 2013b. Particulate matter sources on an hourly time-scale in a rural community during the winter. Journal of the Air and Waste Management Association.

Aryal, R.K., Lee, B.-K., Karki, R., Gurung, A., Baral, B., Byeon, S.-H., 2009. Dynamics of PM2.5 concentrations in Kathmandu Valley, Nepal. Journal of Hazardous Materials 168, 732-738.

Ault, A.P., Moore, M.J., Furutani, H., Prather, K.A., 2009. Impact of emissions from the Los Angeles Port region on San Diego air quality during regional transport events. Environmental Science and Technology 43, 3500-3506.

Begum, B.A., Hopke, P.K., Zhao, W.X., 2005. Source identification of fine particles in Washington, DC, by expanded factor analysis modeling. Environ. Sci. Technol. 39, 1129-1137.

Brown, S.G., Hafner, H.R., (2005). Multivariate Receptor Modelling Workbook. USEPA, Research Triangle Park, NC

Cahill, T.A., Eldred, R.A., Motallebi, N., Malm, W.C., 1989. Indirect measurement of hydrocarbon aerosols across the United States by nonsulfate hydrogen-remaining gravimetric mass correlations. Aerosol Sci. Technol. 10, 421-429.

Carslaw, D.C., (2012). The openair manual - open-source tools for analysing air pollution data. Manual for version 0.7-0. King's College London

Carslaw, D.C., Ropkins, K., 2012. openair - an R package for air quality data analysis. Environmental Modelling & Software 27-28, 52-61.

Chueinta, W., Hopke, P.K., Paatero, P., 2000. Investigation of sources of atmospheric aerosol at urban and suburban residential areas in Thailand by positive matrix factorization. Atmos. Environ. 34, 3319-3329.

Cohen, D., 1998. Characterisation of atmospheric fine particles using IBA techniques. Nucl. Inst. Meth. Phys. Res. B 136-138, 14-22.

Cohen, D., Bailey, G., Kondepudi, R., 1996. Elemental analysis by PIXE and other IBA techniques and their application to source fingerprinting of atmospheric fine particle pollution. Nucl. Inst. Meth. Phys. Res. B 109/110, 218-226.

Cohen, D., Taha, G., Stelcer, E., Garton, D., Box, G., (2000). The measurement and sources of fine particle elemental carbon at several key sites in NSW over the past eight years. *15th Clean Air Conference*, Clean air Society of Australia and New Zealand, Sydney

Cohen, D.D., 1999. Accelerator based ion beam techniques for trace element aerosol analysis. Advances in Environmental, Industrial and Process Control Technologies 1, 139-196.

Craw, D., Chappell, D., Reay, A., 2000. Environmental mercury and arsenic sources in fossil hydrothermal systems, Northland, New Zealand. Environmental Geology 39, 875-887.

Craw, D., Falconer, D., Youngson, J.H., 2003. Environmental arsenopyrite stability and dissolution: Theory, experiment, and field observations. Chemical Geology 199, 71-82.

Davy, P., K., (2007). Composition and Sources of Aerosol in the Wellington Region of New Zealand. PhD Thesis. *School of Chemical and Physical Sciences*, Victoria University of Wellington, Wellington

Davy, P., K., Trompetter, W., Markwitz, A., (2009a). Source apportionment of airborne particles at Wainuiomata, Lower Hutt. GNS Science Client Report 2009/188, Wellington

Davy, P., K., Trompetter, W., Markwitz, A., (2009b). Source apportionment of airborne particles in the Auckland region: 2008 Update. GNS Science Client Report 2009/165, Wellington

Davy, P., K., Trompetter, W., Markwitz, A., (2011a). Concentration, composition and sources of particulate matter in the Johnstone Hills Tunnel, Auckland. GNS Science Client Report 2010/296

Davy, P., K., Trompetter, W.J., Markwitz, A., (2007). Source apportionment of airborne particles in the Auckland region. GNS Science Client Report 2007/314, Wellington

Davy, P., K., Trompetter, W.J., Markwitz, A., (2008). Source apportionment of airborne particles at Seaview, Lower Hutt. GNS Science Client Report 2008/160, Wellington

Davy, P.K., Ancelet, T., Trompetter, W.J., Markwitz, A., Weatherburn, D.C., 2012. Composition and source contributions of air particulate matter pollution in a New Zealand suburban town. Atmospheric Pollution Research 3, 143-147.

Davy, P.K., Trompetter, W.J., Markwitz, A., (2010). Source apportionment of PM10 at Tahunanui, Nelson. GNS Science Client Report 2010/198

Davy, P.K., Trompetter, W.J., Markwitz, A., (2011b). Source apportionment of airborne particles in Dunedin. GNS Science Client Report 2011/131

Davy, P.K., Trompetter, W.J., Markwitz, A., (2011c). Source apportionment of airborne particles in the Auckland region: 2010 Analysis. GNS Science Client Report 2010/262, Wellington

Eberly, S., (2005). EPA PMF 1.1 User's Guide. USEPA

Fine, P.M., Cass, G.R., Simoneit, B.R., 2001. Chemical characterization of fine particle emissions from fireplace combustion of woods grown in the northeastern United States. Environ. Sci. Technol. 35, 2665-2675.

Fine, P.M., Cass, G.R., T., S.B.R., 2002. Chemical characterzation of fine particle emissions from the fireplace combustion of woods grown in the Southern United States. Environmental Science and Technology 36, 1442-1451.

Fitzgerald, J.W., 1991. Marine aerosols: A review. Atmospheric Environment - Part A General Topics 25, 533-545.

Garg, B.D., Cadle, S.H., Mulawa, P.A., Groblicki, P.J., Laroo, C., Parr, G.A., 2000. Brake wear particulate matter emissions. Environmental Science and Technology 34, 4463-4469.

Grange, S.K., Salmond, J.A., Trompetter, W.J., Davy, P.K., Ancelet, T., 2013. Effect of atmospheric stability on the impact of domestic wood combustion to air quality of a small urban township. Atmospheric Environment 70, 28-38.

Helsen, L., van den Bulck, E., 2003. Metal Retention in the Solid Residue after Low-Temperature Pyrolysis of Chromated Copper Arsenate (CCA)-Treated Wood. Environmental Engineering Science 20, 569-580.

Hopke, P.K., Xie, Y.L., Paatero, P., 1999. Mixed multiway analysis of airborne particle composition data. J. Chemomet. 13, 343-352.

Horvath, H., 1993. Atmospheric Light Absorption - A Review. Atmos. Environ, 27A, 293-317.

Horvath, H., 1997. Experimental calibration for aerosol light absorbtion measurements using the integrating plate method - Summary of the data. Aerosol Science 28, 2885-2887.

Jacobson, M.C., Hansson, H.C., Noone, K.J., Charlson, R.J., 2000. Organic atmospheric aerosols: review and state of the science. Reviews of Geophysics 38, 267-294.

Jeong, C.-H., Hopke, P.K., Kim, E., Lee, D.-W., 2004. The comparison between thermal-optical transmittance elemental carbon and Aethalometer black carbon measured at multiple monitoring sites. Atmos. Environ. 38, 5193.

Khalil, M.A.K., Rasmussen, R.A., 2003. Tracers of wood smoke. Atmospheric Environment 37, 1211-1222.

Kim, E., Hopke, P.K., 2008. Source characterization of ambient fine particles at multiple sites in the Seattle area. Atmospheric Environment 42, 6047-6056.

Kim, E., Hopke, P.K., Edgerton, E.S., 2003. Source identification of Atlanta aerosol by positive matrix factorization. J. Air Waste Manage. Assoc. 53, 731-739.

Kim, E., Hopke, P.K., Larson, T.V., Maykut, N.N., Lewtas, J., 2004. Factor analysis of Seattle fine particles. Aerosol Sci. Technol. 38, 724-738.

Lee, E., Chan, C.K., Paatero, P., 1999. Application of positive matrix factorization in source apportionment of particulate pollutants in Hong Kong. Atmos. Environ, 33, 3201-3212.

Lee, J.H., Yoshida, Y., Turpin, B.J., Hopke, P.K., Poirot, R.L., Lioy, P.J., Oxley, J.C., 2002. Identification of sources contributing to Mid-Atlantic regional aerosol. J. Air Waste Manag. Assoc. 52, 1186-1205.

Lide, D.R., CRC Handbook of Chemistry and Physics, 73rd ed, CRC Press Inc (1992).

Maenhaut, W., Malmqvist, K., G., Particle Induced X-ray Emission Analysis. In: R.V. Grieken, Editor, *Handbook of x-ray spectrometry*, Marcel Dekker Inc., Antwerp (2001).

Malm, W.C., Sisler, J.F., Huffman, D., Eldred, R.A., Cahill, T.A., 1994. Spatial and seasonal trends in particle concentration and optical extinction in the United States. J. Geophys. Res. Atmos. 99, 1347-1370.

Maxwell, J.A., Cambell, J.L., Teesdale, W.J., 1989. The Guelph PIXE software package. Nucl. Instr. And Meth. B 43, 218.

Maxwell, J.A., Teesdale, W.J., Cambell, J.L., 1995. The Guelph PIXE software package II. Nucl. Instr. And Meth. B 95, 407.

MfE, (2002). New Zealand Ambient Air Quality Guidelines. New Zealand Government, Wellington

Mitchell, T., Davy, P.K., Kim, N., Ancelet, T., Trompetter, W.J., (2013). Arsenic concentrations in a suburban New Zealand wood burning community. *21st Clean Air Society of Australia and New Zealand Conference*, Sydney

Paatero, P., 1997. Least squares formulation of robust non-negative factor analysis. Chemom. Intell. Lab. Syst. 18, 183-194.

Paatero, P., (2000). PMF User's Guide. University of Helsinki, Helsinki

Paatero, P., Hopke, P.K., 2002. Utilizing wind direction and wind speed as independent variables in multilinear receptor modeling studies. Chemometrics and Intelligent Laboratory Systems 60, 25-41.

Paatero, P., Hopke, P.K., 2003. Discarding or downweighting high-noise variables in factor analytic models. Analytica Chimica Acta 490, 277-289.

Paatero, P., Hopke, P.K., Begum, B.A., Biswas, S.K., 2005. A graphical diagnostic method for assessing the rotation in factor analytical models of atmospheric pollution. Atmospheric Environment 39, 193-201.

Paatero, P., Hopke, P.K., Song, X.H., Ramadan, Z., 2002. Understanding and controlling rotations in factor analytic models. Chemometrics and Intelligent Laboratory Systems 60, 253-264.

Polissar, A.V., Hopke, P.K., Paatero, P., Malm, W.C., Sisler, J.F., 1998. Atmospheric aerosol over Alaska 2. Elemental composition and sources. J. Geophys. Res. Atmos. 103, 19045-19057.

Qin, Y., Kim, E., Hopke, P.K., 2006. The concentrations and sources of PM2.5 in metropolitan New York City. Atmospheric Environment 40, Supplement 2, 312-332.

Ramadan, Z., Eickhout, B., Song, X.-H., Buydens, L.M.C., Hopke, P.K., 2003. Comparison of Positive Matrix Factorization and Multilinear Engine for the source apportionment of particulate pollutants. Chemomet. Intellig. Lab. Syst. 66, 15-28.

Robinson, B., Clothier, B., Bolan, N., Mahimairaja, S., Greven, M., Moni, C., Marchetti, M., Van den Dijssel, C., Milne, G., (2004). Arsenic in the New Zealand Environment. *3rd Australian New Zealand Soils Conference*, Sydney, Australia

Salma, I., Chi, X., Maenhaut, W., 2004. Elemental and organic carbon in urban canyon and background environments in Budapest, Hungary. Atmos. Environ. 38, 27-36.

Schauer, J.J., Lough, G.C., Shafer, M.M., Christensen, W.F., Arndt, M.F., Deminter, J.T., Park, J.-S., 2006. Characterisation of metals emitted from motor vehicles. Research Report 133. Health Effects Institute, Boston.

Scott, A.J., (2006). Source Apportionment and Chemical Characterisation of Airborne Fine Particulate Matter in Christchurch, New Zealand. University of Canterbury, Christchurch

Shah, P., Strezov, V., Stevanov, C., Nelson, P.F., 2006. Speciation of Arsenic and Selenium in Coal Combustion Productsâ€ Energy & Fuels 21, 506-512.

Simmons, S.F., Browne, P.R.L., 2000. Hydrothermal minerals and precious metals in the Broadlands-Ohaaki geothermal system: Implications for understanding low-sulfidation epithermal environments. Economic Geology 95, 971-999.

Song, X.H., Polissar, A.V., Hopke, P.K., 2001. Sources of fine particle composition in the northeastern US. Atmospheric Environment 35, 5277-5286.

Team, R.D.C., (2011). R: A language and environment for statistical computing. R Foundation for Statistical Computing, Vienna, Austria

Thorpe, A., Harrison, R.M., 2008. Sources and properties of non-exhaust particulate matter from road traffic: A review. Science of the Total Environment 400, 270-282.

Trompetter, W., Markwitz, A., Davy, P., K., 2005. Air particulate research capability at the New Zealand Ion Beam Analysis Facility using PIXE and IBA Techniques. International Journal of PIXE 15, 249-255.

Trompetter, W.J., (2004). Ion Beam Analysis results of air particulate filters from the Wellington Regional Council. Geological and Nuclear Sciences Limited, Wellington

Trompetter, W.J., Davy, P.K., (2005). Air Particulate Research Capability at the New Zealand Ion Beam Analysis facility using PIXE and IBA techniques. *BioPIXE 5*, Wellington, New Zealand

Trompetter, W.J., Davy, P.K., Markwitz, A., 2010. Influence of environmental conditions on carbonaceous particle concentrations within New Zealand. Journal of Aerosol Science 41, 134-142.

USEPA, (2008). EPA Positive Matrix Factorization (PMF) 3.0 Fundamentals and User Guide. USEPA National Exposure Research Laboratory: Research Triangle Park, NC

Watson, J.G., Zhu, T., Chow, J.C., Engelbrecht, J., Fujita, E.M., Wilson, W.E., 2002. Receptor modeling application framework for particle source apportionment. Chemosphere 49, 1093-1136.

WHO, (2006). Air quality guidelines. Global update 2005.

Wilton, E., (2006). Air Emission Inventory - Nelson 2006.

APPENDICES

This page is intentionally left blank.

APPENDIX 1: ANALYSIS TECHNIQUES

A1.1 ELEMENTAL ANALYSIS OF AIRBORNE PARTICLES

A1.1.1 Ion beam analysis

Ion beam analysis (IBA) was used to measure the elemental concentrations of particulate matter on the size-resolved filter samples from the St. Vincent Street monitoring site shown in Figure 2.1. IBA is based on the measurement of characteristic X-rays and γ-rays of an element produced by ion-atom interactions using high-energy protons in the 2–5 million electron volt (MeV) range. IBA is a mature and well developed science, with many research groups around the world using IBA in a variety of routine analytical applications, including the analysis of atmospheric aerosols (Maenhaut and Malmqvist, 2001; Trompetter et al., 2005). IBA techniques do not require sample preparation and are fast, non-destructive and sensitive (Cohen, 1999; Maenhaut and Malmqvist, 2001; Trompetter et al., 2005).

IBA measurements for this study were carried out at the New Zealand IBA facility operated by GNS Science. Figure A1.1 shows the PM analysis chamber with its associated X-ray, γ-ray and particle detectors for Proton-Induced X-ray Emission (PIXE), Proton-Induced Gamma-ray Emission (PIGE), Proton Elastic Scattering Analysis (PESA) and Rutherford BackScattering (RBS) measurements.

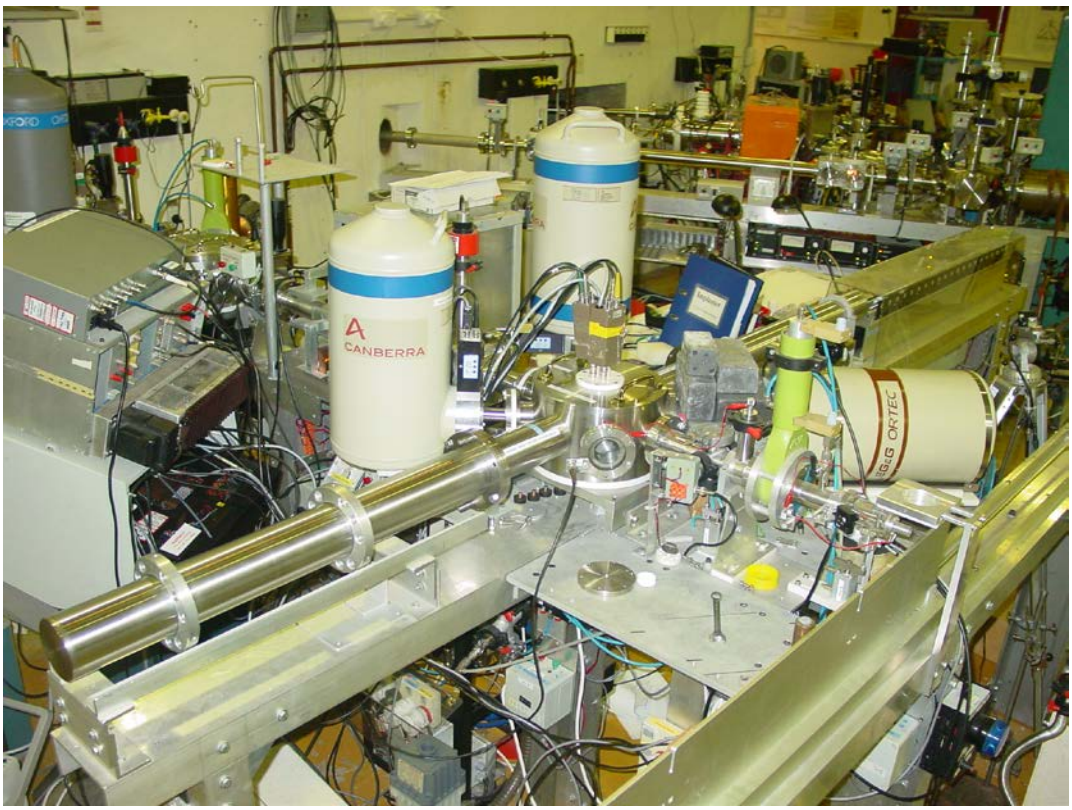

Figure A 1.1 Particulate matter analysis chamber with its associated detectors.

The following sections provide a generalised overview of the IBA techniques used for elemental analysis and the analytical setup at GNS Science (Cohen, 1998; Cohen et al., 1996; Trompetter, 2004; Trompetter and Davy, 2005). Figure A2.2 presents a schematic diagram of the typical experimental setup for IBA of air particulate filters at GNS Science.

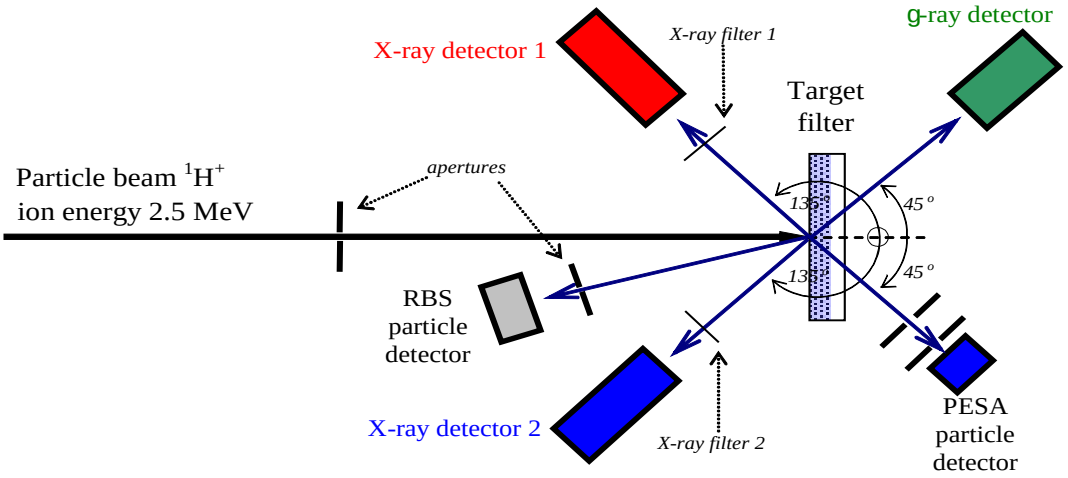

Figure A 1.2 Schematic of the typical IBA experimental setup at GNS Science.

Particle-induced X-ray emission

Particle induced X-ray emission (PIXE), is used to determine elemental concentrations heavier than neon by exposing the filter samples to a proton beam accelerated to 2.5 million volts (MeV) by the GNS 3 MeV van-de-Graaff accelerator. When high energy protons interact with atoms in the sample, characteristic X-rays (from each element) are emitted by ion-electron processes. These X-rays are recorded in an energy spectrum. While all elements heavier than boron emit K X-rays, their production become too few to satisfactorily measure elements heavier than strontium. Elements heavier than strontium are detected via their lower energy L X-rays. The X-rays are detected using a Si(Li) detector and the pulses from the detector are amplified and recorded in a pulse height analyser. In practice, sensitivities are further improved for the lighter elements by using two X-ray detectors, one for light element X-rays and the other for heavier element X-rays, each with different filtering and collimation. Figure A1.3 shows an example of a PIXE spectrum for airborne particles collected on a filter and analysed at the GNS IBA facility.

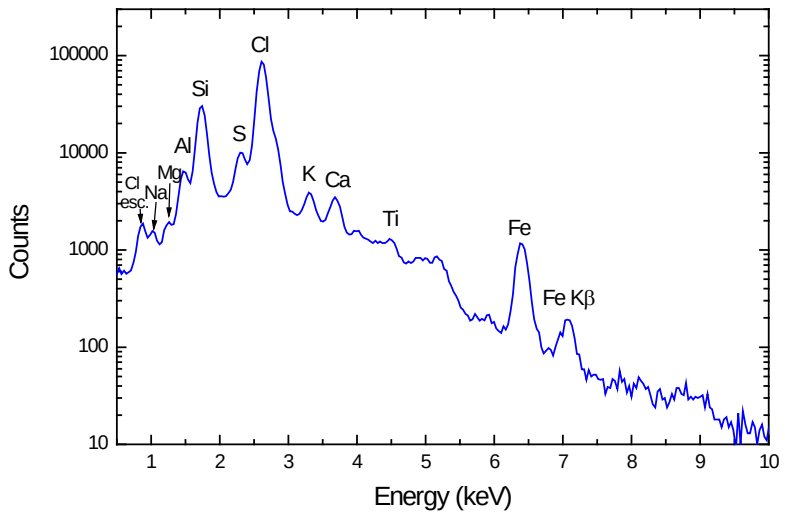

Figure A 1.3 Typical PIXE spectrum for an aerosol sample analysed by PIXE.

As the PIXE spectrum consists of many peaks from different elements (and a Bremsstrahlung background), some of them overlapping, the spectrum is analysed with quantitative X-ray analysis software. In the case of this study, Gupix Software was used to perform the deconvolution with high accuracy (Maxwell et al., 1989; Maxwell et al., 1995). The number of pulses (counts) in each peak for a given element is used by the Gupix software to calculate the concentration of that element. The background and neighbouring elements determine the statistical error and the limit of detection. Note, that Gupix provides a specific statistical error and limit of detection (LOD) for each element in any filter, which is essential for source apportionment studies.

Typically 20–25 elements from Mg–Pb are routinely determined above their respective LODs. Sodium (and fluorine) was determined using both PIXE and PIGE (see next section). Specific experimental details, where appropriate, are given in the results and analysis section.

Particle-induced gamma-ray emission

Particle Induced Gamma-Ray Emission (PIGE) refers to γ-rays produced when an incident beam of protons interacts with the nuclei of an element in the sample (filter). During the de-excitation process, nuclei emit γ-ray photons of characteristic energies specific to each element. Typical elements measured with γ-ray are:

Element	*nuclear reaction*	*gamma ray energy (keV)*
Sodium	$^{23}Na(p,\alpha\gamma)^{20}Ne$	440, 1634
Fluorine	$^{19}F(p,\alpha\gamma)^{16}O$	197, 6129

Gamma rays are higher in energy than X-rays and are detected with a germanium detector. Measurements of a light element such as sodium can be measured more accurately using PIGE because the γ-rays are not attenuated to the same extent in the filter matrix or the detector material, a problem in the measurement of low energy X-rays of sodium. Figure A.4 shows a typical PIGE spectrum.

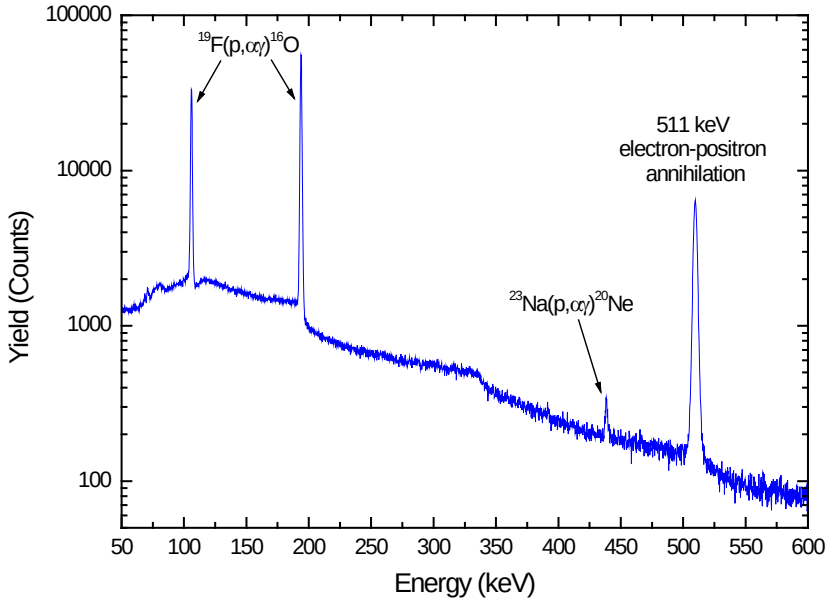

Figure A 1.4 Typical PIGE spectrum for an aerosol sample.

Particle elastic scattering analysis

Particle Elastic Scattering Analysis (PESA) allows hydrogen to be measured quantitatively in air particulate matter collected on a filter providing the filter material contains no or little hydrogen atoms, e.g. Teflon filters. Note that Teflon contains fluorine that introduces a significant background in the X-ray spectra which increases the limits of detection (LODs) of PIXE. Hydrogen can be detected by measuring the elastically scattered protons in a forward direction for a proton beam passing through the air particulate matter filter. At a forward scattering angle of 45º, the protons are elastically scattered from hydrogen with 50 % of the initial proton energy (i.e. for an incident beam of 2.50 MeV the energy of protons scattered off hydrogen is 1.25 MeV) which is much less energy than the energy of the protons scattered from the other heavier elements in the filter. Thus, in the PESA spectrum of a sample filter, a peak corresponding to protons elastically scattered from hydrogen occurs separated from the protons elastically scattered from the other atoms in the air particulate matter filter. The air particulate matter filter is thin enough for this measurement when the hydrogen PESA peak is separated from the noise at the low end of the spectrum and from protons elastically scattered from heavier atoms at the high energy end of the spectrum. For Teflon filters analysed with a 2.5 MeV proton beam, proton scattering energies for PESA are shown in Table A1.1 and Figure A1.5 presents a typical PESA spectrum.

Table A 1.1 Proton scattering energies of various elements for a 2.5MeV proton beam

Element	Energy detected at 45° forward (MeV)
H	1.250
C	2.380
O	2.410
F	2.424
Fe	2.474

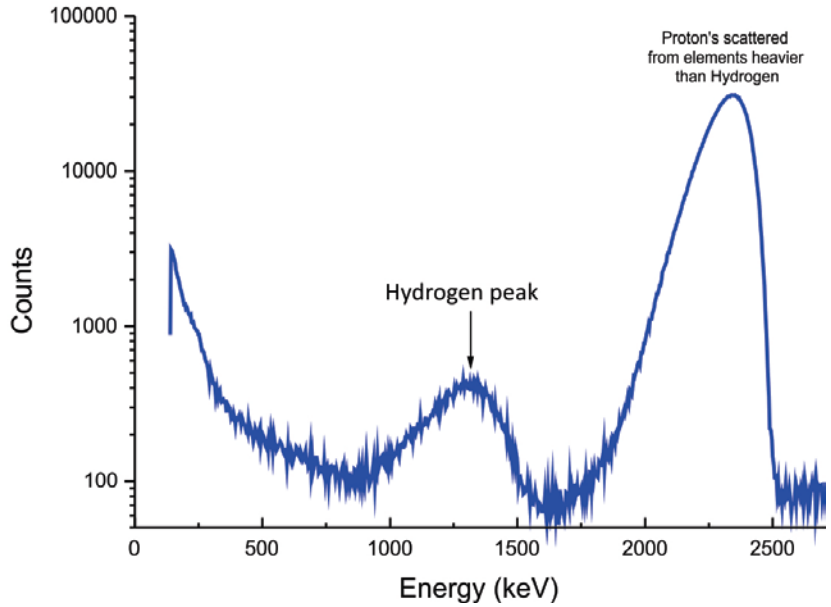

Figure A 1.5 PESA spectrum for an aerosol sample showing the hydrogen peak at 1.250 MeV.

Because PESA, and IBA measurements in general, are conducted in high vacuum (residual gas pressure better than 10^{-6} mbar), free water vapour and VOCs are volatilised before analysis and only bound hydrogen is detected (e.g. SVOCs and ammonium ions) (Cohen, 1999). PESA was used to determine hydrogen concentrations in all samples from St. Vincent Street.

IBA data reporting

Most filters used to collect particulate matter samples for IBA analysis are sufficiently thin that the ion beam penetrates the entire depth producing a quantitative analysis of elements present. Because of the thin nature of the air particulate matter filters, the concentrations reported from the IBA analyses are therefore in aerial density units (ng cm^{-2}) and the total concentration of each element on the filters is calculated by multiplying with the exposed area of the filter. Typically the exposed area is 11.95 cm^2 for filters collected with the Partisol sampler used in this study. For example, to convert from Cl (ng cm^{-2}) into Cl (ng m^{-3}) for filter samples, the equation is:

$$\text{Cl (ng m}^{-3}\text{)} = 11.95(\text{cm}^2) \times \text{Cl (ng cm}^{-2}\text{) / Vol(m}^3\text{)} \quad \text{(A1.1)}$$

Limits of detection for elements determined by IBA

The exact limits of detection for reporting the concentration of each element depends on a number of factors such as:

- the method of detection;
- filter composition;
- sample composition;
- the detector resolution;
- spectral interference from other elements.

To determine the concentration of each element the background is subtracted and peak areas fitted and calculated. The background occurs through energy loss, scattering and interactions of the ion beam as it passes through the filter material or from γ-rays produced in the target and scattered in the detector system (Cohen, 1999). The peaks of elements in spectra that have interferences or backgrounds from other elements present in the air particulate matter, or filter matrix itself, will have higher limits of detection. Choice of filter material is an important consideration with respect to elements of interest as is avoiding sources of contamination. The GNS IBA laboratory routinely runs filter blanks to correct for filter derived analytical artefacts as part of their QA/QC procedures. Figure A1.6 shows the LODs typically achieved by PIXE for each element at the GNS IBA facility. All IBA elemental concentrations determined in this work were accompanied by their respective LODs. The use of elemental LODs is important in receptor modeling applications and is discussed further in Section A1.4.2.

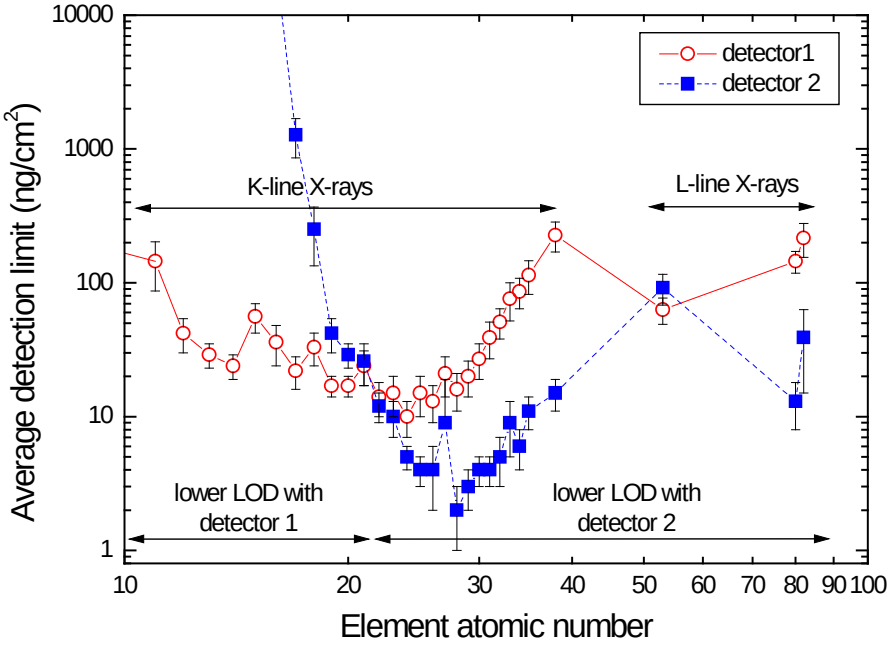

Figure A 1.6 Elemental limits of detection for PIXE routinely achieved as the GNS IBA facility for air filters.

A1.2 BLACK CARBON MEASUREMENTS

Black carbon (BC) has been studied extensively, but it is still not clear to what degree it is elemental carbon (EC (or graphitic) C(0)) or high molecular weight refractory weight organic species or a combination of both (Jacobson et al., 2000). Current literature suggests that BC is likely a combination of both, and that for combustion sources such as petrol and diesel fuelled vehicles and biomass combustion (wood burning, coal burning), EC and organic carbon compounds (OC) are the principle aerosol components emitted (Fine et al., 2001; Jacobson et al., 2000; Salma et al., 2004; Watson et al., 2002).

Determination of carbon (soot) on filters was performed by light reflection to provide the BC concentration. The absorption and reflection of visible light on particles in the atmosphere or collected on filters is dependent on the particle concentration, density, refractive index and size. For atmospheric particles, BC is the most highly absorbing component in the visible light spectrum with very much smaller components coming from soils, sulphates and nitrate (Horvath, 1993, 1997). Hence, to the first order it can be assumed that all the absorption on atmospheric filters is due to BC. The main sources of atmospheric BC are anthropogenic combustion sources and include biomass burning, motor vehicles and industrial emissions (Cohen et al., 2000). Cohen and co-workers found that BC is typically 10 – 40 % of the fine mass ($PM_{2.5}$) fraction in many urban areas of Australia.

When measuring BC by light reflection/transmission, light from a light source is transmitted through a filter onto a photocell. The amount of light absorption is proportional to the amount of black carbon present and provides a value that is a measure of the black carbon on the filter. Conversion of the absorbance value to an atmospheric concentration value of BC requires the use of an empirically derived equation (Cohen et al., 2000):

$$BC\ (\mu g\ cm^{-2}) = (100/2(F\varepsilon))\ \ln[R_0/R] \qquad (A1.2)$$

where:

ε is the mass absorbent coefficient for BC (m^2 g^{-1}) at a given wavelength;

F is a correction factor to account for other absorbing factors such as sulphates, nitrates, shadowing and filter loading. These effects are generally assumed to be negligible and F is set at 1.00;

R_0, R are the pre- and post-reflection intensity measurements, respectively.

Black carbon was measured at GNS Science using the M43D Digital Smoke Stain Reflectometer. The following equation (from Willy Maenhaut, Institute for Nuclear Sciences, University of Gent Proeftuinstraat 86, B-9000 GENT, Belgium) was used for obtaining BC from reflectance measurements on Nucleopore polycarbonate filters or Pall Life Sciences Teflon filters:

$$BC\ (\mu g\ cm^{-2}) = [1000 \times LOG(R_{blank}/R_{sample}) + 2.39] / 45.8 \qquad (A1.3)$$

where:

R_{blank}: the average reflectance for a series of blank filters; R_{blank} is close (but not identical) to 100. GNS always use the same blank filter for adjusting to 100.

R_{sample}: the reflectance for a filter sample (normally lower than 100).

With: 2.39 and 45.8 constants derived using a series of 100 Nuclepore polycarbonate filter samples which served as secondary standards; the BC loading (in µg cm^{-2}) for these samples had been determined by Prof. Dr. M.O. Andreae (Max Planck Institute of Chemistry, Mainz, Germany) relative to standards that were prepared by collecting burning acetylene soot on filters and determining the mass concentration gravimetrically (Trompetter, 2004).

A1.3 POSITIVE MATRIX FACTORISATION

Positive matrix factorisation (PMF) is a linear least-squares approach to factor analysis and was designed to overcome the receptor modeling problems associated with techniques like principal components analysis (PCA) (Paatero et al., 2005). With PMF, sources are constrained to have non-negative species concentrations, no sample can have a negative source contribution and error estimates for each observed data point are used as point-by-point weights. This feature is a distinct advantage, in that it can accommodate missing and below detection limit data that is a common feature of environmental monitoring results (Song et al., 2001). In fact, the signal to noise ratio for an individual elemental measurement can have a significant influence on a receptor model and modeling results. For the weakest (closest to detection limit) species, the variance may be entirely from noise (Paatero and Hopke, 2002). Paatero and Hopke strongly suggest down-weighting or discarding noisy variables that are always below their detection limit or species that have a lot of error in their measurements relative to the magnitude of their concentrations (Paatero and Hopke, 2003). The distinct advantage of PMF is that mass concentrations can be included in the model and the results are directly interpretable as mass contributions from each factor (source).

A1.3.1 PMF model outline

The mathematical basis for PMF is described in detail by Paatero (Paatero, 1997, 2000). Briefly, PMF uses a weighted least-squares fit with the known error estimates of measured elemental concentrations used to derive the weights. In matrix notation this is indicated as:

$$X = GF + E \qquad \text{(A1.5)}$$

where:

X is the known *n* x *m* matrix of *m* measured elemental species in *n* samples;

G is an *n* x *p* matrix of source contributions to the samples;

F is a *p* x *m* matrix of source compositions (source profiles).

E is a residual matrix – the difference between measurement *X* and model *Y.*

E can be defined as a function of factors *G* and *F*:

$$e_{ij} = x_{ij} - y_{ij} = x_{ij} - \sum_{k=1}^{p} g_{ik} f_{kj} \qquad \text{(A1.6)}$$

where:

i = 1,……,*n* elements

j = 1,……,*m* samples

k = 1,……,*p* sources

PMF constrains all elements of *G* and *F* to be non-negative, meaning that elements cannot have negative concentrations and samples cannot have negative source contributions as in real space. The task of PMF is to minimise the function *Q* such that:

$$Q(E) = \sum_{i=1}^{n} \sum_{j=1}^{m} (e_{ik} / \sigma_{kj})^2 \qquad \text{(A1.7)}$$

where σ_{ij} is the error estimate for x_{ij}. Another advantage of PMF is the ability to handle extreme values typical of air pollutant concentrations as well as true outliers that would normally skew PCA. In either case, such high values would have significant influence on the solution (commonly referred to as leverage). PMF has been successfully applied to receptor modeling studies in a number of countries around the world (Begum et al., 2005; Chueinta et al., 2000; Hopke et al., 1999; Jeong et al., 2004; Kim et al., 2003; Kim et al., 2004; Lee et al., 1999; Lee et al., 2002; Song et al., 2001) including New Zealand (Ancelet et al., 2012; Davy, 2007; Davy et al., 2009a, b; Davy et al., 2007, 2008; Scott, 2006).

12.1.1 PMF model used

Two programs have been written to implement different algorithms for solving the least squares PMF problem, these are PMF2 and EPAPMF, which incorporates the Multilinear Engine (ME-2) (Hopke et al., 1999; Ramadan et al., 2003). In effect, the EPAPMF program provides a more flexible framework than PMF2 for controlling the solutions of the factor analysis with the ability of imposing explicit external constraints.

This study used EPAPMF 3.0 (version 3.0.2.2), which incorporates a graphical user interface (GUI) based on the ME-2 program. Both PMF2 and EPAPMF programs can be operated in a robust mode, meaning that "outliers" are not allowed to overly influence the fitting of the contributions and profiles (Eberly, 2005). The user specifies two input files, one file with the concentrations and one with the uncertainties associated with those concentrations. The methodology for developing an uncertainty matrix associated with the elemental concentrations for this work is discussed in Section A1.4.2.

12.1.2 PMF model inputs

The PMF programs provide the user with a number of choices in model parameters that can influence the final solution. Two parameters, the 'signal-to-noise ratio' and the 'species category' are of particular importance and are described below.

Signal-to-noise ratio - this is a useful diagnostic statistic estimated from the input data and uncertainty files using the following calculation:

$$(1/2)\sqrt{\sum_{i=1}^{n}(x_{ij})^2 / \sum_{i=1}^{n}(\sigma_{ij})^2} \qquad \text{(A1.8)}$$

Where x_{ij} and σ_{ij} are the concentration and uncertainty, respectively, of the i^{th} element in the j^{th} sample. Smaller signal-to-noise ratios indicate that the measured elemental concentrations are generally near the detection limit and the user should consider whether to include that species in the receptor model or at least strongly down-weight it (Paatero and Hopke, 2003). The signal-to-noise ratios (S/N ratio) for each element are reported alongside other statistical data in the results section.

Species category - this enables the user to specify whether the elemental species should be considered:

- Strong – whereby the element is generally present in concentrations well above the LOD (high signal to noise ratio) and the uncertainty matrix is a reasonable representation of the errors.
- Weak – where the element may be present in concentrations near the LOD (low signal to noise ratio); there is doubt about some of the measurements and/or the error estimates; or the elemental species is only detected some of the time. If 'Weak' is chosen EPA.PMF increases the user-provided uncertainties for that variable by a factor of 3.
- Bad – that variable is excluded from the model run.

For this work, an element with concentrations at least 3 times above the LOD, a high signal to noise ratio (> 2) and present in all samples was considered 'Strong'. Variables were labelled as weak if their concentrations were generally low, had a low signal to noise ratio, were only present in a few samples or there was a lower level of confidence in their measurement. Mass concentration gravimetric measurements and BC were also down weighted as 'Weak' because their concentrations are generally several orders of magnitude above other species, which can have the tendency to 'pull' the model. Paatero and Hopke recommend that such variables be down weighted and that it doesn't particularly affect the model fitting if those variables are from real sources (Paatero and Hopke, 2003). What does affect the model severely is if a dubious variable is over-weighted. Elements that had a low

signal to noise ratio (< 0.2), or had mostly missing (zero) values, or were doubtful for any reason, were labelled as 'Bad' and were subsequently not included in the analyses.

If the model is appropriate for the data and if the uncertainties specified are truly reflective of the uncertainties in the data, then *Q* (according to Eberly) should be approximately equal to the number of data points in the concentration data set (Eberly, 2005):

Theoretical Q = # samples **x** # species measured (A1.9)

However, a slightly different approach to calculating the Theoretical *Q* value was recommended by (Brown and Hafner, 2005), which takes into account the degrees of freedom in the PMF model and the additional constraints in place for each model run. This theoretical *Q* calculation Q_{th} is given as:

Q_{th} = *(# samples **x** # good species)+[(# samples **x** # weak species)/3] - (# samples **x** factors estimated)* (A1.10)

Both approaches have been taken into account for this study and it is likely that the actual value lies somewhere between the two.

In PMF, it is assumed that only the x_{ij}'s are known and that the goal is to estimate the contributions (g_{ik}) and the factors (or profiles) (f_{kj}). It is assumed that the contributions and mass fractions are all non-negative, hence the "constrained" part of the least-squares. Additionally, EPAPMF allows the user to say how much uncertainty there is in each x_{ij}. Species-days with lots of uncertainty are not allowed to influence the estimation of the contributions and profiles as much as those with small uncertainty, hence the "weighted" part of the least squares and the advantage of this approach over PCA.

Diagnostic outputs from the PMF models were used to guide the appropriateness of the number of factors generated and how well the receptor modelling was accounting for the input data. Where necessary, initial solutions have been 'rotated' to provide a better separation of factors (sources) that were considered physically reasonable (Paatero et al., 2002). Each PMF model run reported in this study is accompanied by the modelling statistics along with comments where appropriate.

A1.4 DATASET QUALITY ASSURANCE

Quality assurance of sample elemental datasets is vital so that any dubious samples, measurements and outliers are removed as these will invariably affect the results of receptor modelling. In general, the larger the dataset used for receptor modelling, the more robust the analysis. The following sections describe the methodology used to check data integrity and provide a quality assurance process that ensured that the data being used in subsequent factor analysis was as robust as possible.

A1.4.1 Mass reconstruction and mass closure

Once the sample analysis for the range of analytes has been carried out, it is important to check that total measured mass does not exceed gravimetric mass (Cohen, 1999). Ideally, when elemental analysis and organic compound analysis has been undertaken on the same sample one can reconstruct the mass using the following general equation for ambient samples as a first approximation (Cahill et al., 1989; Cohen, 1999; Malm et al., 1994):

Reconstructed mass = [Soil] + [OC] + [BC] + [Smoke] + [Sulphate] + [Seasalt] (A1.11)

where:

[Soil] = 2.20[Al] + 2.49[Si] + 1.63[Ca] + 2.42[Fe] + 1.94[Ti]

[OC] = Σ[Concentrations of organic compounds]

[BC] = Concentration of black carbon (soot)

[Smoke] = [K] − 0.6[Fe]

[Seasalt] = 2.54[Na]

[Sulphate] = 4.125[S]

The reconstructed mass (RCM) is based on the fact that the six composite variables or 'pseudo' sources given in equation A1.11 are generally the major contributors to fine and coarse particle mass and are based on geochemical principles and constraints. The [Soil] factor contains elements predominantly found crustal matter (Al, Si, Ca, Fe, Ti) and includes a multiplier to correct for oxygen content and an additional multiplier of 1.16 to correct for the fact that three major oxide contributors (MgO, K_2O, Na_2O) carbonate and bound water are excluded from the equation. Organic carbon concentrations [OC] were estimated using equation A1.12, where PESA was used to determine the hydrogen concentration on filters. In this case, total hydrogen on the filter was assumed to be comprised mainly of H from organic material and ammonium sulphate (assuming sulphate is in fully neutralised form) and therefore organic content (designated [OMH]) was calculated from total H by the following equation (Cohen, 1999; Malm et al., 1994):

[OMH] = 11([H] – 0.25[S]) (A1.12)

Equation A1.12 assumes that average particulate organic matter is composed of 11% H, 71% C, and 20 % O by weight. Where a measure of [OC] was not available, it was assumed that it composed part of the 'remaining mass' (the difference between RCM and gravimetric mass) that includes water and nitrates as major components (Cahill et al., 1989).

[BC] is the concentration of black carbon, measured in this case by light reflectance/absorbance. [Smoke] represents K not included as part of crustal matter and tends to be an indicator of biomass burning.

[Seasalt] represents the marine aerosol contribution and assumes that the NaCl weight is 2.54 times the Na concentration. Na is used as it is well known that Cl can be volatilised from aerosol or from filters in the presence of acidic aerosol, particularly in the fine fraction via the following reactions (Lee et al., 1999):

$$NaCl(p) + HNO_3(ag) \rightarrow NaNO_3(p) + HCL(g) \quad \text{(A1.13)}$$

$$2NaCl(p) + H_2SO_4(ag) \rightarrow Na_2SO_4(p) + 2HCL(g) \quad \text{(A1.14)}$$

Alternatively, where Cl loss is likely to be minimal, such as in the coarse fraction or for both size fractions near coastal locations and relatively clean air in the absence of acid aerosol, then the reciprocal calculation of [Seasalt] = 1.65[Cl] can be substituted, particularly where Na concentrations are uncertain.

Most fine sulphate particles are the result of oxidation of SO_2 gas to sulphate particles in the atmosphere (Malm et al., 1994). It is assumed that sulphate is present in fully neutralised form as ammonium sulphate. [Sulphate] therefore represents the ammonium sulphate contribution to aerosol mass with the multiplicative factor of 4.125[S] to account for ammonium ion and oxygen mass (i.e. $(NH_4)_2SO_4$ = ((14 + 4)2 + 32 + (16x4)/32)).

Additionally, the sulphate component not associated with seasalt can be calculated from equation A1.15 (Cohen 1999):

Non-seasalt sulphate (NSS-Sulphate) = 4.125 ($[S_{tot}]$ - 0.0543[Cl]) (A1.15)

Where the sulphur concentrations contributed by seasalt are inferred from the chlorine concentrations, i.e. [S/Cl]seasalt = 0.0543 and the factor of 4.125 assumes that the sulphate has been fully neutralised and is generally present as $(NH_4)_2SO_4$ (Cahill, Eldred *et al*. 1990; Malm, Sisler *et al*. 1994; Cohen 1999).

The RCM and mass closure calculations using the pseudo-source and pseudo-element approach are a useful way to examine initial relationships in the data and how the measured mass of species in samples compares to gravimetric mass. Note that some scatter is possible because not all aerosols are necessarily measured and accounted for, such as all OC, ammonium species, nitrates and unbound water.

As a quality assurance mechanism, those samples for which RCM exceeded gravimetric mass or where gravimetric mass was significantly higher than RCM were examined closely to assess gravimetric mass and IBA data. Where there was significant doubt either way, those samples were excluded from the receptor modeling analysis. The reconstructed mass calculations and pseudo source estimations are presented in the appendices at the end of this report.

A1.4.2 Dataset preparation

Careful preparation of a dataset is required because serious errors in data analysis and receptor modeling results can be caused by erroneous individual data values. The general methodology followed for dataset preparation was as recommended by (Brown and Hafner, 2005). For this study, all data were checked for consistency with the following parameters:

1. Individual sample collection validation;
2. Gravimetric mass validation;
3. Analysis of RCM versus gravimetric mass to ensure RCM < gravimetric;
4. Identification of unusual values including noticeably extreme values and values that normally track with other species (e.g. Al and Si) but deviate in one or two samples. Scatter plots and time series plots were used to identify unusual values. One-off events such as fireworks displays, forest fires or vegetative burn-offs may affect a receptor model as it is forced to find a profile that matches only that day;
5. Species were included in a dataset if at least 70 % of data was above the LOD and signal-to-noise ratios were checked to ensure data had sufficient variability. Important tracers of a source where less than 70 % of data was above the LOD were included but model runs with and without the data were used to assess the effect;
6. For PCA, % errors and signal-to-noise ratios were used as a guide as to whether a species was too ‘noisy’ to include in an analysis.

In practice during data analyses, the above steps were a reiterative process of cross checking as issues were identified and corrected for, or certain data excluded and the effects of this were then studied.

PMF data matrix population

The following steps were followed to produce a final dataset for use in the PMF receptor model (Brown and Hafner, 2005).

Below detection limit data: For given values, the reported concentration used and the corresponding uncertainty checked to ensure it had a high value.

Missing data: Substituted with the dataset median value for that species.

PMF uncertainty matrix population

Uncertainties can have a large effect on model results so that they must be carefully compiled. The effect of underestimating uncertainties can be severe, while overestimating uncertainties does not do too much harm (Paatero and Hopke, 2003).

Uncertainties for data: Data was multiplied by % fit error provided by IBA analysis to produce an uncertainty in ng m^{-3}.

Below detection limit data: Below detection limit data was generally provided with a high % fit error and this was used to produce an uncertainty in ng m^{-3}. Zero data was given a corresponding uncertainty value of 4×LOD.

Missing data: Uncertainty was calculated as 4 × median value over the entire species dataset.

BC: Because of high mass values for BC, the uncertainties were generated by multiplying mass values by a factor of four to down-weight the variable.

PM gravimetric mass: Uncertainty given as 4 × mass value to down-weight the variable.

Reiterative model runs were used to examine the effect of including species with high uncertainties or low concentrations. In general it was found that the initial uncertainty estimations were sufficient and that adjusting the 'additional modelling uncertainty' function accommodated any issues with modelled variables such as those with residuals outside ± 3 standard deviations.

APPENDIX 2: ELEMENTAL CORRELATION PLOTS FOR PM_{10} AND $PM_{2.5}$

Figures A2.1 and A2.2 present elemental correlation plots for PM_{10} and $PM_{2.5}$ samples collected at St. Vincent Street.

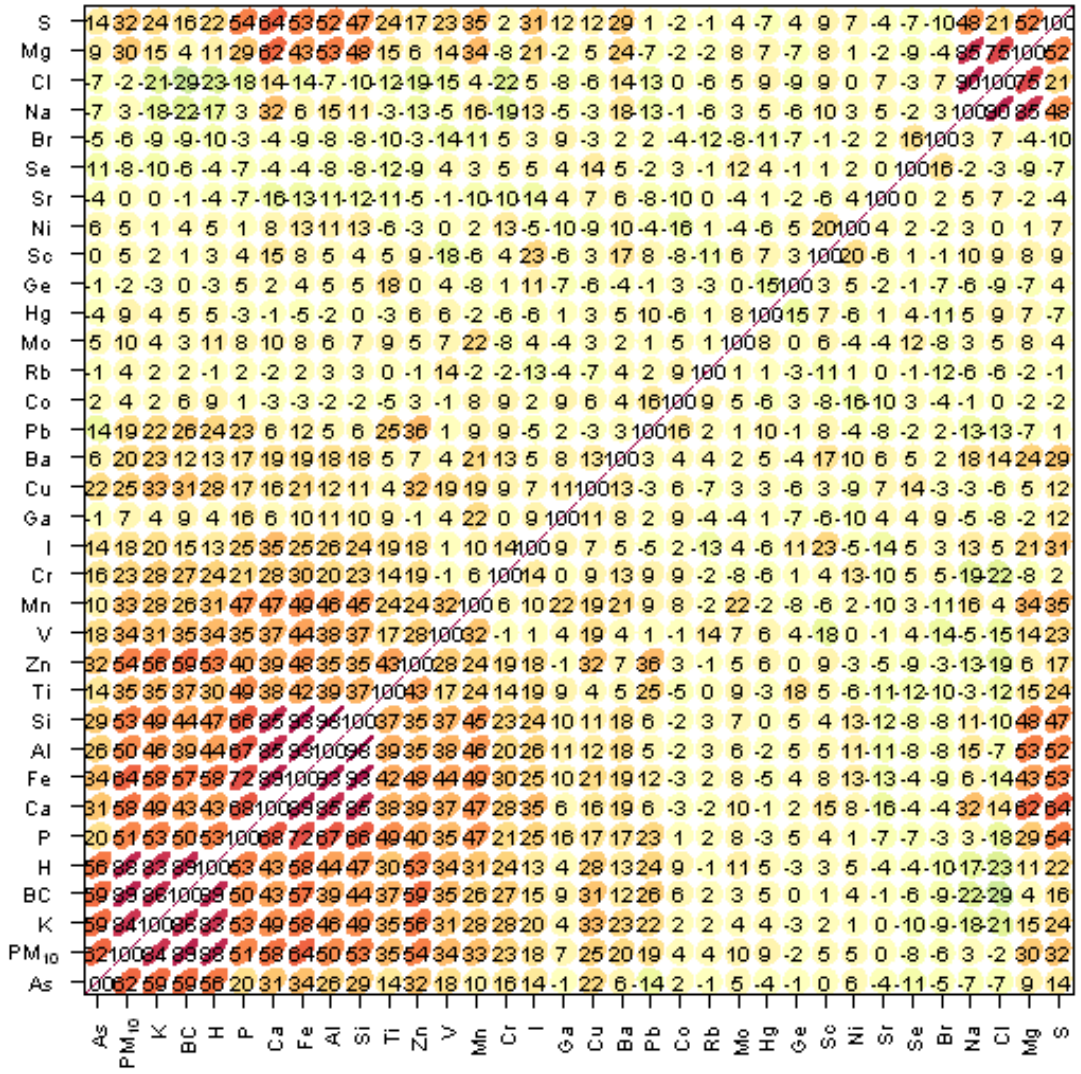

Figure A 2.1 Elemental correlation plot for PM_{10} samples collected at St. Vincent Street.

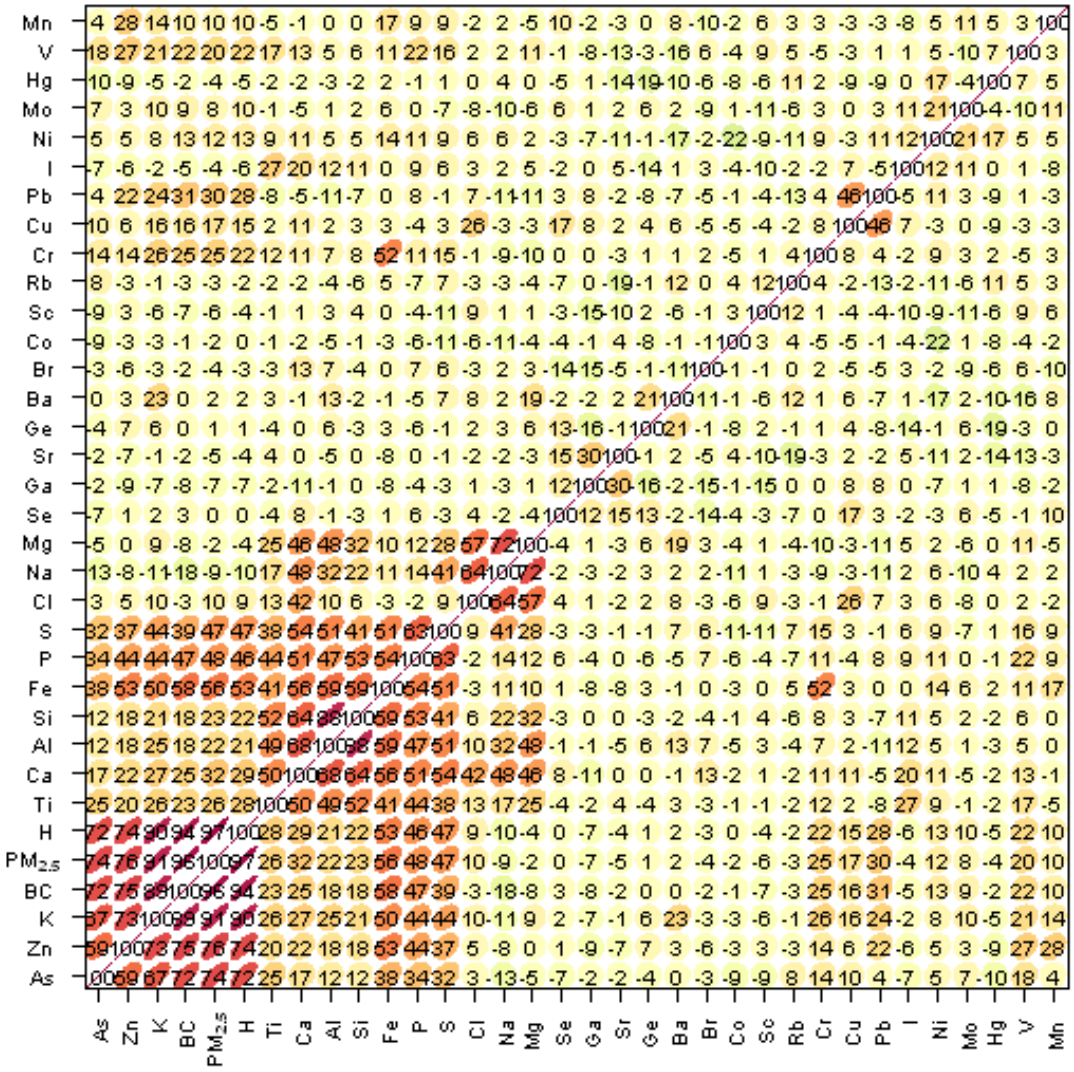

Figure A2.2 Elemental correlation plot for $PM_{2.5}$ samples collected at St. Vincent Street.

APPENDIX 3: EFFECT OF ATMOSPHERIC STABILITY ON THE IMPACT OF DOMESTIC WOOD COMBUSTION TO AIR QUALITY OF A SMALL URBAN TOWNSHIP IN WINTER

Experiments on the vertical and horizontal transport of black carbon in Nelson were performed during the same time period as the hourly particulate matter monitoring campaign discussed in Chapter 6. A manuscript describing the results of the campaign has been published in the international journal *Atmospheric Environment*. The paper, in its entirety, is included here.